TE
662
.A3
no.
FHWA-
RD-
78-
158

rt No. FHWA-RD-78-158

AND INTERPRETATION OF STRONG-MOTION RECORDS FROM HIGHWAY BRIDGES

October 1978

Final Report

DEPARTMENT OF
TRANSPORTATION
MAR 6 1979
LIBRARY

This document is available to the public
through the National Technical Information
Service, Springfield, Virginia 22161

Prepared for

FEDERAL HIGHWAY ADMINISTRATION
Offices of Research & Development
Washington, D.C. 20590

FOREWORD

This report is the result of research conducted at the Seismic Engineering Branch of the U.S. Geological Survey for the Federal Highway Administration (FHWA), Office of Research, under FHWA Purchase Order P.O. 5-3-0195. The report will be of interest to structural researchers, designers, and planners concerned with analyzing and interpreting strong-motion accelerograph records obtained from bridges instrumented to record earthquake response.

Copies of the report are being distributed by FHWA transmittal memorandum. Additional copies may be obtained from the National Technical Information Service, 5285 Port Royal Road, Springfield, Virginia 22161.

Charles F. Scheffey
Director, Office of Research
Federal Highway Administration

NOTICE

This document is disseminated under the sponsorship of the Department of Transportation in the interest of information exchange. The United States Government assumes no liability for its contents or use thereof.

The contents of this report reflect the view of the authors, who are responsible for the facts and the accuracy of the data presented herein. The contents do not necessarily reflect the official views or policy of the Department of Transportation.

This report does not constitute a standard, specification, or regulation.

The United States Government does not endorse products or manufacturers. Trademarks or manufacturers' names appear herein only because they are considered essential to the object of this document.

TE
662
.A3
no.
FHWA-
RD-
78-158

Technical Report Documentation Page

1. Report No. FHWA-RD-78-158	2. Government Accession No.	3. Recipient's Catalog No.
4. Title and Subtitle Use and Interpretation of Strong-Motion Records from Highway Bridges		5. Report Date October 1978
		6. Performing Organization Code
7. Author(s) J. D. Raggett and Christopher Rojahn		8. Performing Organization Report No.
9. Performing Organization Name and Address U.S. Geological Survey Menlo Park, California 94025		10. Work Unit No. (TRAIS) 35A2-052 FCP
		11. Contract or Grant No. 5-3-0195 P.O.
12. Sponsoring Agency Name and Address Offices of Research and Development Federal Highway Administration U.S. Department of Transportation Washington, D.C. 20590		13. Type of Report and Period Covered Final Report
		14. Sponsoring Agency Code S0809

15. Supplementary Notes

FHWA Contract Manager: James D. Cooper, HRS-11.

16. Abstract

This report describes how strong-motion records obtained from the earthquake induced motions of highway bridges may be analyzed for use in the evaluation of bridge designs and bridge design procedures.

This report is divided into five principal sections. The first section describes strong-motion instrumentation and strong-motion records. In the second section, a mathematical model for the dynamic response of bridges to strong ground shaking is formulated. The third section describes how analog records scaled by hand can be analyzed. Force levels throughout bridges and mathematical model parameters are found from hypothetical strong motions for two example bridges. The fourth section describes how digitized records can be analyzed. A linear least-squares fitting procedure in the time domain for identifying mathematical model parameters from recorded strong motions is described. Hypothetical motions for three example bridges are analyzed using this procedure to yield best-fit mathematical models. The last section consists of appendices. Included are a more extensive introduction to dynamics of structures and listings of the programs used to identify the best-fit mathematical models.

DEPARTMENT OF TRANSPORTATION
MAR 6 1979
LIBRARY

17. Key Words Earthquake, Bridges, Records, Strong Motion	18. Distribution Statement No restrictions. This document is available to the public through the National Technical Information Service, Springfield, Virginia 22161.		
19. Security Classif. (of this report) Unclassified	20. Security Classif. (of this page) Unclassified	21. No. of Pages 170	22. Price

Form DOT F 1700.7 (8-72) Reproduction of completed page authorized

CONTENTS

	Page
Introduction	1
I. Strong-motion instrumentation and records	3
II. Formulation of a mathematical model for the dynamic behavior of bridges	7
III. Analysis of analog records	16
A. Introduction	16
B. Force levels in bridges from strong-motion records	16
C. Identification of the mathematical model from strong-motion records	31
D. Example analyses	44
IV. Analysis of digitized strong-motion records with the assistance of a high-speed computer	91
A. Introduction	91
B. Time domain analysis procedure	95
C. Transformation to normal coordinates	100
D. Example analyses	103
V. Concluding remarks	142
References	144
Appendix A - Glossary of terms	146
B - Introduction to structural dynamics of bridges	150
C - Computer program listings	164
D - Conversion factors	168

INTRODUCTION

This manual describes some standard, general methods to analyze strong-motion accelerograph records of highway bridge motions. These analysis methods are appropriate for typical highway grade separation bridges. These bridges may be steel or concrete, simple spans or continuous, straight or curved, but are restricted to being moderate in length. The assumption that all bridge support motions are identical requires that bridge lengths be moderate.

Methods are described for the analysis of analog records visually without the need of a high-speed digital computer and for the analysis of digitized data with the use of a computer. The objectives of both types of analysis are (1) to find force levels throughout the bridge for a particular earthquake, and (2) to find parameters of a mathematical model which best describes the measured response. There are many secondary objectives that may be considered also, but for brevity only these two primary objectives are considered here.

The analyst is assumed to be familiar with structural engineering and to have some knowledge of structural dynamics. Appendix B includes a section on structural dynamics in which those concepts that are needed for the specific analysis procedures outlined here are developed. A greater understanding of structural dynamics may be obtained from standard texts (Biggs, 1964; Clough and Penzien, 1975; Hurty and Rubinstein, 1964).

A few words of caution are in order about the use of this manual. There are few uncertainties in obtaining force levels in bridges from strong-motion records. Force levels are computed from an extension of the expression

$$(\text{Force}) = (\text{Mass})(\text{Acceleration})$$

Masses can be estimated quite accurately from drawings, and accelerations can be measured accurately at specific points. There are always uncertainties in describing complete bridge accelerations from the accelerations of a few points, but with the judicious selection of instrument locations these uncertainties can be minimized. Therefore, force level analyses can be performed with confidence.

On the other hand, when strong-motion records are analyzed to obtain model properties, many uncertainties exist. In this manual properties are sought for only a linear mathematical model. This model is chosen because it is commonly used in structural dynamics, because general solution methods exist to solve the resulting set of equations, and because that solution is relatively easy to obtain. This model is not selected because it happens to be the best, although fortunately it is quite good for non-damaging levels of motion. It may not be appropriate for high-level damaging motions or for motions involving significant foundation compliance.

It is beyond the scope of this manual to discuss higher order mathematical bridge models, which are appropriate for nonlinear or inelastic response. It would also be very difficult since there is no single, general higher order model; there are many. This whole field of nonlinear higher order, model identification from strong-motion records is in an early stage of development. Even the methods suggested here to identify model properties for the linear model are not well established at this time. Rapid advancement is expected in the next few years, particularly with regard to the automatic analysis of digitized records on high speed digital computers.

I. STRONG-MOTION INSTRUMENTATION AND RECORDS

A strong-motion record is defined here as the record of structural motion caused by a relatively large earthquake. This strong motion may be recorded in a number of ways. It may be a light trace on film, a line on a strip of paper, or an analog or digital signal on magnetic tape. In all cases the motion is recorded as a function of time.

The motion recorded is that for a point moving along a single axis and may have dimensions of displacement, velocity, or acceleration. Most often acceleration is recorded. The motion is recorded as an electrically or mechanically generated signal which is proportional to the motion within some acceptable error.

The adjective "strong" is included to differentiate these recordings from recordings taken with other common seismographs used to determine earthquake magnitudes and epicentral distances. Such seismographs are capable of detecting earthquakes almost anywhere in the world, and are necessarily very sensitive. Strong motions would cause these seismograph recordings to be off scale. In general, strong motions could cause damage to structures, and are recorded near earthquake epicenters. The actual level of ground motion above which motions are "strong" is not well defined. Typically, ground motions with a peak acceleration greater than 0.01 g trigger strong-motion accelerometers, those greater than 0.05 g are of structural interest, and those greater than 0.10 g are potentially damaging.

In the United States, strong-motion records are normally recorded on accelerographs. The accelerographs are of two general types: analog or digital. In either case, acceleration is sensed by accelerometers and recorded as a continuous function of time. In the analog instrument, it is recorded on light-sensitive film or paper and in the digital instrument, it

is recorded in digital form on magnetic tape. Both instrument types are powered by batteries, are triggered into operation by the strong motion itself (i.e., motion having an acceleration equal to or greater than a pre-set triggering level, commonly 0.01 g, and are available either as self-contained triaxial instruments or remote accelerometer/central recording instruments. In the self-contained variety, all major components--accelerometers, recorder, and trigger--are housed in one container, whereas in the remote recording type, these elements can be physically separated but are interconnected by low-voltage data cable.

A typical analog film record from a three-component self-contained accelerograph is shown in figure 1 (records from remote accelerometer/central recording systems are similar although they normally contain more data traces). The record contains time ticks, two fixed traces, three acceleration data traces and a WWVB time code. The time ticks denote film speed and normally appear every half second; each fixed trace is a reference

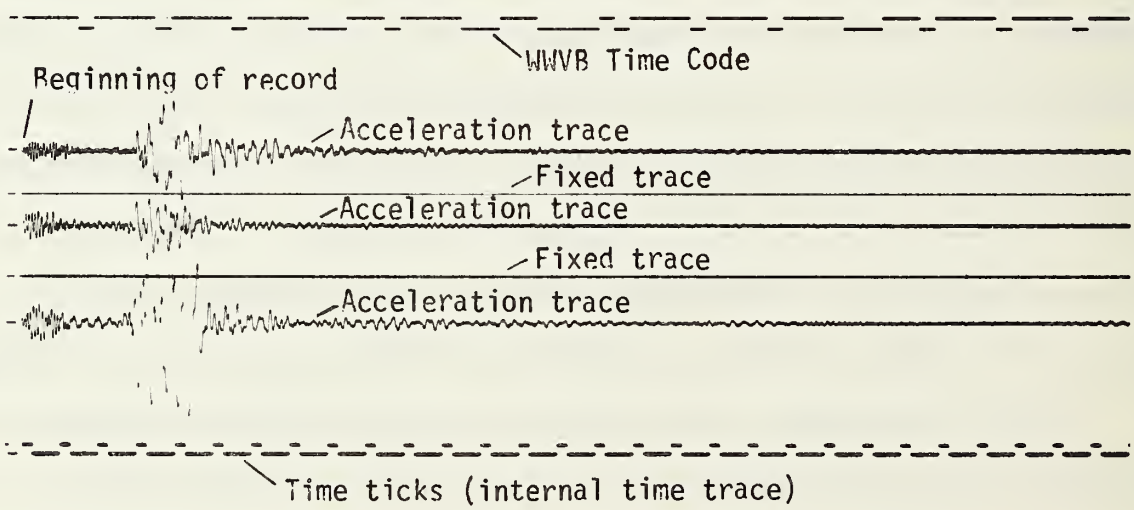

Figure 1.- Copy of a typical three-component strong-motion accelerograph record.

trace that is used to extract long-period errors from the data due to film distortion or the film drive mechanism; and the WWVB time code is used to identify when the event occurred. The most important elements of the record, the acceleration data traces, have values of amplitude that are approximately proportional to real values of recorded acceleration. For most instruments in present use, the sensitivity of the acceleration traces is on the order of 1.90 cm/g. The sensitivity is calibrated during or before installation and should appear on the record or accompany it. Other relevant information that should accompany the record includes orientation, location, natural frequency, damping of each accelerometer, film speed, instrument serial number, and location of the recorded earthquake. If such information does not accompany a record, most of it should be available either from the instrument owner, the manufacturer, or the agency or organization maintaining the instrument.

Records from a typical digital instrument are normally recorded in digital form on one- or four-track cassette tape and are not immediately available in analog form. Analog records are made from a digital instrument by processing the digital data with a digital-to-analog converter and plotter. Hardware of this type has been developed by the firms that manufacture the digital instruments and should be available either through these firms or the agency or organization that maintains the instrument.

In order to convert both the analog film and digital cassette records into a digital form that can be processed on high-speed digital computers, additional processing is required. Analog records are converted into digitized form on systems known as digitizers. In such a system, a handheld cursor or automatic scanning device is used to follow the trace and assign numerical coordinate values (normally Cartesian) to all points of interest.

Such points are normally selected at equal intervals or at all peaks, valleys and points of inflection. The numerical values are recorded on computer-compatible cards or on magnetic tape. Data from a digital strong-motion instrument is immediately available in digitized form on cassettes but requires processing for conversion into a computer-compatible format. The processing is handled by hardware designed by the instrument manufacturer. Its availability should be known by the strong-motion instrument manufacturer or the agency or organization maintaining the instrument.

After conversion into a high-speed-computer-compatible format, the digitized data can be corrected to extract errors introduced during the recording and digitization process and to account for the dynamic characteristics of the recording instrument. Procedures for correcting the data are well established (Brady and Perez, 1976; Miklofsky and Mancini, 1977; Trifunac and Lee, 1973) and are presently performed routinely by the U.S. Geological Survey. When the processing is completed, the digitized data are then ready for analysis. Procedures for standardized analysis of three-component ground motion records are also well established (Brady and Perez, 1976; Trifunac and Lee, 1973) and are routinely performed. The analysis of a set of earthquake records from a particular bridge, however, is not yet a routine procedure. The methodology described below has been designed for that purpose.

II. FORMULATION OF A MATHEMATICAL MODEL FOR THE DYNAMIC BEHAVIOR OF BRIDGES

As indicated above, the two primary objectives in the analysis of strong-motion records are: (1) to verify, modify, or improve the mathematical models used to design a bridge to resist earthquake motion and (2) to find force levels throughout a bridge. If a number of analyses lead to a consistent set of modeling assumptions, then this set of assumptions can be used with confidence in the design of new bridges. It is hoped that the analyses verify rather than modify the initial design assumptions.

A mathematical model of the bridge is formulated from the initial design of the bridge. Numerous assumptions are made in the formulation of this model and these assumptions are to be verified from the measured records. The bridge response motions, or output motions, are computed using the mathematical bridge model and a given design earthquake. From these output motions force and stress levels at selected points in the bridge are computed. These force and stress levels are then compared with allowable levels. If the computed levels exceed the allowable levels, then the bridge design must be modified and reanalyzed after a new mathematical model has been formulated.

Experimentally it is desirable to measure the input ground motions and a sufficient number of bridge response motions to describe the complete bridge motion to within some acceptable error. From the output motions alone, the force and stress levels throughout the bridge may be computed and compared with corresponding acceptable levels. The force levels for a specific earthquake are not of general interest because that particular

earthquake or any scale multiple of it is never likely to repeat itself. Of far greater general interest is to identify the mathematical model that would have duplicated the measured output motions for the measured input motions. A comparison of this model and the model used to design the bridge will test the assumptions made to formulate the model for design.

In general, mathematical models of dynamic bridge behavior are formulated during the design process to predict what distortions are expected relative to the ground when a bridge is subjected to an earthquake. It is important to recognize that these distortions are in addition to the absolute displacements of the bridge following the ground motions. If there are no distortions (the bridge is essentially rigid) there will still be significant earthquake forces in the bridge equal to the products of bridge masses and ground accelerations. We hope to learn from the dynamic model of the bridge whether or not these distortions are significant relative to the absolute ground displacements. In some cases the distortions are very small relative to the absolute displacements of the bridge. For such cases, the accuracy of the dynamic model is unimportant because the contribution to the total inertial load from the flexible distortions is so small. For certain loads, the bridge may "resonate" producing very large distortions from a relatively small input. Such vibrations rarely result from earthquakes. For very flexible structures, distortions one to four times the absolute ground displacements may be expected (Newmark and Rosenblueth, 1971; Wiegel, 1970). For relatively rigid bridges, distortions much less than the absolute ground motion are likely.

The importance of the mathematical model of dynamic behavior depends upon the bridge being analyzed. Therefore, there is no absolute measure of

the accuracy of mathematical models for all bridges, but it must be evaluated for each class of bridges.

A few fundamental assumptions, generally made in the formulation of a dynamic mathematical model, will be made in this report. It is first assumed that a linear elastic model may describe adequately the dynamic distortions of the bridge. Forces are assumed to be linearly related to bridge displacements and velocities relative to the ground, and linearly related to absolute bridge accelerations. The second fundamental assumption is that all supports of the bridge are subjected to the same ground motion at the same time. For this assumption to hold, the bridge length must be small with respect to the wave lengths of the ground motion waves which produce the most significant bridge response, presumably at the lower natural frequencies of the bridge. This assumption seems reasonable for typical highway bridges on firm foundation material, but may be erroneous if the foundation material varies significantly from one end of the bridge to the other.

Both of these assumptions are made not necessarily because they will lead to the most accurate model, but because they will lead to mathematical equations that can be solved with comparative ease. Once these assumptions are made the mathematical model is well defined and the model parameters may be determined from the response of the structure. If the model is not assumed to be linear, the problem is not well defined and there is no end to the possible forms that the model may take.

Ultimately, these two modeling assumptions must be evaluated by analyzing actual strong-motion records. If model parameters can be found with accuracy such that a mathematical model, based upon the above two

assumptions, can duplicate the measured response well, then it can be deduced that the two assumptions are reasonable. If model parameters cannot be found, then the assumptions are poor. It is beyond the scope of this report to suggest higher order models that may be evaluated. For information on higher order models the reader should consult Clough and Penzien (1975) and Hurty and Rubinstein (1964).

Within the context of these two assumptions, the mathematical model will take one of three forms depending upon the coordinate system chosen to describe the bridge distortions.

The first and most common form of mathematical model is

$$[M]\{\ddot{u}\}+[C]\{\dot{u}\}+[K]\{u\} = -\{M_x\}\ddot{U}_{xg}-\{M_y\}\ddot{U}_{yg}-\{M_z\}\ddot{U}_{zg} \qquad (1)$$

where

$\{u\}$	is a vector of bridge displacements relative to the ground at a finite number of preselected points,
$[M]$	is a matrix of masses lumped at, and corresponding to, the physical coordinates chosen to describe the bridge distortions,
$[C]$	is a damping matrix,
$[K]$	is a stiffness matrix,
$\ddot{U}_{xg}$, $\ddot{U}_{yg}$, $\ddot{U}_{zg}$	are mutually orthogonal ground accelerations,
$(\dot{\ })=d/dt$	is differentiation with respect to time, and
$\{M_x\}$, $\{M_y\}$, $\{M_z\}$	are vectors of participation factors corresponding to the ground motions $\ddot{U}_{xg}$, $\ddot{U}_{yg}$, $\ddot{U}_{zg}$, respectively.

The participation factor M_{xi} is the quasi-static force in the ith coordinate direction produced by a unit acceleration, $\ddot{U}_{xg}(t)=1$. Similar definitions hold for the participation factors M_{yi} and M_{zi}.

This mathematical model is called a lumped-mass model in physical coordinates. It can be used to identify mathematical models for short simple-span bridges and very long multi-span continuous bridges. It is called a lumped-mass model because the mass of the bridge is typically lumped (for analysis purposes) at a selected number of points. The coordinates are physical because they are translations and rotations at selected points which are measureable.

For many bridges, particularly short continuous bridges, it may be more appropriate to describe the bridge distortions in generalized coordinates. This is the second form of mathematical model. In this coordinate system, bridge distortions are expanded in terms of a set of r assumed distorted shapes.

$$\tilde{u}(s,t) = \sum_{i=1}^{r} \tilde{\psi}_i(s)\alpha_i(t) \tag{2}$$

where

$\tilde{u}(s,t)$ is a vector of bridge distortions as a function of time, t, and s, the distance along the centerline of the bridge element (bridges typically can be modeled as a collection of one-dimensional elements),

$\tilde{\psi}_i(s)$ is a vector description of the ith <u>assumed</u> distorted shape and

$\alpha_i(t)$ is a time-dependent, generalized displacement associated with the ith assumed distorted shape.

At any time the vector of distortions at a location s is given by

$$\tilde{u}(s,t) = u_x(s,t)\tilde{i}+u_y(s,t)\tilde{j}+u_z(s,t)\tilde{k} \tag{3}$$

where $\tilde{i}$, $\tilde{j}$, and $\tilde{k}$ are unit vectors in the mutually perpendicular directions

x, y, z respectively parallel to the recorded ground accelerations $\ddot{U}_{xg}(t)$, $\ddot{U}_{yg}(t)$, $\ddot{U}_{zg}(t)$. The vector description of the assumed distorted shapes, $\tilde{\psi}_i(s)$, similarly can be written in terms of its orthogonal components in the x, y, and z directions. Note that the generalized displacements, $\alpha_i(t)$, cannot be measured directly, but must be computed from displacements in physical coordinates, $u_i(t)$, by the inverse of the transformation

$$\{u(t)\} = [\psi]\{\alpha(t)\} \tag{4}$$

The matrix element ψ_{ij} is the displacement in the ith physical coordinate direction for the jth assumed distorted shape.

The mathematical model describing the dynamic bridge distortions can now be given by

$$[m]\{\ddot{\alpha}\}+[c]\{\dot{\alpha}\}=[k]\{\alpha\} = -\{m_x\}\ddot{U}_{xg}-\{m_y\}\ddot{U}_{yg}-\{m_z\}\ddot{U}_{zg} \tag{5}$$

The inertial terms, integrated over all elements of the bridge, are

$$m_{ij} = \int M(s)\tilde{\psi}_i(s)\cdot\tilde{\psi}_j(s)ds \tag{6}$$

$$m_{xi} = \int M(s)\tilde{\psi}_i(s)\cdot\tilde{i}ds \tag{7}$$

$$m_{yi} = \int M(s)\tilde{\psi}_i(s)\cdot\tilde{j}ds \tag{8}$$

$$m_{zi} = \int M(s)\tilde{\psi}_i(s)\cdot\tilde{k}ds \tag{9}$$

and typically are computed from material properties, the geometry of the bridge being analyzed, and the assumed deflected shapes. The quantity M(s) is an inertia per unit length of bridge (a mass when $\tilde{\psi}(s)$ is a displacement and a rotational inertia when $\tilde{\psi}(s)$ is a rotation). Analytical expressions for the damping coefficients, c_{ij} and stiffness coefficients k_{ij}, can also be formulated. However, these are the unknowns to be obtained from the strong-motion records.

Although this formulation, in terms of generalized coordinates, $\alpha_i(t)$,

looks identical to the model formulation in terms of physical coordinates, $u_i(t)$, there is one significant advantage for most short continuous bridges. To achieve the same degree of accuracy describing structure distortions, it will require fewer coordinates $\alpha_i(t)$ than $u_i(t)$. Since one transducer is needed to record each distortion, in either coordinate system, the system with the fewer coordinates required will require fewer transducers. Another way of interpreting this advantage is that the coordinate system requiring the fewest number of coordinates to describe the bridge distortions for a given accuracy will describe the bridge distortions most accurately for the same number of transducers.

For all bridges, distortions can be described most accurately, with the fewest number of coordinates, if normal coordinates are used (Clough and Penzien, 1975). This is the third form of the mathematical model. Here bridge distortions are expanded in terms of normal mode shapes

$$\tilde{u}(s,\tau) = \sum_{i=1}^{n} \tilde{\phi}_i(s)\eta_i(t) \tag{10}$$

where

$\tilde{\phi}_i(s)$ is the ith normal (or natural) mode shape, and

$\eta_i(t)$ is a displacement in normal coordinates associated with the ith normal mode shape.

In normal coordinates, the matrix equation of motion describing structure distortions takes the unique form

$$[M]\{\ddot{\eta}\}+[C]\{\dot{\eta}\}+[K]\{\eta\}=-\{M_x\}\ddot{U}_{xg}-\{M_y\}\ddot{U}_{yg}-\{M_z\}\ddot{U}_{zg} \tag{11}$$

where all off-diagonal terms of $[M]$, $[C]$, and $[K]$ equal zero. The inertial terms, integrated over elements of the bridge, are again given by

$$M_i = \int M(s)\tilde{\phi}_i(s)\cdot\tilde{\phi}_i(s)ds \tag{12}$$

$$M_{xi} = \int M(s)\tilde{\phi}_i(s)\cdot\tilde{i}ds \tag{13}$$

$$M_{yi} = \int M(s)\tilde{\phi}_i(s)\cdot\tilde{j}ds \tag{14}$$

$$M_{zi} = \int M(s)\tilde{\phi}_i(s)\cdot\tilde{k}ds \tag{15}$$

It is particularly advantageous to describe bridge motions in terms of normal coordinates because the individual equations in the matrix equation, equation 11, are uncoupled. Specifically, each normal displacement is governed by the single equation of motion (here for example, the ith)

$$M_i\ddot{\eta}_i+C_i\dot{\eta}_i+K_i\eta_i = -M_{xi}\ddot{U}_{xg}-M_{yi}\ddot{U}_{yg}-M_{zi}\ddot{U}_{zg} \tag{16}$$

Typically these equations are normalized to have modal masses, M_i, equal unity (Clough and Penzien, 1975). For such a normalization, equation 16 takes the form

$$\ddot{\eta}_i+2\xi_i\omega_i\dot{\eta}_i+\omega_i^2\eta_i=-\gamma_{xi}\ddot{U}_{xg}-\gamma_{yi}\ddot{U}_{yg}-\gamma_{zi}\ddot{U}_{zg} \tag{17}$$

in terms of the common dynamic response characteristics

$\omega_i = \sqrt{K_i/M_i}$	a natural circular frequency of vibration (radians/sec),
$\xi_i = C_i/2\sqrt{K_iM_i}$	a modal viscous damping ratio, and
γ_{xi}, γ_{yi}, γ_{zi}	renormalized participation factors: M_{xi}/M_i, M_{yi}/M_i and M_{zi}/M_i respectively.

In this form, a participation factor is a measure of the degree to which a mode of vibration is excited by a ground motion relative to the response of a simple spring-mass oscillator having the same natural frequency and damping ratio.

It is desirable to describe the distortions of all bridges in terms of normal modes because the fewest coordinates are needed for a given accuracy. Similarly, for a given number of normal coordinates there are the fewest unknown model parameters to be determined from the strong-motion records

because all off-diagonal terms of $[M]$, $[C]$, and $[K]$ by definition equal zero. Unfortunately, when model parameters are to be determined from strong-motion records as they are in this report, bridge distortions cannot be described in normal coordinates before analysis because the normal mode shapes $\tilde{\phi}_i(s)$ are unknowns that are to be determined from the analysis of the strong-motion records. These mode shapes must be known to compute the normal displacements, $\eta_i(t)$. Again the normal displacements $\eta_i(t)$ are not directly measureable, but must be computed by the inverse of the transformation

$$\{u(t)\}=[\phi]\{\eta(t)\} \tag{18}$$

where ϕ_{ij} is the displacement of the jth normal mode shape in the ith physical coordinate direction.

Therefore, for the methods of analysis described here, bridge distortions must be described in either physical or generalized coordinates. The lumped-mass model in physical coordinates should be used for simple span or long multi-span bridges, whereas the model in generalized coordinates is more appropriate for short continuous bridges. Once model parameters are identified from the strong-motion records, the identified mathematical model can be transformed readily from physical or generalized coordinates (equations 1 or 5) to the decoupled form in normal coordinates (equation 17). Methods to make this transformation from either physical or generalized coordinates to normal coordinates can be found in any text on structural dynamics (Biggs; 1964, Clough and Penzien, 1975; Hurty and Rubinstein, 1964).

If the reader is interested in a more complete development of the equations presented above, Appendix B should be consulted or the referenced texts on structural dynamics. Gere and Weaver, 1965, give a complete development of matrix algebra.

III. ANALYSIS OF ANALOG RECORDS

A. Introduction

This section describes methods of analyzing analog recordings of strong-motion records from bridges. For use in the procedures described, the ground motion and bridge response values may be visually scaled from the raw recordings. Also, analysis methods described in this section may be performed without a high-speed digital computer.

As mentioned in Section II there are two principal objectives of the strong-motion record analysis procedures. The first is to determine force levels throughout the bridge for the measured earthquake. The second is to deduce from the ground motion and bridge response records the mathematical model of the bridge which best duplicates the bridge response. Mathematical models are most often characterized by natural frequencies, damping ratios, and mode shapes. In order to find force levels there is no need to formulate a mathematical model describing the bridge motion as complete and as complex as those formulated in the previous section (equations 1, 5, 11, and 17). Instead, force levels can be computed from the recorded bridge motions, known geometry of the bridge, and known mass distribution in the bridge. The recorded bridge motions, however, must be described mathematically in terms of one of the three coordinate systems described in Section II.

B. Force Levels in Bridges from Strong-Motion Records

It is assumed that accelerations are measured as raw data. This may seem to be overly restrictive, but in practice nearly all strong-motion

instruments do record acceleration as raw data.

A second more important assumption is that the bridge is properly instrumented in the first place. By proper instrumentation it is meant that there exist a sufficient number of time-correlated bridge accelerations to describe all significant bridge motions. This is absolutely necessary if accurate force levels are to be measured from the experimental data without the use of a mathematical model. Many instrumentation programs have as their principal objective the verification of a particular mathematical model. Relatively few strong-motion instruments may be required to verify a mathematical model adequately, but these may be totally inadequate for the calculation of force levels in the bridge without the use of a mathematical model. Therefore, it is important to determine first whether or not there are enough recordings to perform a force analysis. If there are not, a force analysis can still be made but only with the assistance of a mathematical model. The mathematical model is first verified by the experimental data, and then force levels are computed from the mathematical model.

For a typical bridge deck it is assumed that all significant horizontal distortions can be described in terms of four modes of vibration: a lateral translation relative to the ground, a rotation about a vertical axis, a lateral flexural mode, and a longitudinal translation relative to the ground. These four modes of vibration and the corresponding, assumed, displacement shapes relative to the ground are shown in figure 2. In order that force levels be found throughout the bridge, bridge motions in all of these modes of vibration must be recorded. In general there must exist at least one recorded motion for each mode of vibration of interest. These

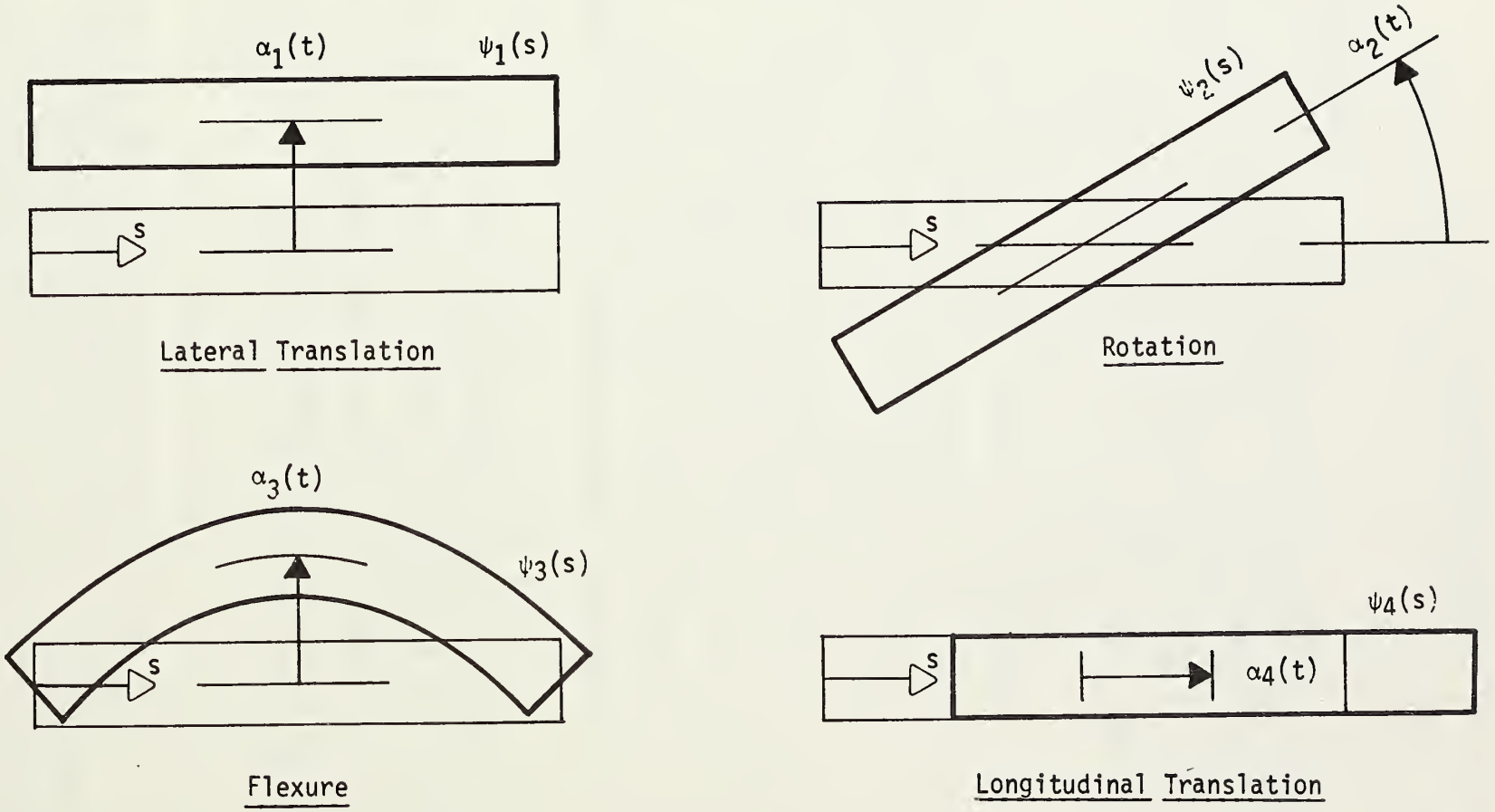

Figure 2.- Example modes of vibration.

recorded motions, however, must be recordings of independent motions to describe the above modes of vibration sufficiently. For example, the four instrument motions shown in figure 3a may have been recorded in hopes of detecting the modes of vibration. The motions $\ddot{U}_1(t)$ and $\ddot{U}_2(t)$ can be combined to yield lateral translation and rotation but cannot be combined to yield any information regarding deck flexure. Furthermore, either $\ddot{U}_3(t)$ or $\ddot{U}_4(t)$ can be used to record the longitudinal deck motion. Since longitudinal deck extension is likely to be minimal, $\ddot{U}_3(t)$ and $\ddot{U}_4(t)$ will be nearly identical and hence one is redundant. Therefore, there are only three independent motions recorded, and all four expected modes of vibration cannot be detected by these three motions. A more suitable instrumentation plan is shown in figure 3b. Corresponding to the assumed deflected shapes $\tilde{\psi}_i(s)$shown in figure 2, generalized accelerations can be expressed in terms of the measured <u>absolute</u> accelerations by

$$\ddot{\alpha}_1(t) = (\ddot{U}_1(t)+\ddot{U}_3(t))/2-\ddot{U}_{yg}(t) \tag{19}$$

$$\ddot{\alpha}_2(t) = (\ddot{U}_3(t)-\ddot{U}_1(t))/L \tag{20}$$

$$\ddot{\alpha}_3(t) = (2\ddot{U}_2(t)-\ddot{U}_1(t)-\ddot{U}_3(t))/2 \tag{21}$$

$$\ddot{\alpha}_4(t) = \ddot{U}_4(t)-\ddot{U}_{xg}(t) \tag{22}$$

These equations are equivalent to the inverse of the transformation from physical to generalized coordinates, equation 4. The generalized accelerations, $\ddot{\alpha}_i(t)(i=1,2,3,4)$ can now be used to determine force levels in the bridge associated with the four modes of vibration shown in figure 2.

As a second example of the instrumentation required to compute force levels throughout a structure accurately, consider a bridge deck composed of many independent simple spans. If each deck is considered to be rigid in a horizontal plane, then all significant horizontal deck motions relative to

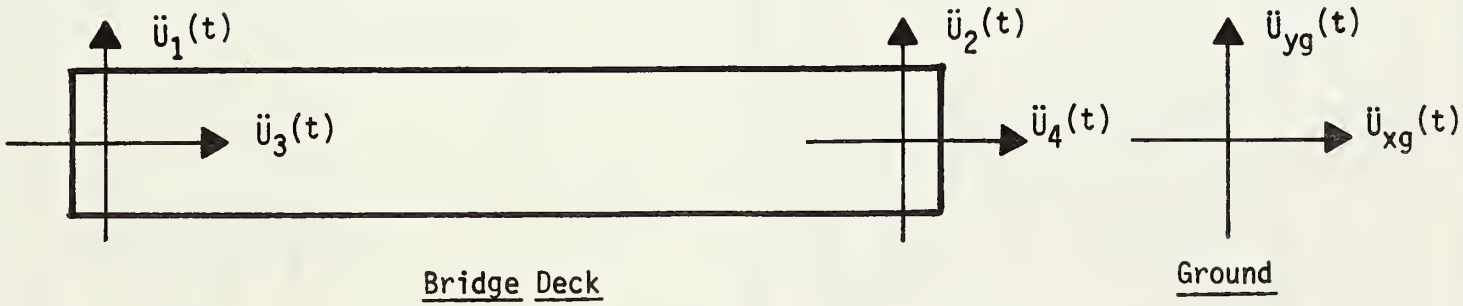

(a) Incorrect Instrumentation

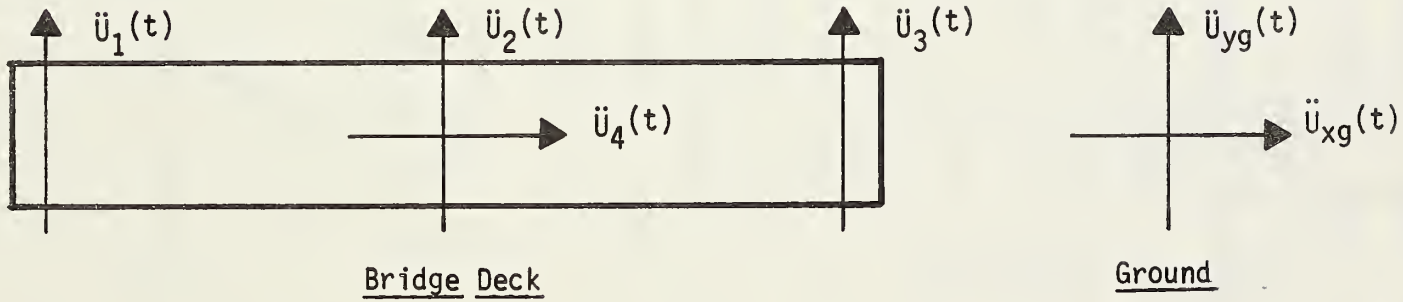

(b) Correct Instrumentation

Figure 3.- Instrumentation schemes.

the ground can be described in terms of lateral and longitudinal translation, and rotation about a vertical axis. Specifically for each span, the instrumentation shown in figure 4 may be used to describe lateral deck translation relative to the ground, $(\ddot{U}_1(t) + \ddot{U}_2(t))/2 - \ddot{U}_{yg}(t)$; deck rotation about a vertical axis, $(\ddot{U}_2(t) - \ddot{U}_1(t))/L$; and longitudinal deck translation relative to the ground, $\ddot{U}_3(t) - \ddot{U}_{xg}(t)$. Force levels in this deck can then be computed from these generalized accelerations. Force levels throughout the multispan bridge may be found experimentally only if each individual span is instrumented in a similar manner.

Force levels throughout the bridge may be found readily from a generalization of the relation F = ma. At any instant in time in the ith coordinate direction (whether in physical coordinates, generalized coordinates, or normal coordinates),

$$F_{mi} + F_{ci} + F_{ki} = 0 \tag{23}$$

where

F_{mi}	is an inertial force;
F_{ci}	is a dissipative force; and
F_{ki}	is a restoring force.

In general, the peak dissipative, or damping, forces are small with respect to the peak inertial and restoring forces and occur at different times (Clough and Penzien, 1975; Newmark and Rosenblueth, 1971). Therefore

$$F_{mi}\big|_{max} \cong -F_{ki}\big|_{max} \tag{24}$$

Maximum restoring forces are of greatest concern because they are related to stresses, strains, and possible failure. Since accelerations are recorded as raw data, and since masses can be computed quite accurately, maximum inertial forces are easiest to compute.

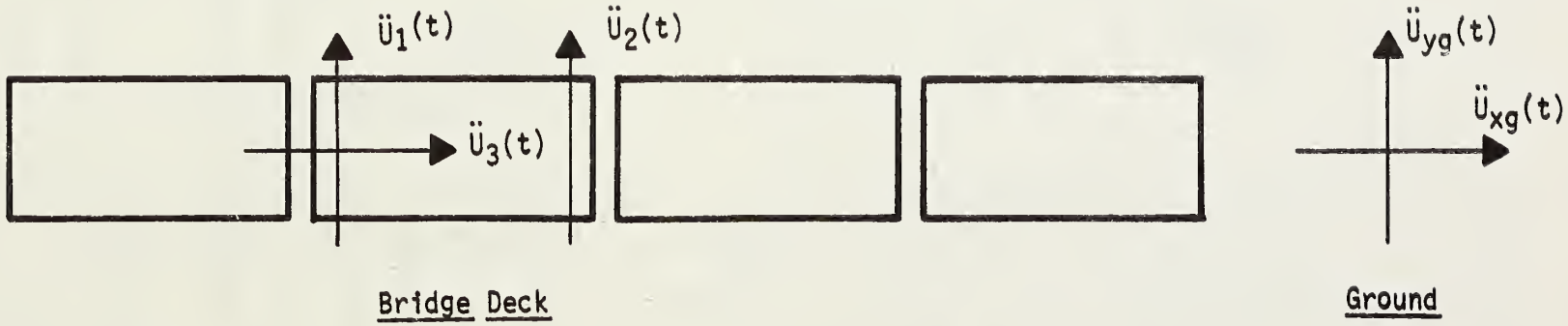

Figure 4.- Multiple simple span bridge instrumentation.

A general approach to the computation of force levels throughout a bridge takes three steps: (1) compute inertial forces acting on bridge, (2) compute reactions to those inertial forces, and (3) compute any desired internal action from inertial forces and reactions. Forces will be computed for structures described by physical as well as generalized coordinates. Force levels in bridges described in normal coordinates can be computed exactly as for bridges described by generalized coordinates if the functions $\tilde{\phi}_i(s)$ are substituted for $\tilde{\psi}_i(s)$, and $\eta_i(t)$ for $\alpha_i(t)$in the equations which follow in this section.

Inertial loads acting on bridges are computed most easily for lumped mass models described in physical coordinates. At any time, the inertial force acting on the ith mass is simply

$$\tilde{F}_i(t) = M_i\ddot{\tilde{U}}_i(t) \tag{25}$$

where $\ddot{U}_i(t)$ is the recorded absolute acceleration at the ith mass. The complete inertial force distribution on the bridge is obtained by computing inertial forces on all masses for the same instant in time.

The computation of inertial forces acting on a bridge whose distortions are described in generalized coordinates is somewhat more difficult. At any instant in time, t, for any location along a bridge, s, the inertial force per unit length of bridge is given by

$$\tilde{F}(s,t) = M(s)\ddot{\tilde{U}}(s,t) \tag{26}$$

where $\ddot{\tilde{U}}(s,t)$ is the absolute acceleration at that point on the bridge. If these absolute accelerations are expanded in terms of ground accelerations and generalized accelerations

$$\ddot{\tilde{U}}(s,t) = \sum_{i=1}^{n} \tilde{\psi}_i(s)\ddot{\alpha}_i(t) + \ddot{U}_{xg}(t)\tilde{i} + \ddot{U}_{yg}(t)\tilde{j} + \ddot{U}_{zg}(t)\tilde{k} \tag{27}$$

then the inertial forces can be expanded in like manner:

$$\tilde{F}(s,t) = M(s)\sum_{i=1}^{n}\tilde{\psi}_i(s)\ddot{\alpha}_i(t)+M(s)[\ddot{U}_{xg}(t)\tilde{i}+\ddot{U}_{yg}(t)\tilde{j}+\ddot{U}_{zg}(t)\tilde{k}] \quad (28)$$

The generalized accelerations, $\ddot{\alpha}_i(t)$, are readily computed from the vector of bridge distortions in physical coordinates $\{\ddot{u}(t)\}$ using the inverse of equation 4, namely

$$\{\ddot{\alpha}(t)\} = [\psi]^{-1}\{\ddot{u}(t)\} \quad (29)$$

Inertial forces acting on the bridge can then be computed using equation 28.

The second step in computing force levels throughout a bridge is to compute reactions resisting those inertial forces. These can be computed using any acceptable procedure of structural engineering. One such technique using the principle of virtual work (Clough and Penzien, 1975) will be discussed in detail. Reactions will be computed first for bridges whose motions are described in physical coordinates; and second, in generalized coordinates.

As an example, the horizontal reaction at one end of a simply supported bridge span will be computed. This reaction and the lumped-mass model of the span is shown in figure 5. Let $\tilde{r}_i(s)$ be a vector deformed shape that the bridge takes if the left support is deformed a unit amount corresponding to the unknown reaction, $R_i(t)$. In addition, let $\tilde{r}_{ij}$ be the vector displacement due to this unit support displacement at the jth mass. The $\tilde{r}_i(s)$ and $\tilde{r}_{ij}$ are also shown schematically in figure 5.

By the principle of virtual work when a bridge, which is in static or dynamic equilibrium under the action of a set of forces, is subjected to a virtual displacement, the total work (force x displacement) done by those forces equals zero (Clough and Penzien, 1975). The forces acting on this example bridge deck are all the reactions and the inertial forces

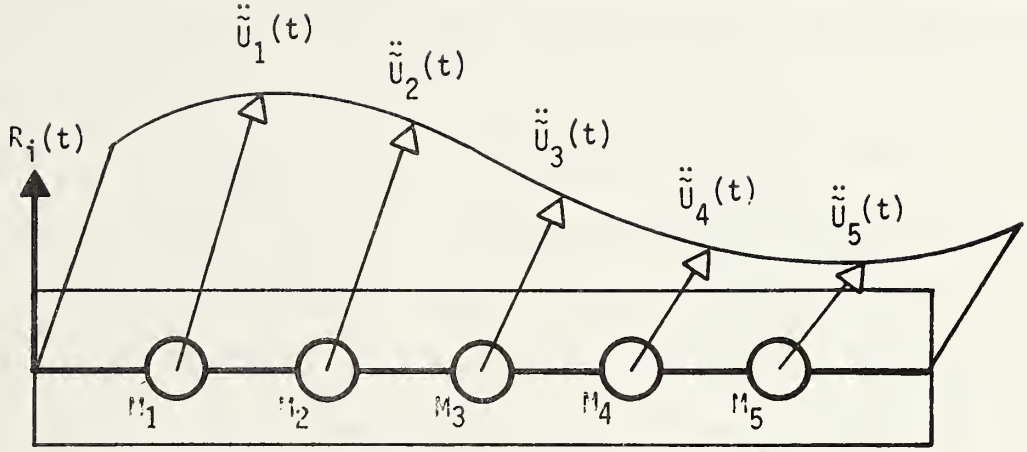

Lumped Mass Model And Recorded Accelerations

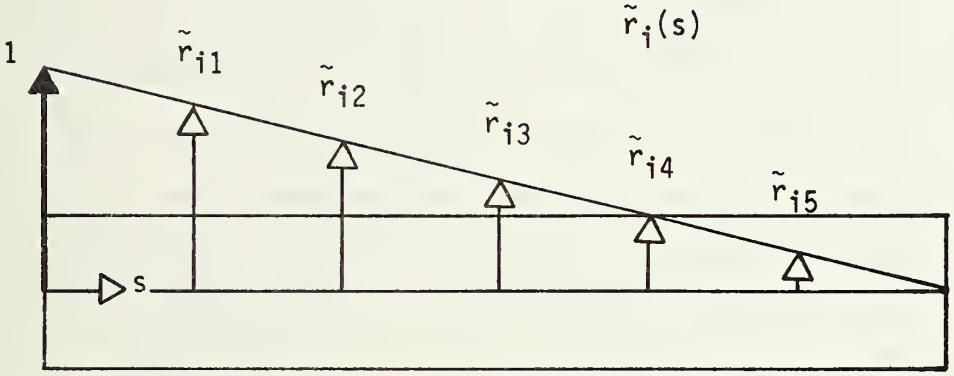

Deformed Shape Due To Unit Displacement Corresponding To R_i (t)

Figure 5.- Definition of shape functions.

$$\tilde{F}_i(t) = M_i\ddot{\tilde{U}}_i(t) \tag{25}$$

If the entire bridge is subjected to a single virtual displacement, δr_i, corresponding to the unknown reaction, $R_i(t)$, then the total virtual work is given by

$$R_i(t)\delta r_i + \sum_{j=1}^{n} M_j\ddot{\tilde{U}}_j(t)\cdot\tilde{r}_{ij}\delta r_i = 0 \tag{30}$$

and for this example the number of masses, n, is five. There are many other non-zero reactions besides the ith but their virtual displacements are by definition zero, so they produce no virtual work. Since δr_i is small but non-zero it may be divided from equation 30. Hence

$$R_i(t) = -\sum_{j=1}^{n} M_j\ddot{\tilde{U}}_j(t)\cdot\tilde{r}_{ij} \tag{31}$$

Such an equation can be derived for all reactions, whether they be forces or moments (if the reaction is a moment, then $\tilde{r}(s)$ is the deformed shape of the bridge due to a unit support rotation corresponding to the unknown moment).

If the distortions of the bridge are described in generalized coordinates, it is easiest to find all the reactions to unit generalized accelerations, and unit ground accelerations, and then linearly combine the results for the actual values of $\ddot{\alpha}_i(t)$, $\ddot{U}_{xg}(t)$, $\ddot{U}_{yg}(t)$, and $\ddot{U}_{zg}(t)$ measured.

Consider first the ith reaction of the same simply supported bridge deck to a unit generalized acceleration, $\ddot{\alpha}_j(t)$. Let this reaction be $R_{ij}(t)$. This reaction and the jth unit generalized acceleration are shown schematically in figure 6. For this unit generalized acceleration, the inertial force per unit length along the axis of the bridge

$$\tilde{F}_j(s,t) = M(s)\tilde{\psi}_j(s)\ddot{\alpha}_j(t) \tag{32}$$

and because $\ddot{\alpha}_j(t) = 1$, by assumption,

$$\tilde{F}_j(s) = M(s)\tilde{\psi}_j(s) \tag{33}$$

Again define $\tilde{r}_i(s)$ as the vector deformed shape that the bridge takes if the

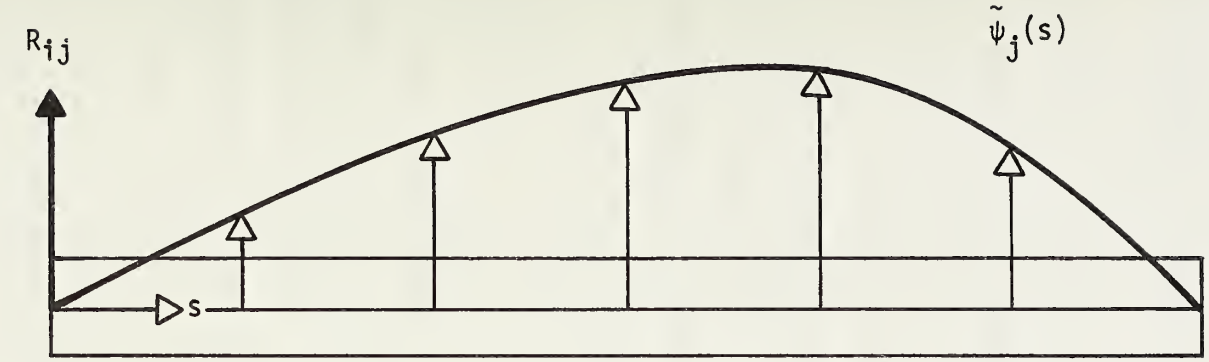

Assumed Deformed Shape

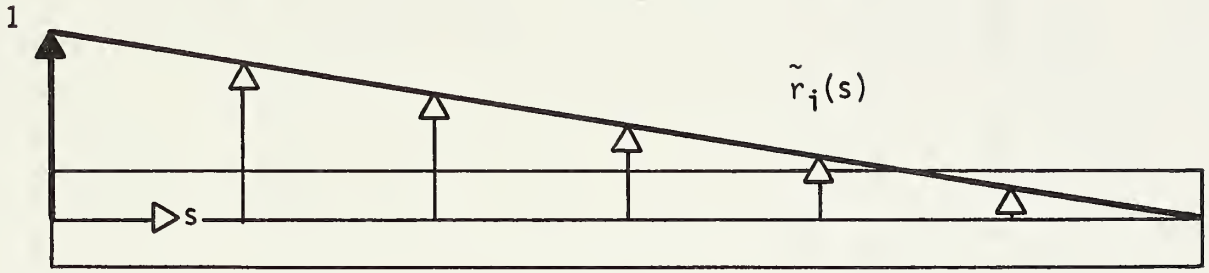

Deformed Shape Due To Unit Displacement Corresponding To R_{ij}

Figure 6.- Definition of shape functions.

left support is deformed by a unit amount which corresponds to the unknown reaction, R_{ij}. By the principle of virtual work, the total work produced by all inertial forces and reactions, when subjected to a virtual displacement δr_i, must equal zero:

$$R_{ij}\delta r_i + \int M(s)\tilde{\psi}_j(s)\cdot\tilde{r}_i(s)\delta r_i ds = 0 \qquad (34)$$

Again since δr_i is small but non-zero, it may be divided from equation (34) and so after minor rearrangement,

$$R_{ij} = -\int M(s)\tilde{r}_i(s)\cdot\tilde{\psi}_j(s)ds \qquad (35)$$

There is no relation between the number of reactions, i, and the number of assumed deformed shapes, j. Equation 35 similarly is completely valid for statically determinate or statically indeterminate structures. For statically indeterminate structures, the only difficulty arises in the computation of the $\tilde{r}_i(s)$. Because typical highway grade separation bridges rarely have many degrees of indeterminacy, this does not seem to be an insurmountable problem. In many cases these deformed shapes may be approximated with suitable accuracy.

In certain cases it may be desireable to find the <u>total</u> reaction in a certain direction due to a unit generalized acceleration in the jth direction. The principle of virtual work can again be used to advantage. For example, the total reaction in the x-direction (parallel to the recorded ground acceleration, $\ddot{U}_{xg}$) will be found. If all supports are displaced by a unit amount in the x-direction, the entire bridge will undergo a rigid body translation, without distortion, in the x-direction by a unit amount. This rigid body translation can be described by the vector function $\tilde{r}(s) = \tilde{i}$, where $\tilde{i}$ is a unit vector in the x-direction.

Again, the inertial force per unit length of bridge due to a unit generalized acceleration in the jth direction is

$$\tilde{F}_j(s) = M(s)\tilde{\psi}_j(s) \tag{36}$$

By the principle of virtual work, the total work produced by all inertial forces and reactions must equal zero when subjected to a virtual displacement. In calculating the total reactive force in the x-direction it is convenient to let the virtual displacement be a virtual rigid body translation in the x-direction.

$$\delta\tilde{r}_x(s) = \tilde{r}_x(s)\delta r_x = \tilde{i}\delta r_x \tag{37}$$

Therefore, the total work produced by all forces acting on the bridge is

$$(R_{1jx}\delta r_x + R_{2jx}\delta r_x + \ldots + R_{mjx}\delta r_x) + \int M(s)\tilde{\psi}_j(s)\cdot\tilde{i}\delta r_x ds = 0 \tag{38}$$

where there are assumed to be m reactions and R_{ij} is the ith reaction in the x-direction due to a unit generalized acceleration in the jth direction. The total reaction in the x-direction due to a unit generalized acceleration in the jth direction is given by

$$R_{tjx} = R_{1jx} + R_{2jx} + \cdot\cdot + R_{mjx}. \tag{39}$$

Then

$$R_{tjx}\delta r_x + \int M(s)\tilde{\psi}_j(s)\cdot \tilde{i}\delta r_x ds = 0 \tag{40}$$

and hence

$$R_{tjx} = -\int M(s)\tilde{\psi}_j(s) \cdot \tilde{i}\, ds \tag{41}$$

Similarly for $\tilde{j}$ and $\tilde{k}$ unit vectors in the y- and z-directions, the total reactive forces in those two directions respectively due to a unit generalized acceleration in the jth direction are

$$R_{tjy} = -\int M(s)\tilde{\psi}_j(s) \cdot \tilde{j}\, ds \tag{42}$$

and

$$R_{tjz} = -\int M(s)\tilde{\psi}_j(s) \cdot \tilde{k}\, ds \tag{43}$$

In addition to the reactions produced by the unit generalized accelerations, there are reactions due to unit rigid body translations in the $\ddot{U}_{xg}(t)$, $\ddot{U}_{yg}(t)$, and $\ddot{U}_{zg}(t)$ directions. The inertial forces per unit

length of bridge, produced by unit ground accelerations $\ddot{U}_{xg}(t) = 1$, $\ddot{U}_{yg}(t) = 1$, and $\ddot{U}_{zg}(t) = 1$ are respectively

$$\tilde{F}_x(s) = M(s)\tilde{i} \tag{44}$$

$$\tilde{F}_y(s) = M(s)\tilde{j} \tag{45}$$

$$\tilde{F}_z(s) = M(s)\tilde{k} \tag{46}$$

Following the logic used in the computation of the reaction R_{ij}, the ith reactions due to unit rigid body accelerations in the $\ddot{U}_{xg}(t)$, $\ddot{U}_{yg}(t)$, and $\ddot{U}_{zg}(t)$ directions are respectively

$$R_{ix} = -\int M(s)\tilde{i}\cdot\tilde{r}_i(s)ds \tag{47}$$

$$R_{iy} = -\int M(s)\tilde{j}\cdot\tilde{r}_i(s)ds \tag{48}$$

and

$$R_{iz} = -\int M(s)\tilde{k}\cdot\tilde{r}_i(s)ds \tag{49}$$

It is often advantageous to know the total reaction of a rigid body response to a unit ground acceleration. Following the logic used to derive the previous reaction equations, and for $\tilde{i}\cdot\tilde{i} = 1$, the total reaction in the x-direction of a rigid body response to $\ddot{U}_{xg} = 1$ is

$$R_{tx} = -\int M(s)ds \tag{50}$$

Similarly the total rigid body reactions in the y- and z-directions due to unit accelerations $\ddot{U}_{yg} = 1$ and $\ddot{U}_{zg} = 1$ respectively are

$$R_{ty} = -\int M(s)ds \tag{51}$$

$$R_{tz} = -\int M(s)ds \tag{52}$$

Total rigid body reactions normal to the direction of the ground acceleration will obviously be zero.

For any instant in time, the total ith reaction must include all of the effects from the n generalized coordinates and the three rigid body ground translations. Specifically,

$$R_i(t) = R_{i1}\ddot{\alpha}_1(t) + \ldots + R_{in}\ddot{\alpha}_n(t) + R_{ix}\ddot{U}_{xg}(t) + R_{iy}\ddot{U}_{yg}(t) + R_{iz}\ddot{U}_{zg}(t) \tag{53}$$

Once the distribution of inertial forces over the entire bridge and all reactions have been found, the entire force field on the complete bridge, isolated as a rigid body, is known. These forces are found using equations 25 and 31 if bridge distortions are described using physical coordinates, or equations 28 and 53 if bridge distortions are described using generalized coordinates (or normal coordinates if $\tilde{\phi}_i(s)$ is substituted for $\tilde{\psi}_i(s)$, and $\eta_i(t)$ for $\alpha_i(t)$). Since most bridges can be modeled as a composition of one-dimensional elements, all internal actions acting on the bridge can be computed from statics alone, knowing the reactions and the distribution of inertial loads. Specifically, for the free-body shown in figure 7, the internal forces N_x, V_y, and V_z and internal moments M_x, M_y, and M_z may readily be found from the six equations of equilibrium on the free-body. The reader should note that in most cases, distributions of forces throughout a bridge should be computed using generalized or normal coordinates, rather than physical coordinates and a lumped-mass model, unless many masses spaced closely together are used in the latter.

Finding a maximum reaction, or a maximum internal action, may require a trial and error approach. In general, however, the time where the maximum occurred should be easy to determine. The accelerations can be measured in intervals throughout this region and tabulated in a systematic manner. Reactions or internal actions can then be computed in a standardized manner, and the maxima can easily be identified. These procedures are demonstrated in the example analyses.

C. Identification of the Mathematical Model from Strong-Motion Records

At best, only a portion of the mathematical model can be expected to be identified by visual analysis of the strong-motion records. It is most

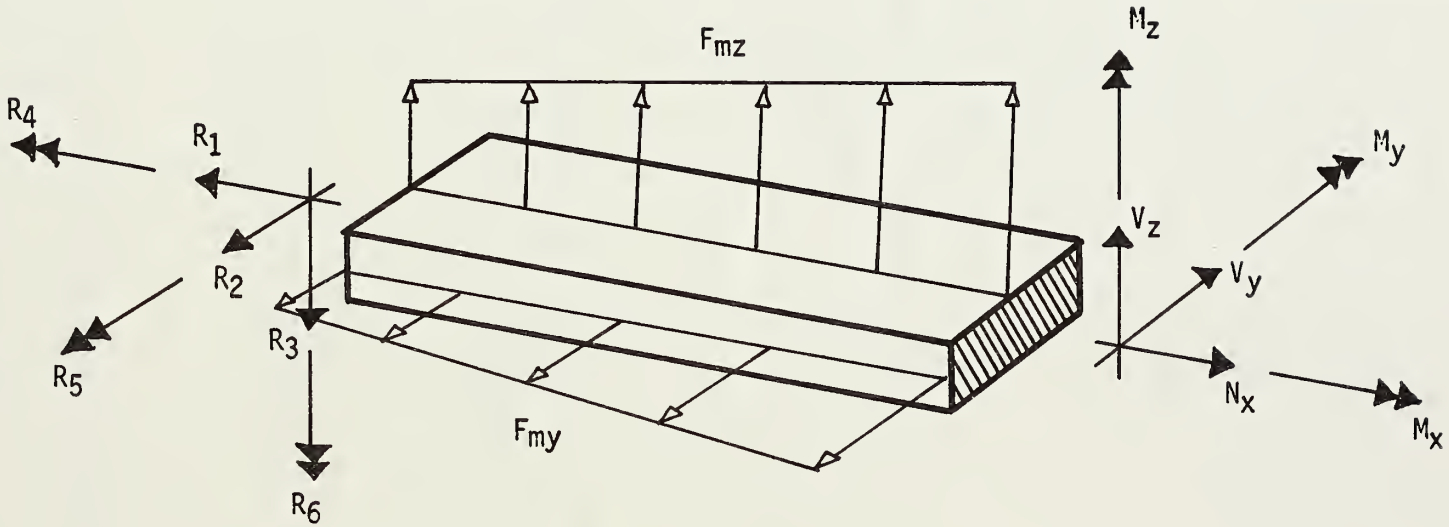

Figure 7.- Internal actions on bridge deck.

reasonable to obtain model properties in normal coordinates. In normal coordinates each mode of vibration is characterized by the equation

$$\ddot{\eta}_i+2\xi_i\omega_i\dot{\eta}_i+\omega_i^2\eta_i = -\gamma_{xi}\ddot{U}_{xg}-\gamma_{yi}\ddot{U}_{yg}-\gamma_{zi}\ddot{U}_{zg} \tag{54}$$

where

ω_i = natural circular frequency of vibration

ξ_i = viscous damping ratio

$\gamma_{xi},\gamma_{yi},\gamma_{zi}$ = participation factors

The total relative displacement vector is a combination of modal responses

$$\tilde{u}(s,t) = \tilde{\phi}_1(s)\eta_1(t)+\tilde{\phi}_2(s)\eta_2(t)+\cdots+\tilde{\phi}_n(s)\eta_n(t) \tag{55}$$

where the $\tilde{\phi}_i(s)$ are the normal modes of vibration. For ideal data we can expect to obtain only a few natural frequencies, ω_i, corresponding mode shapes, $\tilde{\phi}_i(s)$, and corresponding participation factors, γ_{xi},γ_{yi}, and γ_{zi}. Little information about the damping ratios can be expected to be found without some computational effort on a digital computer. Even this small amount of information gained may be significant. A brief discussion of the behavior of lightly damped bridges will demonstrate this.

Motions of bridges that behave in a linear manner can be described as the sum of n independent normal mode motions (equation 55). If the ground vibrated continuously with a frequency equal to one of the natural frequencies of the bridge, ω_i, the well-known phenomenon of resonance would occur; namely, the bridge would vibrate in that mode with an amplitude of motion many times greater than the ground motion. Naturally occurring earthquakes do not vibrate at constant frequencies for any appreciable length of time, but have vibrational energy at many frequencies with amplitudes varying with time. Since the ground motion is not steady, resonance will not occur, but amplified response motions at the natural

frequencies generally will occur. Not all modes of vibration will be excited to great amplitudes; usually only the first few or at least those with model frequencies matched by the frequency content of the earthquake's energy. It follows that, even for a very large value of n, the total bridge distortion often may be well approximated by a truncated sum, such as:

$$\tilde{u}(s,t) = \tilde{\phi}_1(s)\alpha_1(t)+\tilde{\phi}_2(s)\alpha_2(t)+\tilde{\phi}_3(s)\alpha_3(t)+\varepsilon \qquad (56)$$

where ε represents insignificant higher modal distortions. If the properties of only a few significant modes of vibration are found, the significant motion of the bridge may be modeled. A general rule of thumb is that if a mode responds significantly to an earthquake, its properties may be found. The danger of using only those modes that are excited significantly by one earthquake to predict the bridge motion to a future earthquake, is that the first earthquake may not excite a particular mode of vibration that might be excited significantly by a future earthquake. It is therefore most important to have, in addition to a mathematical model deduced from the earthquake records, a mathematical model formulated from basic principles.

A mode will vibrate only at its natural frequency, ω_i, if excited at that frequency, or if allowed to vibrate freely without any input ground motion. A steady-state input motion with frequency ω will produce a steady-state modal response also at that frequency, ω, and not at the natural frequency of the mode, ω_i. Fortunately, the modal response to an earthquake is not a great deal unlike the response to a series of impulses. Between impulses vibration is free, and hence at the natural frequency ω_i. Because of the erratic arrival time of impulses (approximating an earthquake) the modal response will have varying amplitudes, but still will be predominantly at the natural frequency, ω_i. If the earthquake lasts for

a long time relative to the natural period of the mode ($T_i=2\pi/\omega_i$), then the ground-motion energy at the frequency ω_i will tend to amplify that modal response on the order of two to four times the amplitude of the ground motion at a frequency of ω_i, depending on the modal damping. If the duration of the earthquake is short, that modal response simply does not have time to be amplified to a significant level.

The accuracy of the modal properties found depends upon how large the bridge distortions are relative to the ground motion. Accelerometers measure absolute acceleration. If the bridge response is identical to the ground motion, there are no bridge distortions, and nothing can be learned about the specifics of the dynamic mathematical model. However, significant results may still be obtained for purposes of design. If there are no bridge distortions there is no dynamic amplification, implying that an equivalent <u>static</u> model may be used to model the earthquake behavior for this bridge. Reactions may be computed directly from the equations, repeated here,

$$R_{ix} = -\int M(s)\tilde{r}_i(s)\cdot\tilde{i}ds \tag{57}$$

$$R_{iy} = -\int M(s)\tilde{r}_i(s)\cdot\tilde{j}ds \tag{58}$$

$$R_{ix} = -\int M(s)\tilde{r}_i(s)\cdot\tilde{k}ds \tag{59}$$

and used to find any internal actions as outlined previously. If, on the other hand, the bridge distortions are significant, mode shapes, natural frequencies, and participation factors may be found as outlined below.

Often it can be assumed, if the relative response is large with respect to the ground motion, that the relative response is approximately equal to the absolute response, especially at the dominant natural frequencies. This assumption will be made for this example.

Dominant frequencies of motion are first identified and assumed to equal natural frequencies of the bridge. It is important to check the ground motion to make sure that the dominant frequencies observed in the response are not simply ground motions transmitted without amplification to the bridge. For the example traces shown in figure 8, two dominant frequencies of motion exist having frequencies $\omega_1=2\pi/T_1$ and $\omega_2=2\pi/T_2$. Note that if motions having a few dominant frequencies do not occur consistently throughout all traces, the bridge is not likely to be responding significantly in its natural modes of vibration. In this example the first two periods of vibration are estimated from a single period of vibration each. Errors are generally minimized if periods are measured from as many cycles of motion as possible. In figure 8, the solid lines represent recorded motions, including all modal responses whereas the dashed lines have been drawn as estimates of the first mode of response (lowest frequency mode).

Mode shapes are obtained by comparing the relative amplitudes of the modal responses for one instant in time. Usually that time is taken at a modal peak to minimize errors. At time t_1 (corresponding to a peak in the lowest frequency mode) the relative responses for traces 1, 2, and 3 are 2.0, 3.0, and 2.0, respectively. These are shown plotted on a plan of the bridge in figure 9 from which the continuous normal mode shape $\tilde{\phi}_1(s)$ can be estimated. Since mode shapes depict relative displacements, any convenient scale may be used. For instance, instead of the values 2.0, 3.0, 2.0 the values 10, 15, 10; 0.667, 1.000, 0.667; or any other scale multiple may be used. Once chosen they must remain unchanged for the rest of the analysis.

Similarly, at time t_2 the second modal peak values <u>relative</u> to the fundamental mode response may be measured as 1.0, 0.0, -1.0 for traces 1, 2,

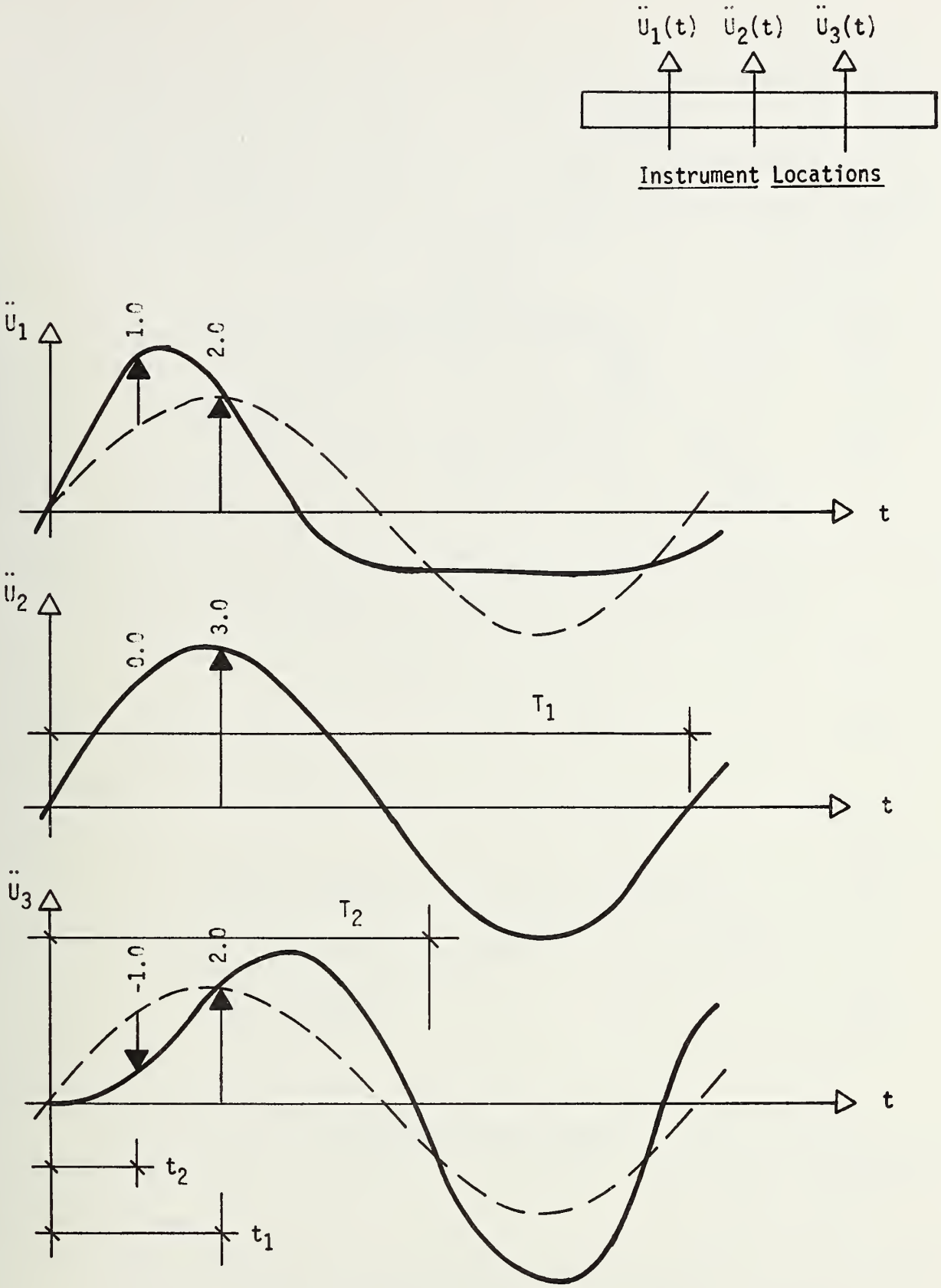

Figure 8.- Example accelerations.

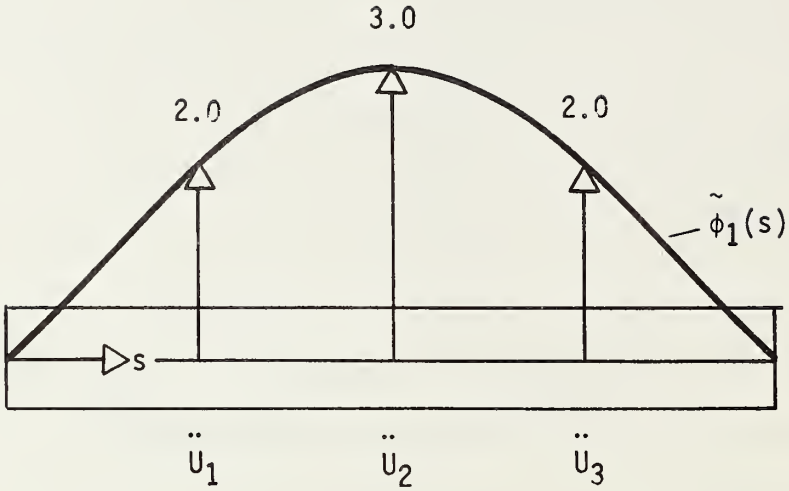

First Mode Of Vibration

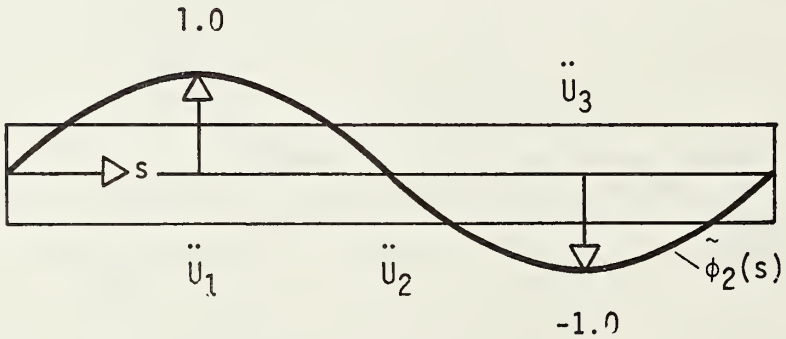

Second Mode Of Vibration

Figure 9.- Natural modes of vibration.

and 3 respectively. These values are plotted and shown in figure 9, from which the continuous mode shape $\tilde{\phi}_2(s)$ can be estimated.

Assuming the mass distribution of the bridge to be known, the participation factors may be computed from equations 12 through 15, expanded here:

$$\gamma_{xi} = \int M(s)\tilde{\phi}_i(s)\cdot\tilde{i}ds/\int M(s)\tilde{\phi}_i(s)\cdot\tilde{\phi}_i(s)ds \tag{60}$$

$$\gamma_{yi} = \int M(s)\tilde{\phi}_i(s)\cdot\tilde{j}ds/\int M(s)\tilde{\phi}_i(s)\cdot\tilde{\phi}_i(s)ds \tag{61}$$

$$\gamma_{zi} = \int M(s)\tilde{\phi}_i(s)\cdot\tilde{k}ds/\int M(s)\tilde{\phi}_i(s)\cdot\tilde{\phi}_i(s)ds \tag{62}$$

If in the above example $\tilde{i}$ is the unit vector in the direction of s; $\tilde{j}$, perpendicular to s in the plane of the paper; and $\tilde{k}$, directed vertically out of the paper, then the estimated mode shapes can be rewritten as

$$\tilde{\phi}_1(s) = \phi_1(s)\tilde{j} \tag{63}$$

$$\tilde{\phi}_2(s) = \phi_2(s)\tilde{j} \tag{64}$$

Because $\tilde{i}\cdot\tilde{j} = \tilde{i}\cdot\tilde{k} = \tilde{j}\cdot\tilde{k} = 0$ then

$$\gamma_{x1} = \gamma_{x2} = 0 \tag{65}$$

$$\gamma_{y1} = \int M(s)\phi_1(s)ds/\int M(s)\phi_1{}^2(s)ds \tag{66}$$

$$\gamma_{y2} = \int M(s)\phi_2(s)ds/\int M(s)\phi_2{}^2(s)ds \tag{67}$$

$$\gamma_{z1} = \gamma_{z2} = 0 \tag{68}$$

where the integrals no longer contain vector functions.

The damping ratios ξ_1 and ξ_2 cannot be obtained visually from the induced vibrations as sketched. Only in certain circumstances can damping ratios be obtained.

If response spectra (Clough and Penzien, 1975; Newmark and Rosenblueth, 1971; Wiegel, 1970) are published for the earthquake and the site in

question (or if published spectra are assumed to be valid for the site) then modal damping ratios may be found by comparing measured peak modal accelerations to peak values for various damping ratios. The damping ratio at which the two peak modal responses coincide, is assumed to equal the actual modal damping ratio.

Specifically, a response spectrum is a collection of points, each one of which is the peak response of a simple oscillator governed by the equation of motion with parameters ω and ξ

$$\ddot{y}+2\xi\omega\dot{y}+\omega^2 y = -\ddot{U}_{xg} \text{ (or } \ddot{U}_{yg} \text{ or } \ddot{U}_{zg}) \tag{69}$$

subjected to the single ground motion input. A typical set of response spectra for a single ground motion is shown in figure 10. If the modal response is excited by a single component of the ground motion, as in this example, then the damping ratios can be found as follows. Let $\ddot{\eta}_{1\ max}$ and $\ddot{\eta}_{2\ max}$ be the maximum modal accelerations measured, corresponding to the mode shapes $\tilde{\phi}_1(s)$ and $\tilde{\phi}_2(s)$. The maximum corresponding, simple oscillator responses are

$$S_a(\omega_1) = \ddot{\eta}_{1\ max}/\gamma_{yi} \tag{70}$$

$$S_a(\omega_2) = \ddot{\eta}_{2\ max}/\gamma_{y2} \tag{71}$$

By comparing these spectral values measured to the spectral values computed at frequencies ω_1 and ω_2 it can be deduced that the modal damping ratios are

$$\xi_1 = 0.05 \text{ (5\%)}$$

$$\xi_2 = 0.03 \text{ (3\%)}$$

If the modal responses are the result of multiple ground motion inputs (more than one non-zero participation factor) then the response spectrum method of determining modal damping ratios cannot be used.

It should be noted that response spectra cannot be computed easily

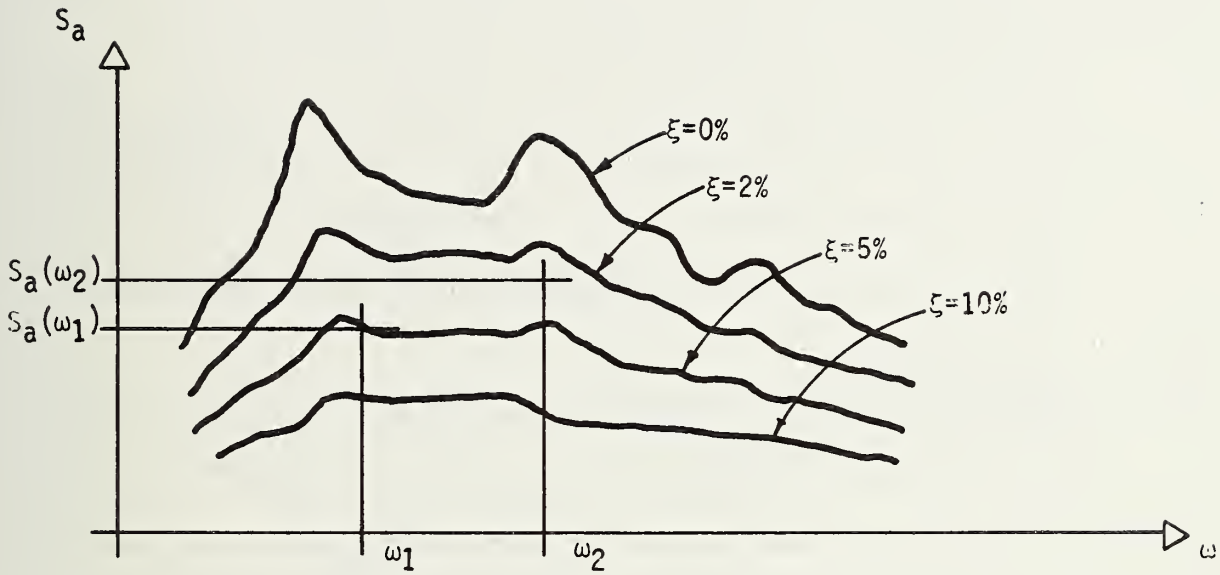

Figure 10.- Response spectrum for $\ddot{U}_{yg}$.

without the aid of a digital computer. If a response spectrum is not published by others from nearby ground motions, it is not reasonable to pursue this analysis approach. If the traces are digitized in order that a response spectrum be computed, general computer aided methods of analysis of the strong-motion records (described in the next section) preferably may be used to obtain modal properties.

A second method of obtaining damping ratios visually from analog records is possible if there exists a distinct free-vibration portion of the response at the end of the record. For some earthquakes, particularly near the source, the ground motion ceases shortly after it begins. If at that time of cessation, the relative bridge response is significant, it will continue to vibrate freely until all kinetic energy is dissipated by the damping mechanisms. One of several possible modal free vibrations is sketched in figure 11.

The envelope of a viscously damped free vibration, shown by the dashed line, is given in terms of the frequency and damping ratio by $e^{-\xi\omega t}$ (Clough and Penzien, 1975). For C equal to some constant, the ratio of peak modal amplitudes at the times t and t+nT is

$$\frac{\eta(t)}{\eta(t+nT)} = \frac{Ce^{-\xi\omega t}}{Ce^{-\xi\omega(t+nT)}} \tag{72}$$

$$= \frac{e^{-\xi\omega t}}{e^{-\xi\omega t}e^{-\xi\omega nT}} = e^{\xi\omega nt} \tag{73}$$

If natural logarithms are taken of this ratio then

$$\ln(\eta(t)/\eta(t+nT)) = \xi\omega nT \tag{74}$$

or finally

$$\xi = \frac{1}{2\pi n}\ln(\eta(t)/\eta(t+nT)) \tag{75}$$

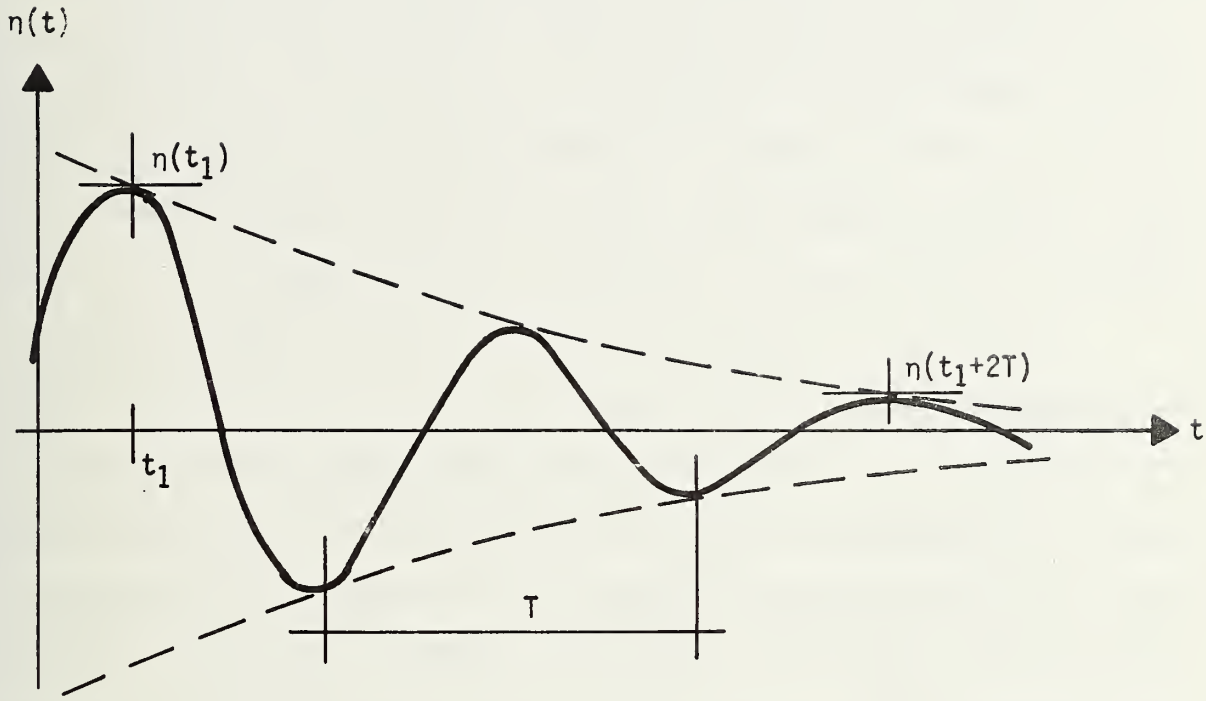

Figure 11.- Example free vibration.

for $T = 2\pi/\omega$. Unfortunately, the ground motion often continues to be significant for a sufficient length of time so that no distinct free-vibration portion of the record exists. It may be advisable to test the bridge to find these modal damping ratios. The bridge may be perturbed to produce a free vibration by a heavy truck stopping abruptly on the bridge, or if convenient it may be pulled and released by a tractor (Douglas, 1976; Newmark and Rosenblueth, 1971; Wiegel, 1970). In both cases the free vibrations recorded may be analyzed by the method outlined above.

It should be noted that force levels throughout the bridge may be obtained using normal modes and normal coordinates exactly as outlined in the beginning of this section. In place of the assumed deflected shapes $\tilde{\psi}_i(s)$, the normal modes $\tilde{\phi}_i(s)$ are used. Similarly, in place of the coordinates $\alpha_i(t)$, the normal coordinates $\eta_i(t)$ are used.

D. Example Analyses

In this section, hypothetical strong-motion records for two bridge designs will be analyzed. For both examples, absolute bridge accelerations have been generated theoretically (using the finite-element program SAP IV (Bathe, Wilson, and Peterson, 1973)) from actual recorded ground motions at the D. Johnson Ranch, Oroville, Calif. on 6 August 1975 (Sherburne and Hauge, 1975). These theoretically generated acceleration traces are then analyzed as if they had been recorded as raw data.

For both examples, force levels are found as well as the dynamic response characteristics. The two examples include a bridge of three simple spans, and a continuous two-span bridge. As will become evident, the motion of a simple continuous two-span bridge is very complex. Although it is entirely feasible, it is impractical to analyze more complex bridges

visually from analog records in as systematic a manner as is done for these two examples.

Three-Span Simply-Supported Bridge - The subject bridge and the strong-motion instrument locations are shown in figure 12. The absolute accelerations recorded, corresponding to the instrument locations, are

$\ddot{U}_{xg}, \ddot{U}_{yg}, \ddot{U}_{zg}$	ground accelerations
$\ddot{U}_1, \ddot{U}_2, \ddot{U}_3$	structure accelerations

Because of symmetry, the two lateral pier cap motions are assumed to be identical so only one need be recorded. Shown in figure 13 are the three recorded ground motions, and in figure 14 the three hypothetical structure motions $\ddot{U}_1$, $\ddot{U}_2$, and $\ddot{U}_3$.

Before the traces can be analyzed, some assumptions regarding the bridge behavior must be made. It is assumed that the three deck elements behave as rigid plates, restrained longitudinally at one end, and restrained vertically and laterally at both ends. It is expected that vertical flexural motions will exist, but they cannot be identified with the instrumentation shown on figure 12. It is also assumed that the vertical flexural motions are uncoupled from the lateral and longitudinal motions to be analyzed. Torsional motions about the bridge centerline axis are also ignored for the following two reasons. First, torsional components of the ground motion are not likely to be large. And second, secondary torsional motions of the bridge deck due to lateral translations will not be excited at the bents because the pair of columns at each bent prevents the pier cap from rotating about the centerline axis. Although the lateral and longitudinal ground motions are recorded at a single point only, it is assumed that both abutments and all pier bases experience motions identical

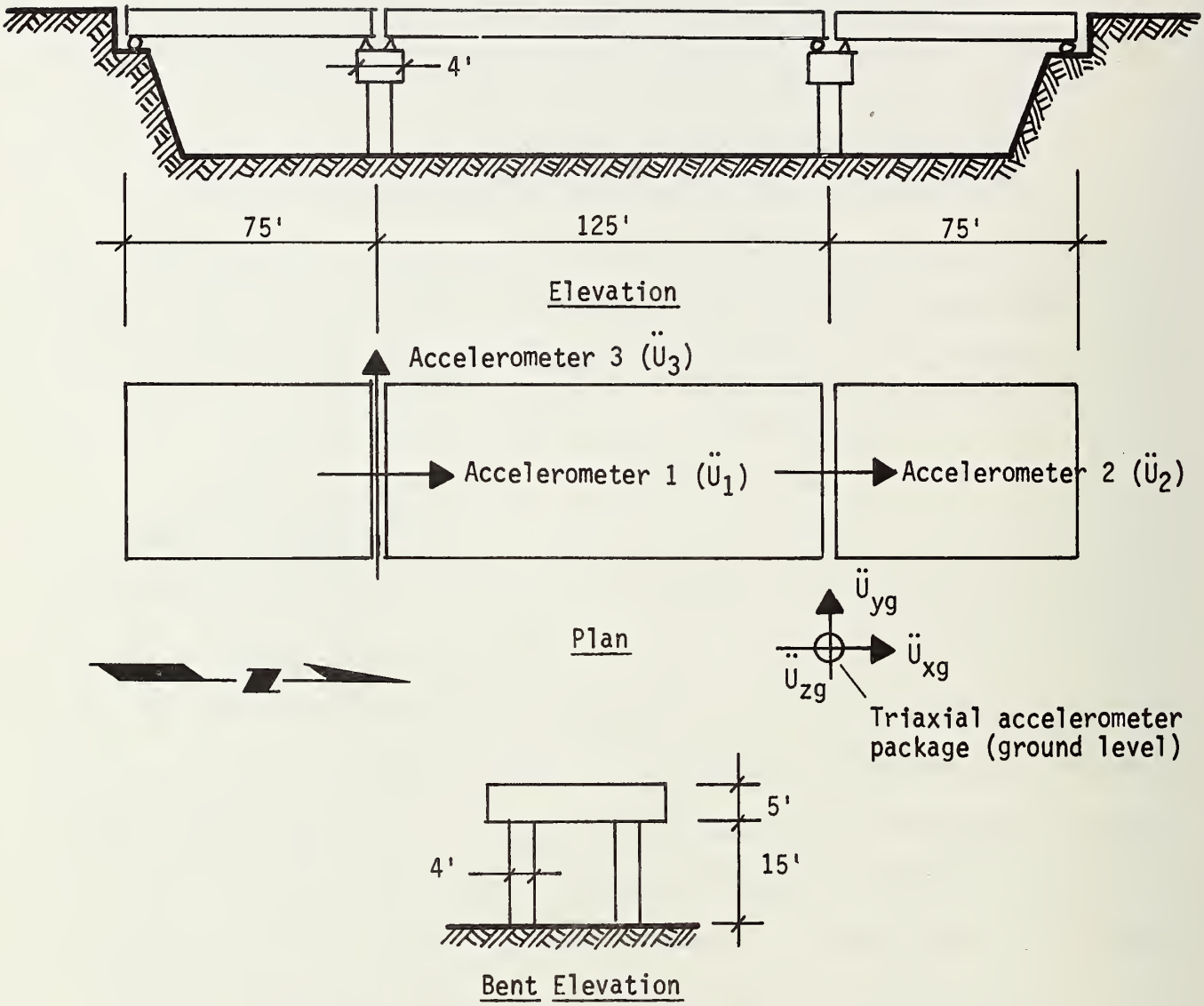

Figure 12.- Three-span simply supported bridge, geometry and strong-motion instrumentation.

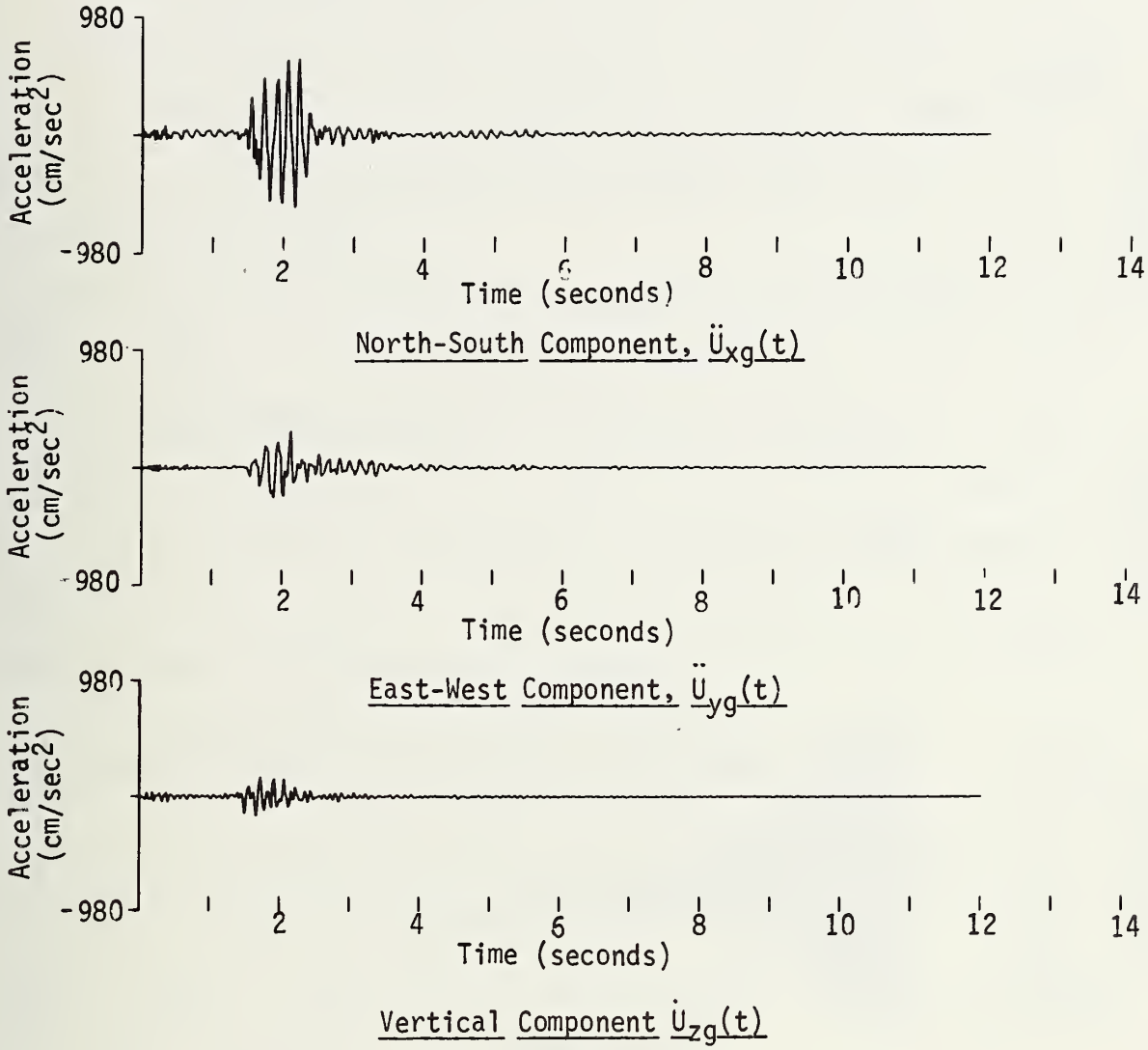

Figure 13.- August 6, 1975 earthquake aftershock ground motion recorded at the D. Johnson Ranch, Oroville, Calif.

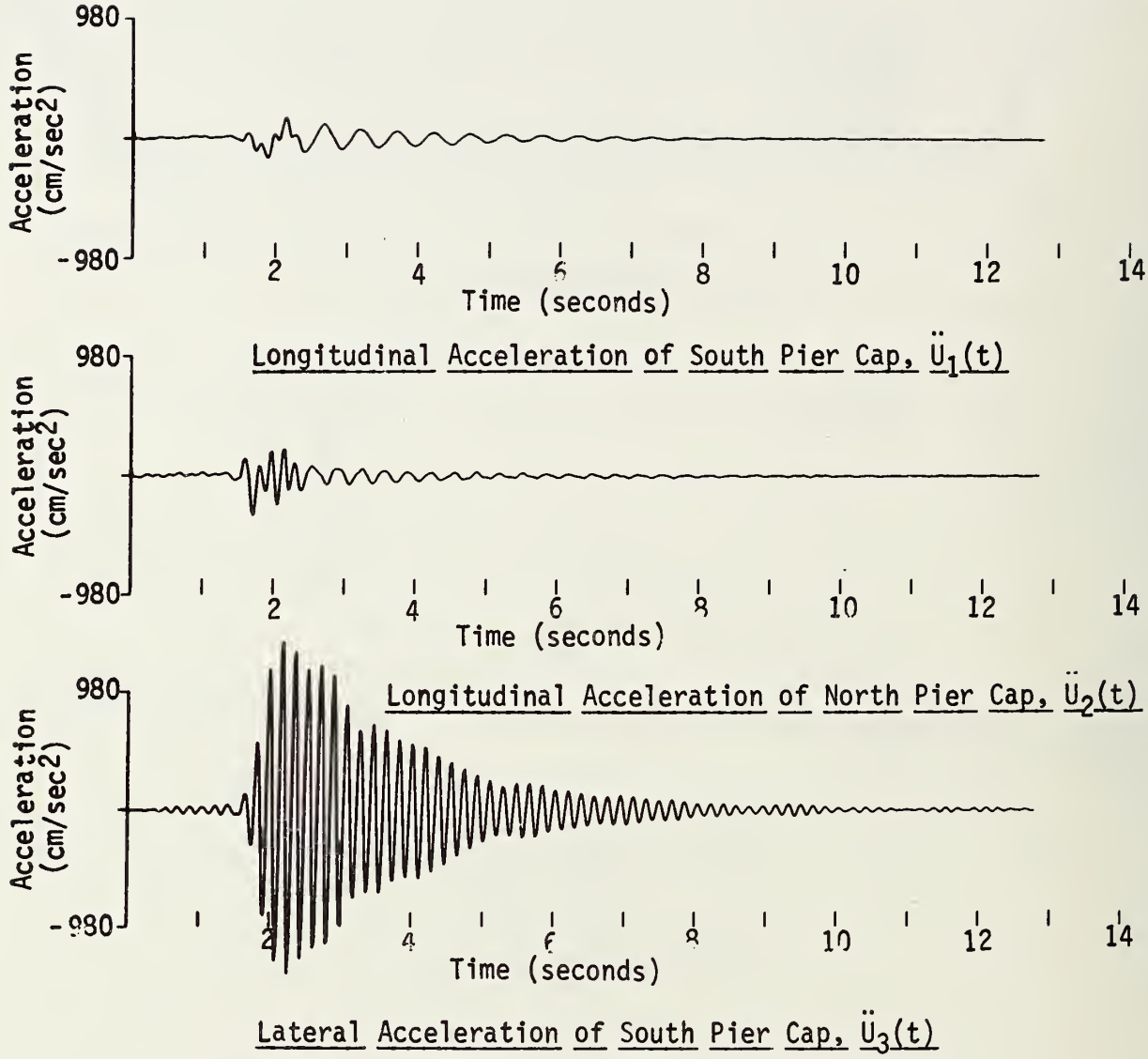

Figure 14.- Three-span simply supported bridge, structure motions.

to those recorded.

Because of the simple and discontinuous nature of this bridge, physical coordinates are used and masses corresponding to bridge degree of freedom are assumed to be lumped at the accelerometer (and coordinate) locations. The mass of a column cap and the two columns is 3.863 kip-sec^2/ft, and the mass per foot of deck is 0.303 kip-sec^2/ft^2. The masses corresponding to each degree of freedom are shown shaded in figure 15.

(1) Maximum Force Levels

For this example the maximum force reactions experienced will be found. Since the degrees of freedom are both inertially as well as elastically uncoupled, maximum force reactions (figure 16) corresponding to each degree of freedom are found simply as the product of mass (figure 15) times the corresponding peak absolute acceleration. The reactions to be found are shown in figure 16. The mass M_{end} is used in calculating lateral and vertical reactions at the ends of the bridge.

The maximum accelerations, masses, and maximum reactions are shown on table 1. Note that the maximum reactions do not occur at the same instant but at many different times. At any given instant, all reactions and distributed inertial forces could be found in a similar manner. Then from equations of dynamic equilibrium for any free-body all internal member forces could be computed.

(2) Structural Model Parameters

Because of the simple, uncoupled behavior of this bridge, structural model parameters may be found rather easily from a hand analysis of the records.

As described in the previous section, the mathematical model is

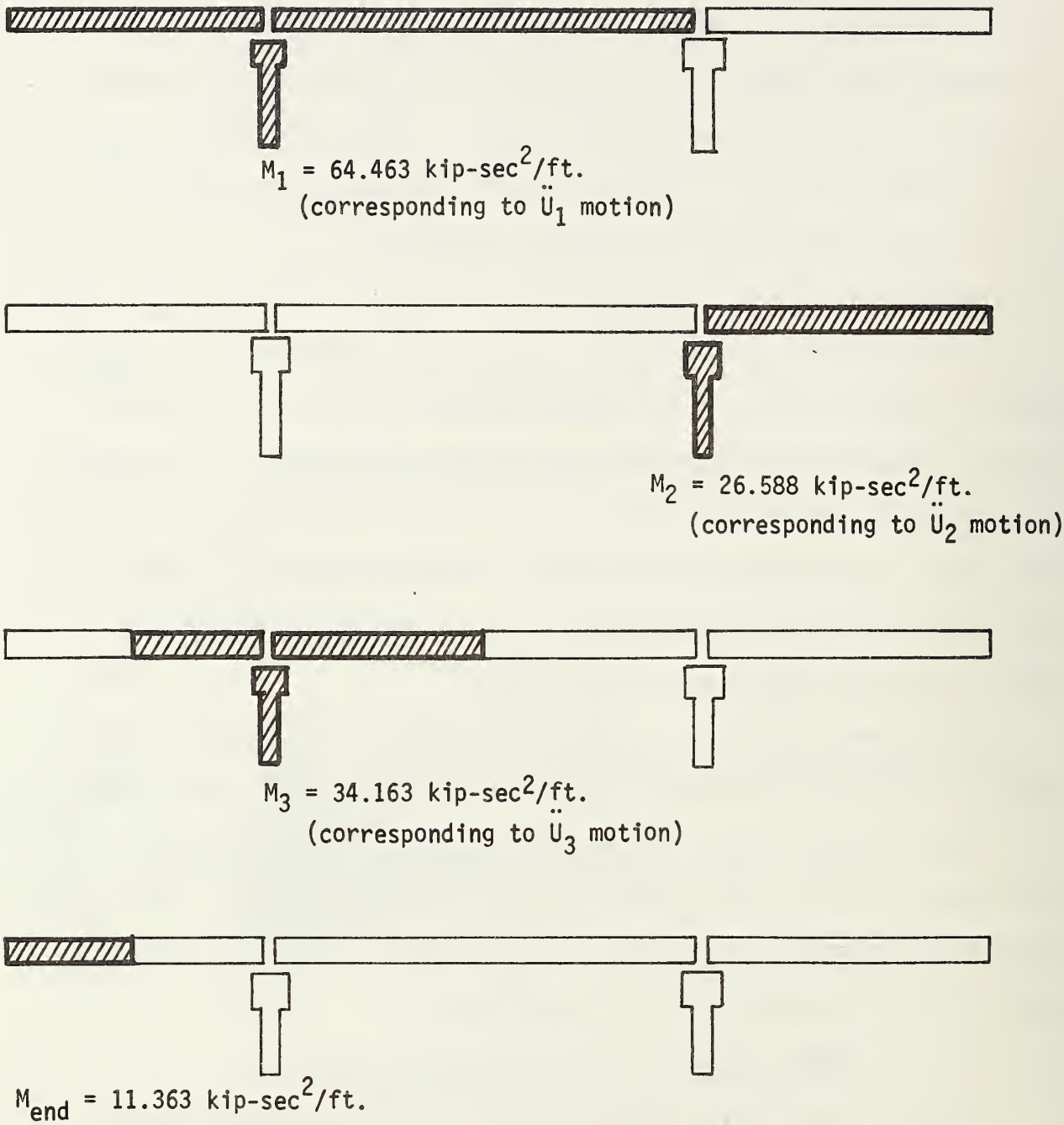

Figure 15.- Three-span simply supported bridge mass.

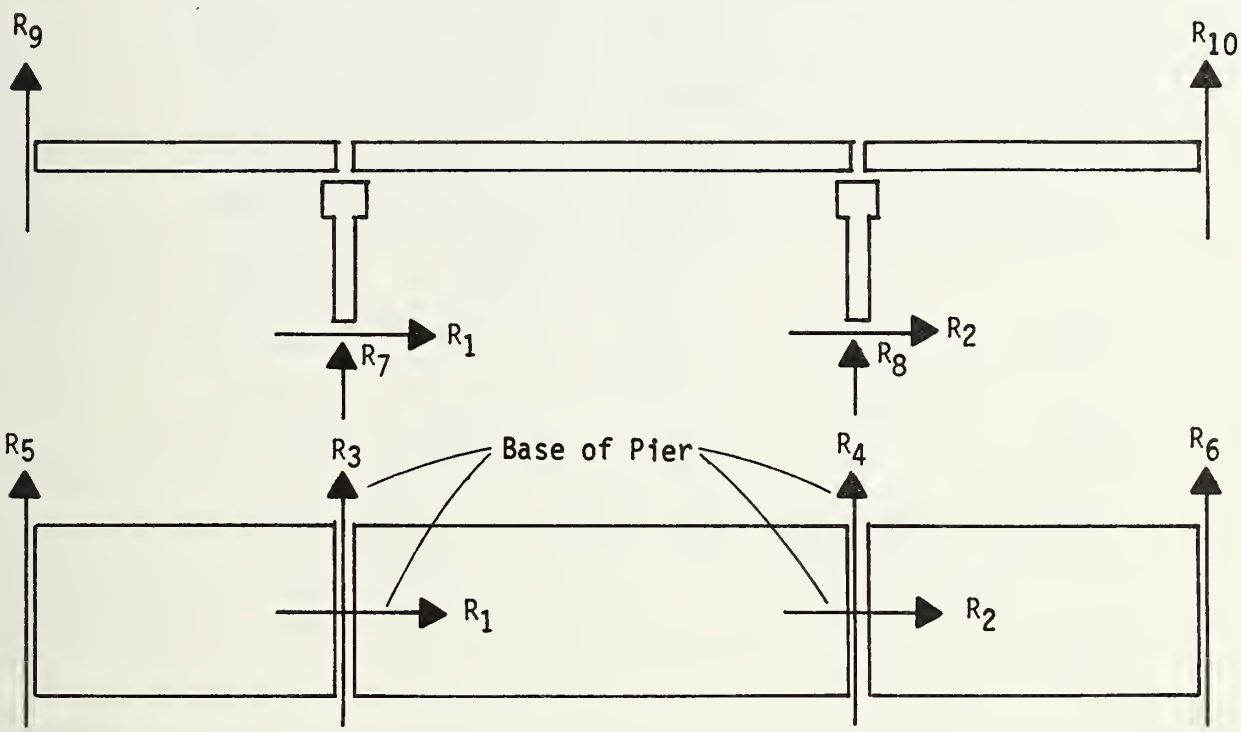

Figure 16.- Three-span simply supported bridge, unknown reactions.

Reaction	Acceleration	Max Value (fps^2)	Mass ($\frac{kip\text{-}sec^2}{ft}$)	Force (kips)
1	$\ddot{U}_1$	3.0663	64.463	197.661
2	$\ddot{U}_2$	10.634	26.588	282.742
3	$\ddot{U}_3$	45.830	34.163	1565.69
4	$\ddot{U}_3$	45.830	34.163	1565.69
5	$\ddot{U}_{yg}$	9.899	11.363	112.48
6	$\ddot{U}_{yg}$	9.899	11.363	112.48
7	$\ddot{U}_{zg}$	5.439	34.163	185.82
8	$\ddot{U}_{zg}$	5.439	34.163	185.81
9	$\ddot{U}_{zg}$	5.439	11.363	61.81
10	$\ddot{U}_{zg}$	5.439	11.363	61.81

Table 1.-Three-Span Simply Supported Bridge, Maximum Reactions

inertially uncoupled, i.e., $M_{ij} = 0$ for all $i \neq j$. Due to the expansion joints and structural symmetry of this bridge, it is obvious that the bridge also is elastically uncoupled, that is, $K_{ij} = 0$ for all $i \neq j$. It is also assumed that the bridge motions are not coupled by off-diagonal damping terms, C_{ij}. Therefore all bridge distortions may be modeled by

$$\begin{bmatrix} M_1 & 0 & 0 \\ 0 & M_2 & 0 \\ 0 & 0 & M_3 \end{bmatrix} \begin{Bmatrix} \ddot{\eta}_1 \\ \ddot{\eta}_2 \\ \ddot{\eta}_3 \end{Bmatrix} + \begin{bmatrix} C_1 & 0 & 0 \\ 0 & C_2 & 0 \\ 0 & 0 & C_3 \end{bmatrix} \begin{Bmatrix} \dot{\eta}_1 \\ \dot{\eta}_2 \\ \dot{\eta}_3 \end{Bmatrix} + \begin{bmatrix} K_1 & 0 & 0 \\ 0 & K_2 & 0 \\ 0 & 0 & K_3 \end{bmatrix} \begin{Bmatrix} \eta_1 \\ \eta_2 \\ \eta_3 \end{Bmatrix} = -\begin{Bmatrix} M_1 \\ M_2 \\ 0 \end{Bmatrix} \ddot{U}_{xg} - \begin{Bmatrix} 0 \\ 0 \\ M_3 \end{Bmatrix} \ddot{U}_{yg} \tag{76}$$

where η_i are relative modal displacements (in what are already normal coordinates) defined by

$$\eta_1(t) = U_1(t) - U_{xg}(t) \tag{77}$$

$$\eta_2(t) = U_2(t) - U_{yg}(t) \tag{78}$$

$$\eta_3(t) = U_3(t) - U_{zg}(t) \tag{79}$$

Equation (76) rearranged becomes

$$\ddot{\eta}_i + 2\xi_i\omega_i\dot{\eta}_i + \omega_i^2\eta_i = -\gamma_{xi}\ddot{U}_{xg} - \gamma_{yi}\ddot{U}_{yg} \tag{80}$$

where again

$$\omega_i = \sqrt{K_i/M_i} \tag{81}$$

and for this example

$$\xi_i = C_i/2\sqrt{K_iM_i} \tag{82}$$

and for this example

$$\gamma_{x1} = 1 \qquad \gamma_{x2} = 1 \qquad \gamma_{x3} = 0$$

$$\gamma_{y1} = 0 \qquad \gamma_{y2} = 0 \qquad \gamma_{y3} = 1$$

It is intended to find both ω_i and ξ_i from the strong-motion records; and then knowing M_i, C_i and K_i may be found from equations 81 and 82.

Figure 13 indicates that approximately 3 seconds into the earthquake, the ground motion has died out, and the bridge vibrated freely without additional significant ground motion input. Natural frequencies can simply be measured by counting the cycles in this free vibration period, and the damping can be estimated from the logarithmic decrement of the decaying records. For t>3 seconds, it is assumed that $\ddot{U}_{xg} = \ddot{U}_{yg} = 0$ so $\ddot{\eta}_i = \ddot{U}_i$ (i=1,2,3). Shown in table 2 is a summary of the frequency information obtained from figure 14. Similarly damping ratios are found by computing the logarithmic decrements for t>3 seconds. These damping ratios are summarized in table 3.

Shown in tables 2 and 3 are the actual values of ω_i and ξ_i which were used to generate these hypothetical records for this example analysis. As can be seen the natural frequencies can be found with excellent accuracy, but the damping ratios with less accuracy. The free vibration portion of these records are exceptionally clean considering that they were created from real earthquake motions. Even for these clean records, however, the damping ratio estimates are not particularly accurate. Estimating damping from less clean strong-motion records is likely to be highly inaccurate.

Since mode shapes are relations between structure displacements for a given natural mode, and since these bridge motions are naturally decoupled, no mode shapes exist as such. More precisely, in terms of displacements η_1, η_2, η_3 the mode shapes are

$$\{\phi_1\} = \begin{Bmatrix} 1 \\ 0 \\ 0 \end{Bmatrix} \qquad \{\phi_2\} = \begin{Bmatrix} 0 \\ 1 \\ 0 \end{Bmatrix} \qquad \{\phi_3\} = \begin{Bmatrix} 0 \\ 0 \\ 1 \end{Bmatrix}$$

<u>Two-Span Continuous Bridge</u> - For this example force levels and structural model parameters will be found from hand analyses from the strong-motion

Degree of Freedom	No. of cycles	Time	Period	ω_i	ω_{actual}
1	10	5.103	.510	12.313	12.236
2	14	4.600	.329	19.123	19.052
3	25	4.500	.183	34.282	33.615

Table 2.- Three-Span Simply Supported Bridge, Natural Frequencies

DOF	No. of cycles	η_{io}	η_{in}	ξ_i	$\xi_{(actual)}$
1	9	1.30	.18	0.035	0.040
2	15	6.30	1.20	0.018	0.040
3	20	21.00	2.00	0.019	0.020

Table 3.- Three-Span Simply Supported Bridge, Damping Ratios

records of a continuous two-span grade separation bridge. Hypothetical absolute accelerations have again been generated at the proposed instrument locations and again will be analyzed as if they had actually been recorded.

The bridge to be analyzed is shown schematically in figure 17. Shown in figure 18 are the instrument locations. The ground-motion time histories used are the same ones used for the previous example and are shown in figure 13. The hypothetical bridge motions which are to be analyzed are shown in figures 19, 20, and 21.

A few general assumptions are again made with regard to the expected behavior of this bridge. Although ground motions have been recorded at a single point, it has been assumed that the abutment motions and the column base motions are identical to those ground motions recorded. Furthermore, it is assumed that the vertical motion of the bridge deck directly above the central column equals the vertical ground motion. The ends of the bridge deck are free to move longitudinally, are free to rotate about a transverse axis and are free to rotate about a vertical axis, but are fixed transversely, vertically, and rotationally about a longitudinal axis. The central column is assumed to be fixed at both its top and bottom.

(1) Maximum Force Levels - For this example the maximum force reactions will again be found from a hand analysis of the hypothetical bridge motions. Those reactions sought are shown in figure 22. Because the example bridge is continuous, it is not advisable to use physical coordinates and a lumped mass model; instead it is advisable to use generalized masses and a corresponding generalized coordinate system as described Section II. Such a coordinate system can describe structure distortions accurately with relatively few coordinates.

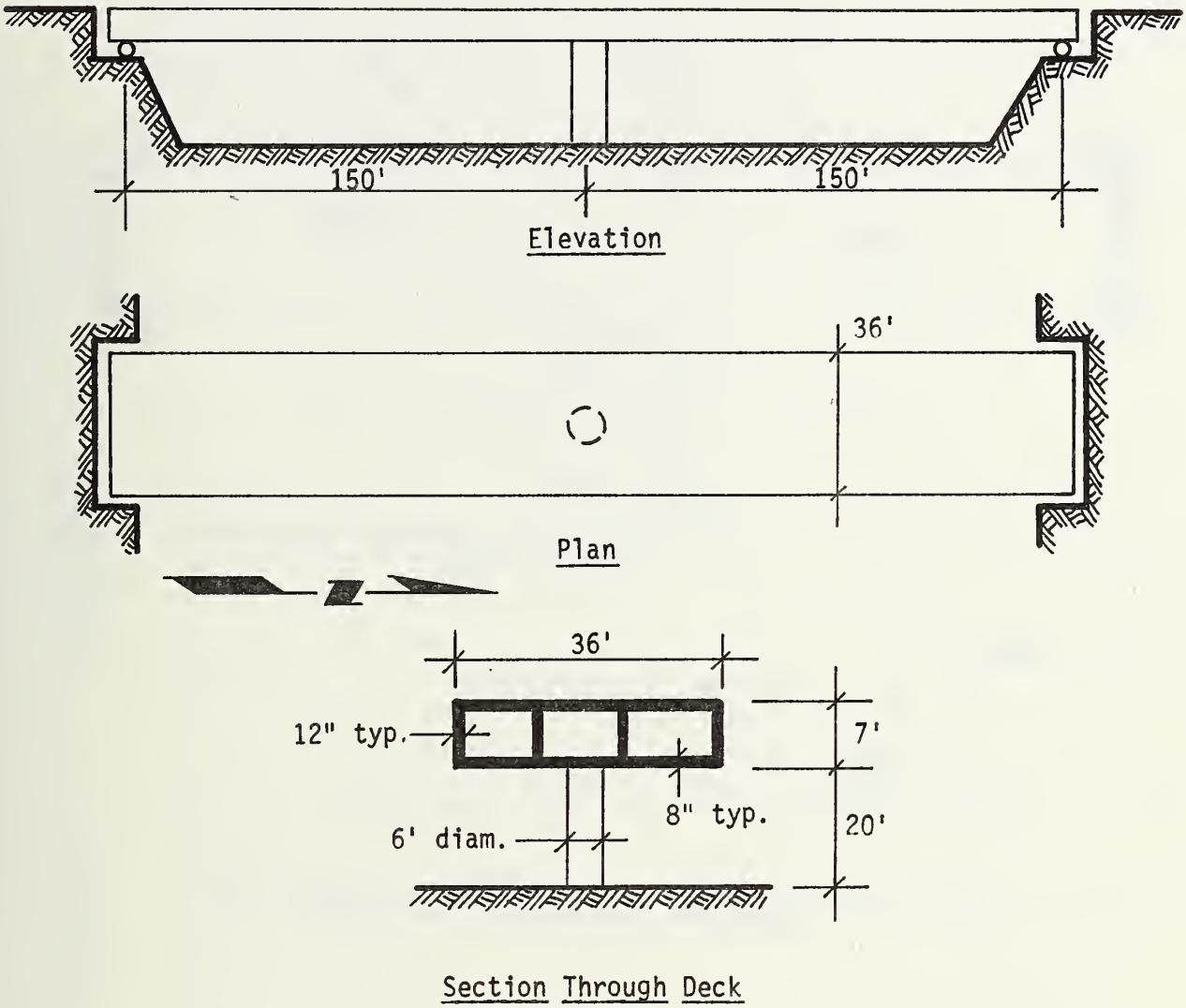

Figure 17.- Continuous two-span bridge.

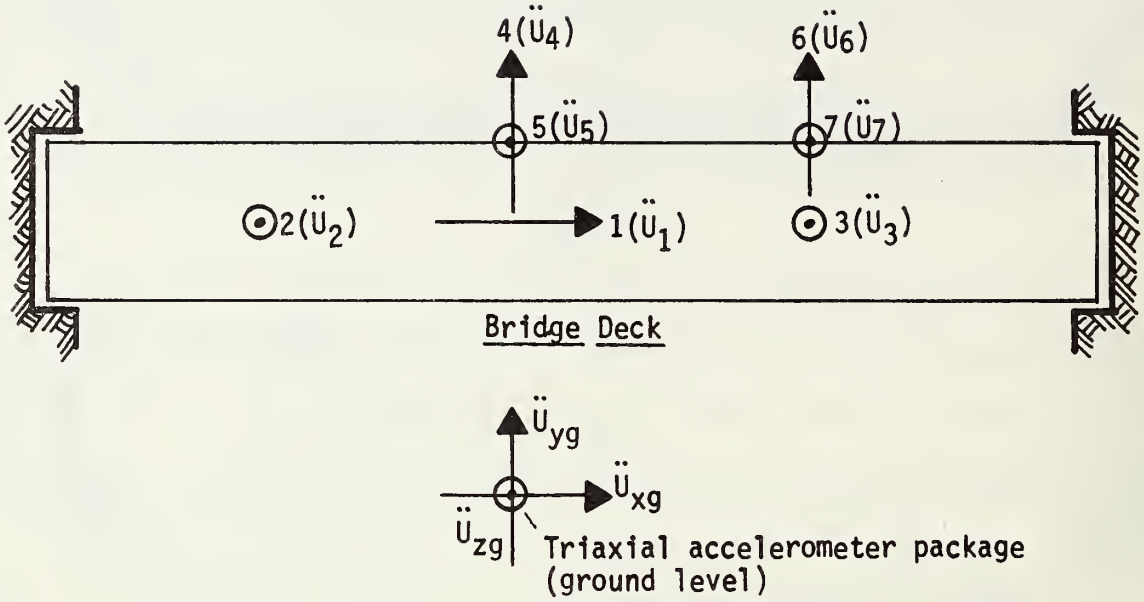

Legend:

⊙ Vertical accelerometer

→ Horizontal accelerometer

Figure 18.- Continuous two-span bridge, strong-motion instrument numbers and locations.

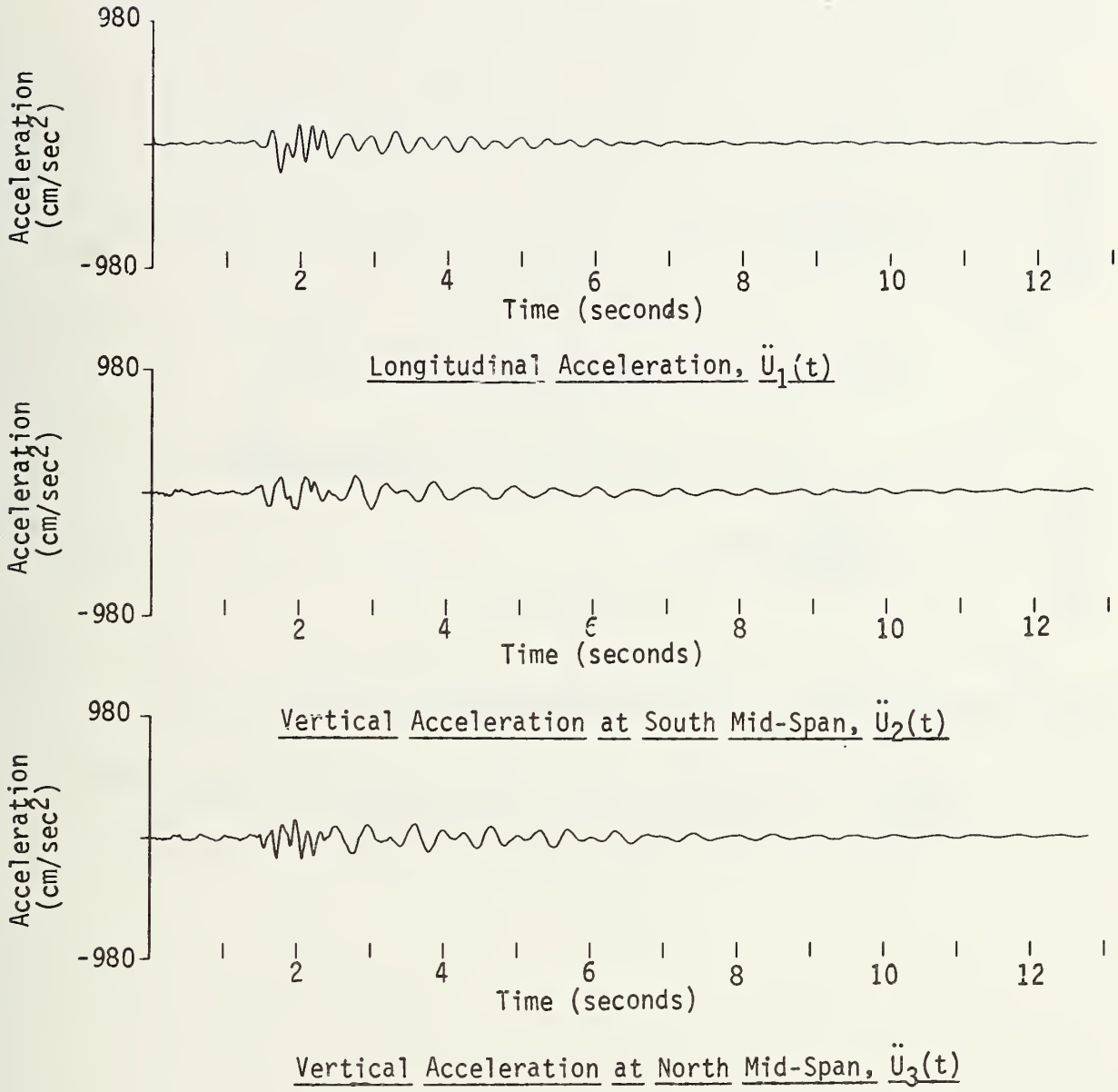

Figure 19.- Continuous two-span bridge structure motions.

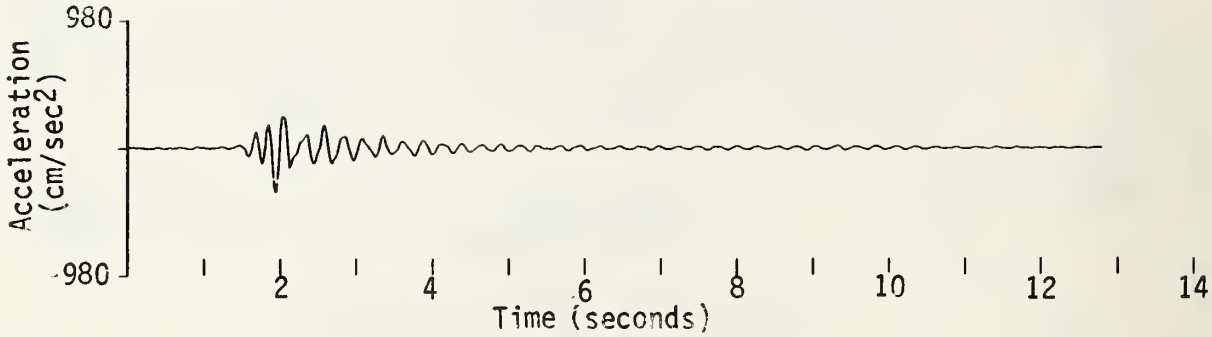

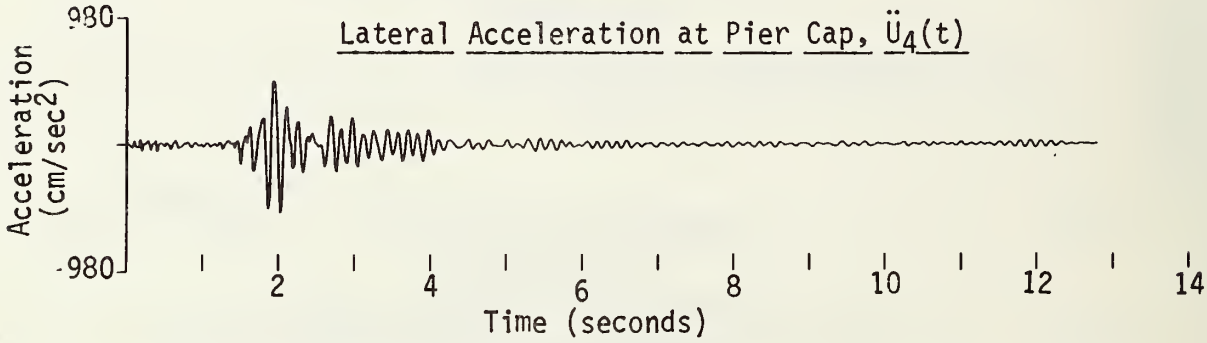

Vertical Acceleration at West Edge of Deck at Pier Cap, $\ddot{U}_5(t)$

Figure 20.- Continuous two-span bridge, structure motions.

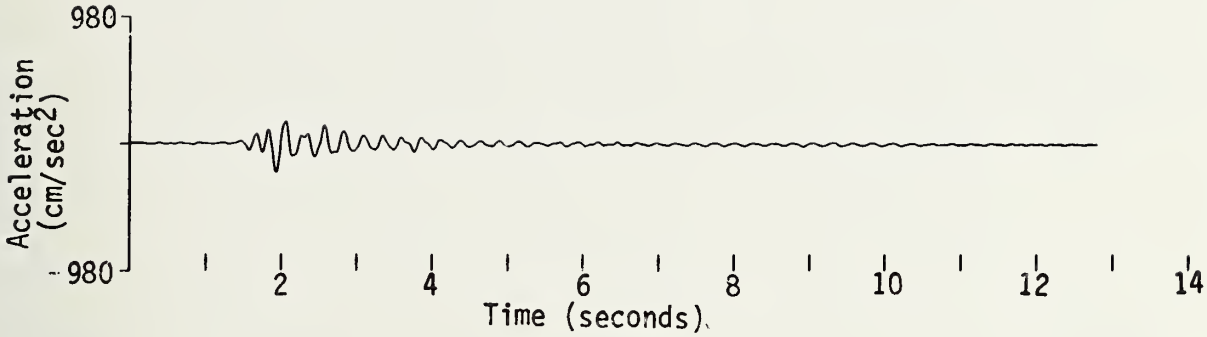

Lateral Acceleration at North Mid-Span, $\ddot{U}_6(t)$

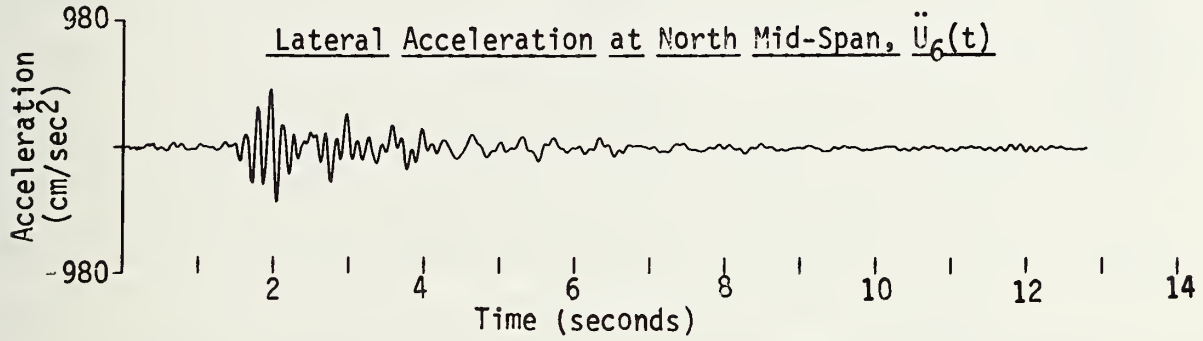

Vertical Acceleration at West Edge of Deck at North Mid-Span, $\ddot{U}_7(t)$

Figure 21.- Continuous two-span bridge structure motions.

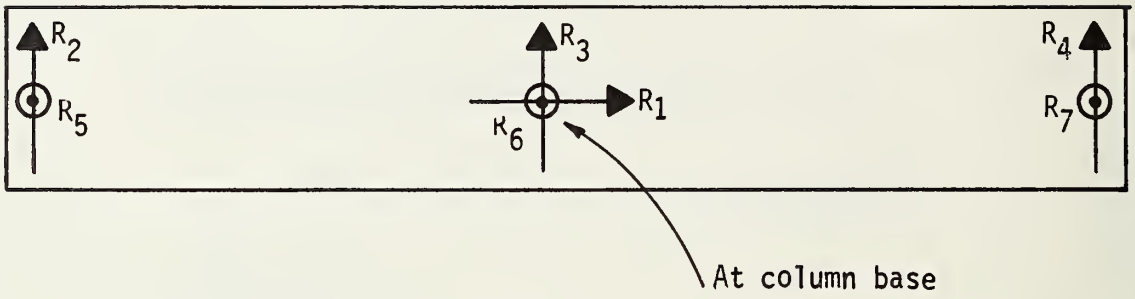

Figure 22.- Continuous two-span bridge, desired force reactions.

It is assumed that all structure distortions can be described adequately as a linear combination of the assumed distortions shown in figure 23. (Note that it is assumed that all structure motions can be described adequately as a linear combination of these assumed distortions and the rigid body translations.) The vectors $\tilde{i}$, $\tilde{j}$, and $\tilde{k}$ are unit vectors in the x-, y-, and z-directions respectively. For use in calculating reactions from the above distortions, distortions due to unit displacements corresponding to the unknown reactions must be found or assumed. Those distortions needed are shown in figure 24. In addition, for use in computing the total reactive forces in the three mutually perpendicular directions, the distortions $\tilde{r}_x(x)=\tilde{i}$, $\tilde{r}_y(x)=\tilde{j}$ and $\tilde{r}_z(x)=\tilde{k}$ are used.

Reactions to unit generalized accelerations are obtained using equation 35 and a simple numerical integration procedure. For symmetric $\tilde{\psi}_i(x)$, the central reaction is found using equation 35. Each end reaction is then found as half of the difference between the total reaction and the central reaction. For the mass per unit length of deck equal to 0.3295 kips-sec^2/ft^2, and ignoring the column mass, the force reactions to unit values 1 ft/sec^2 of the generalized accelerations are given in figure 25. Similarly reactions for unit rigid body motions are found as shown in figure 26. The reactions in figure 26 are found using equations 47, 48, and 49.

Now that all reactions due to unit generalized and rigid-body accelerations have been found, it remains to find the actual generalized and rigid-body accelerations experienced by the bridge during the hypothetical earthquake. For the calculation of maximum force levels, the recorded time histories have been expanded to show only four seconds of the strongest motion. These expanded time histories are shown in figures 27, 28, 29, and 30.

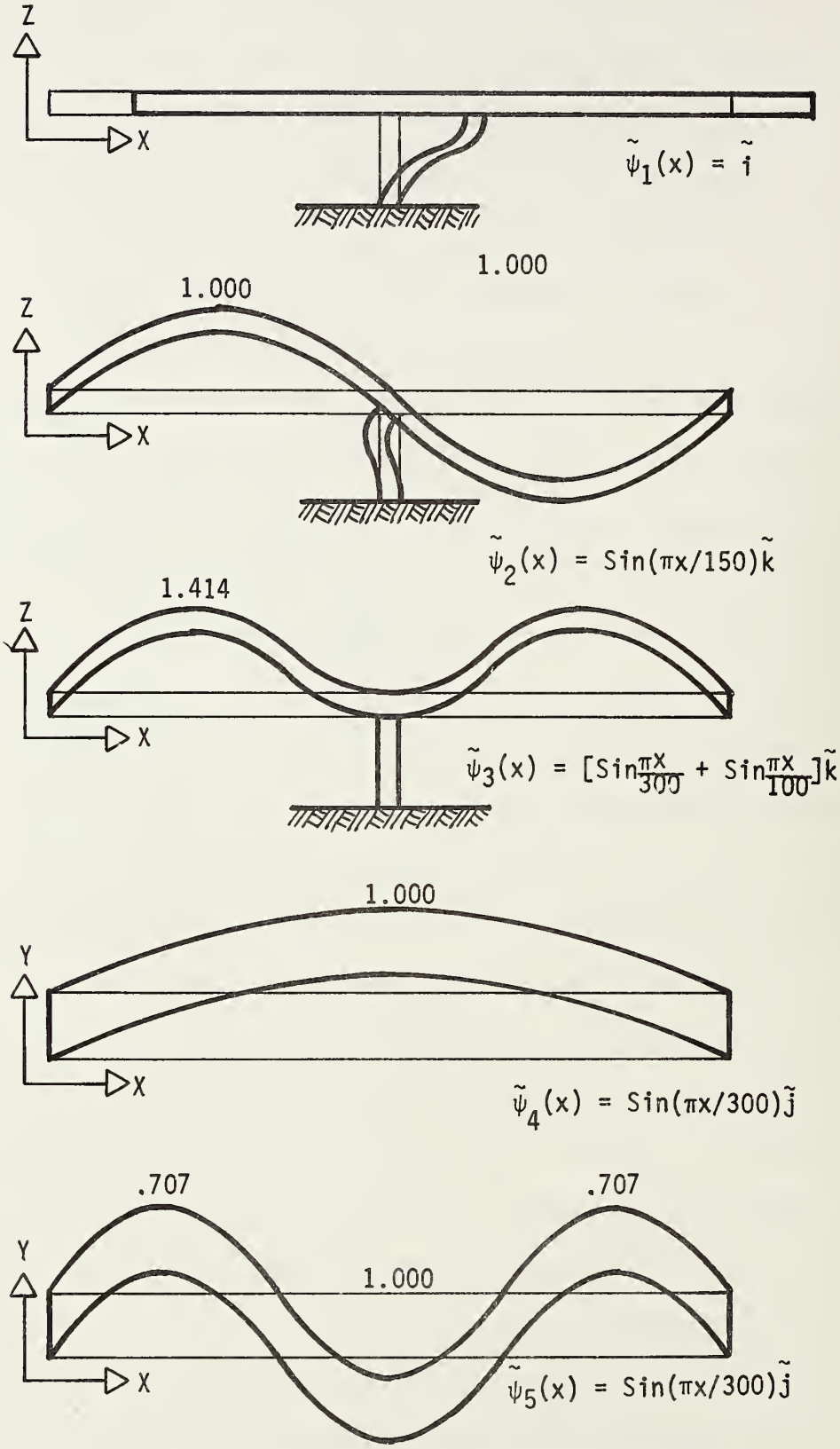

Figure 23.- Continuous two-span bridge, assumed distortions.

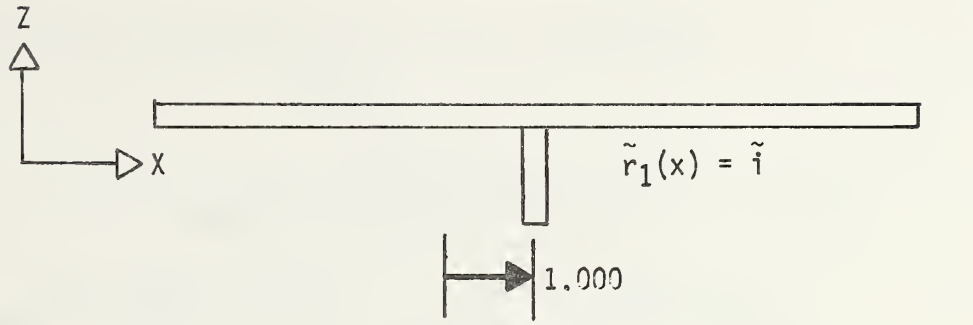

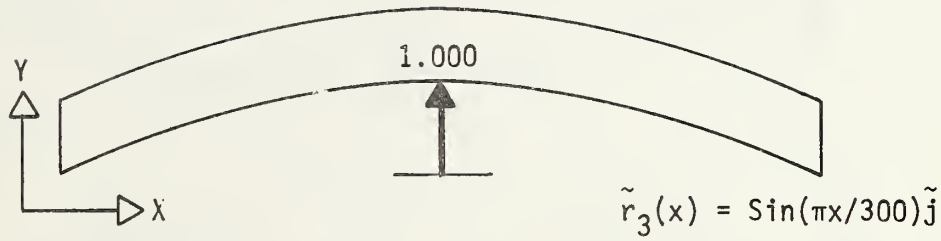

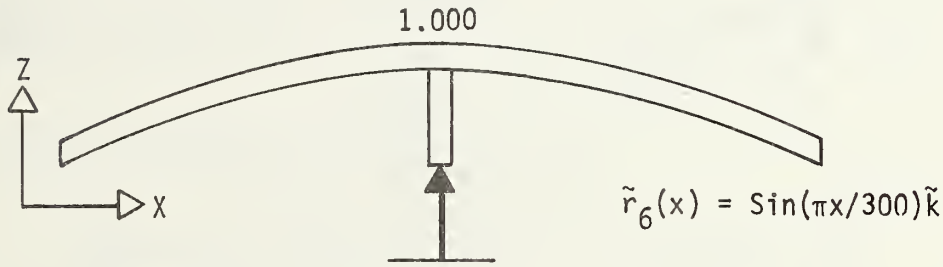

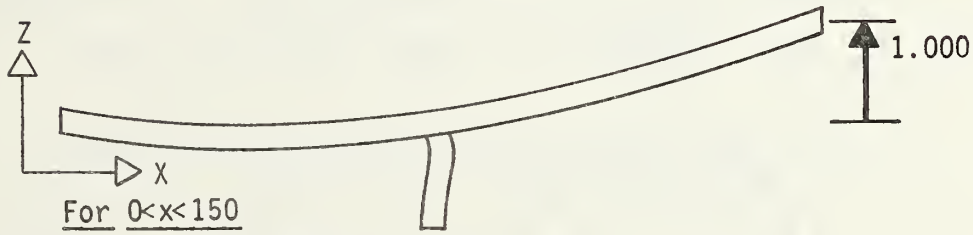

For $0<x<150$

$$\tilde{r}_7(x) = \frac{x3/6-3750x}{2250000}\tilde{k}$$

For $150<x<300$

$$\tilde{r}_7(x) = \frac{150x^2-x^3/6-26250x+1125000}{2250000}\tilde{k}$$

Figure 24.- Continuous two-span bridge, distortions for unit displacements corresponding to reactions.

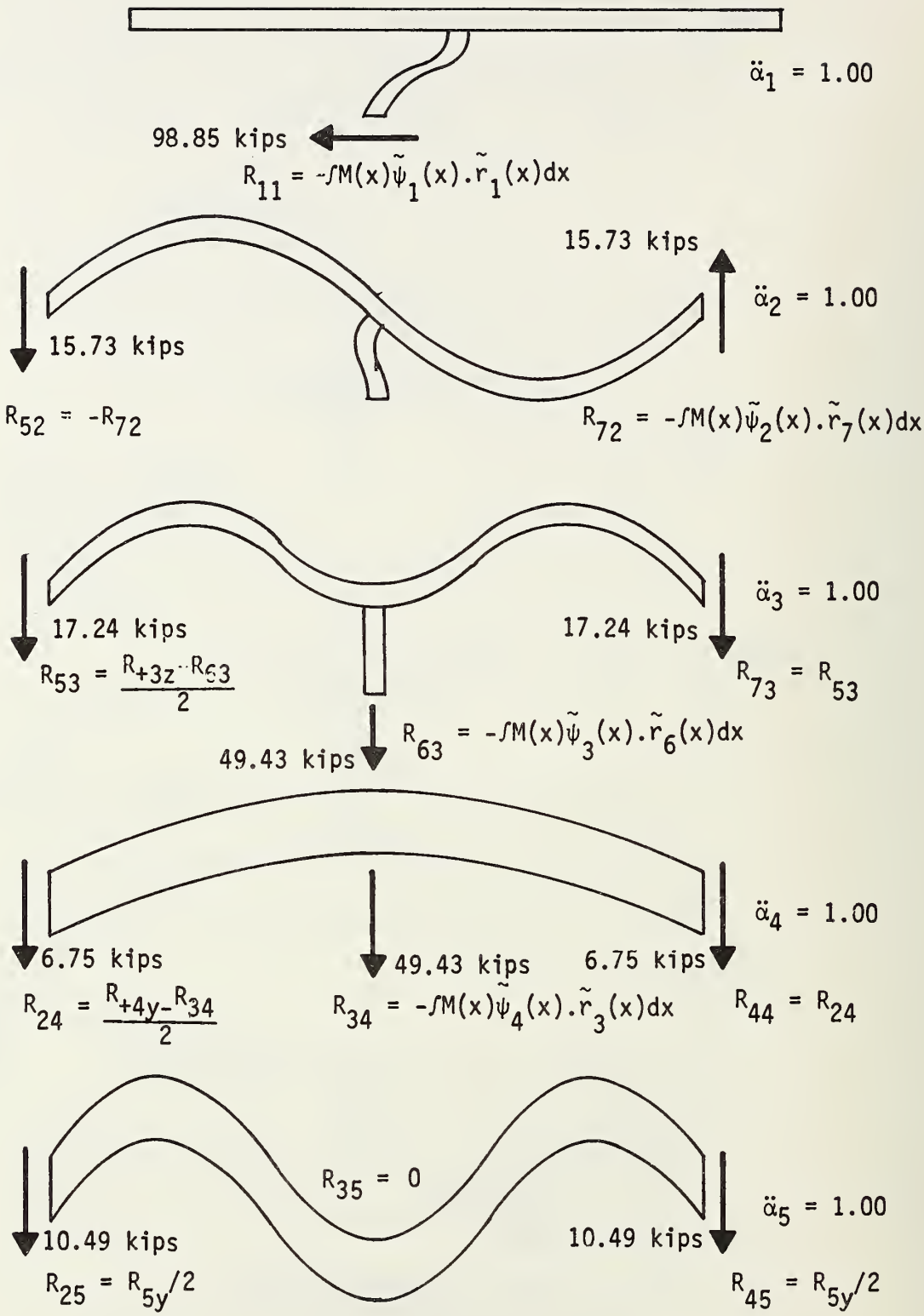

Figure 25.- Continuous two-span bridge, reactions due to unit generalized accelerations.

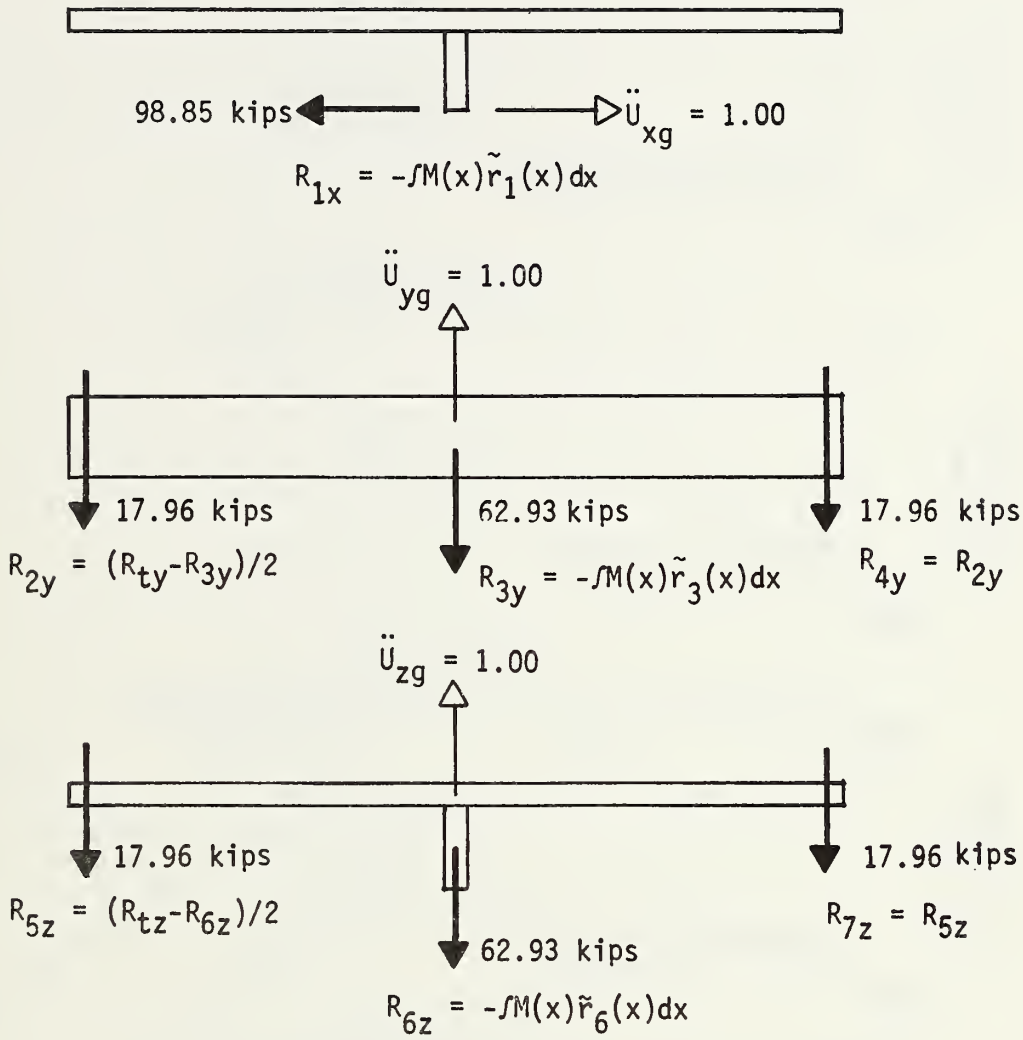

Figure 26.- Continuous two-span bridge, reactions due to unit, rigid body accelerations.

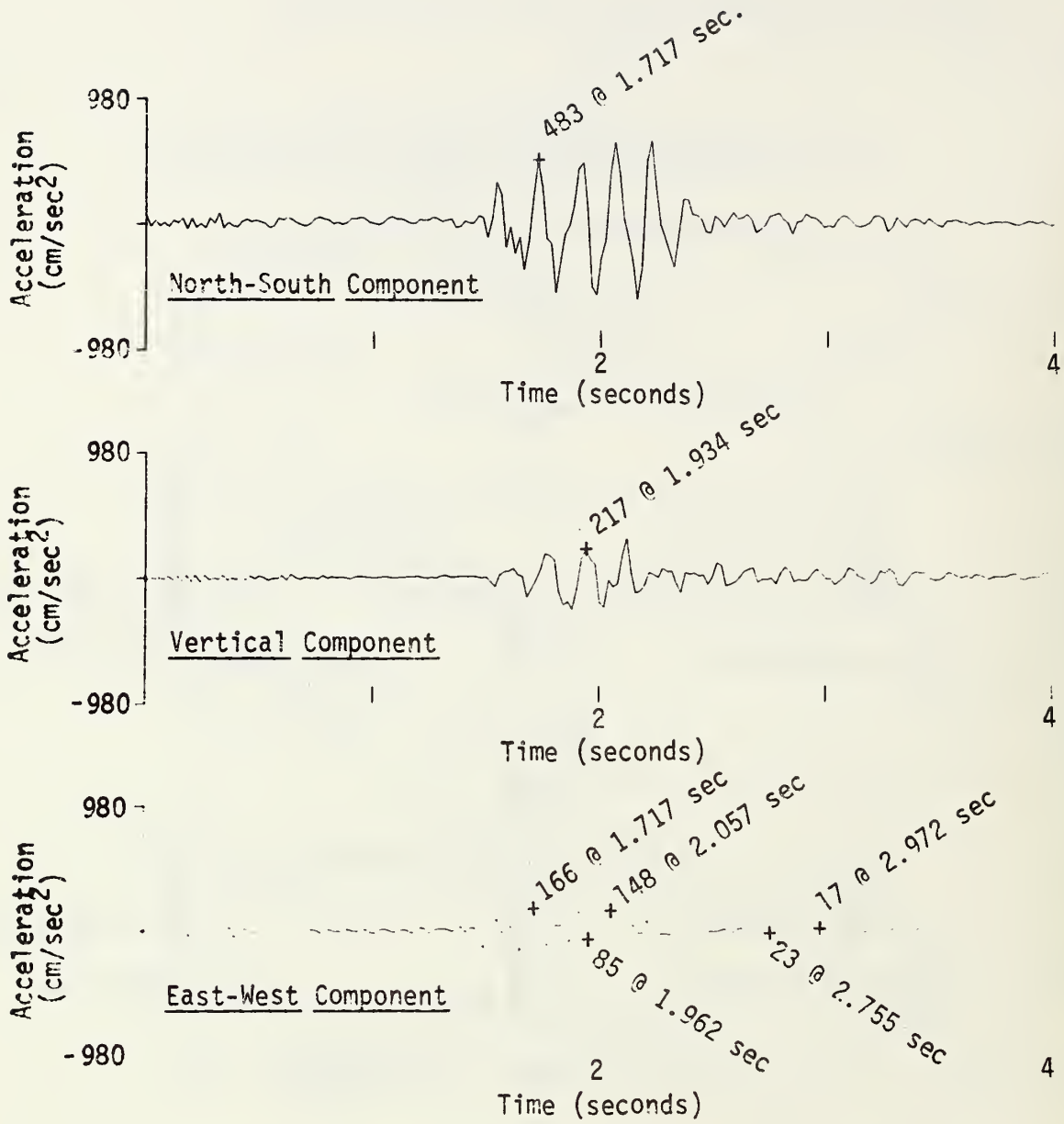

Figure 27.- Continuous two-span bridge, ground accelerations.

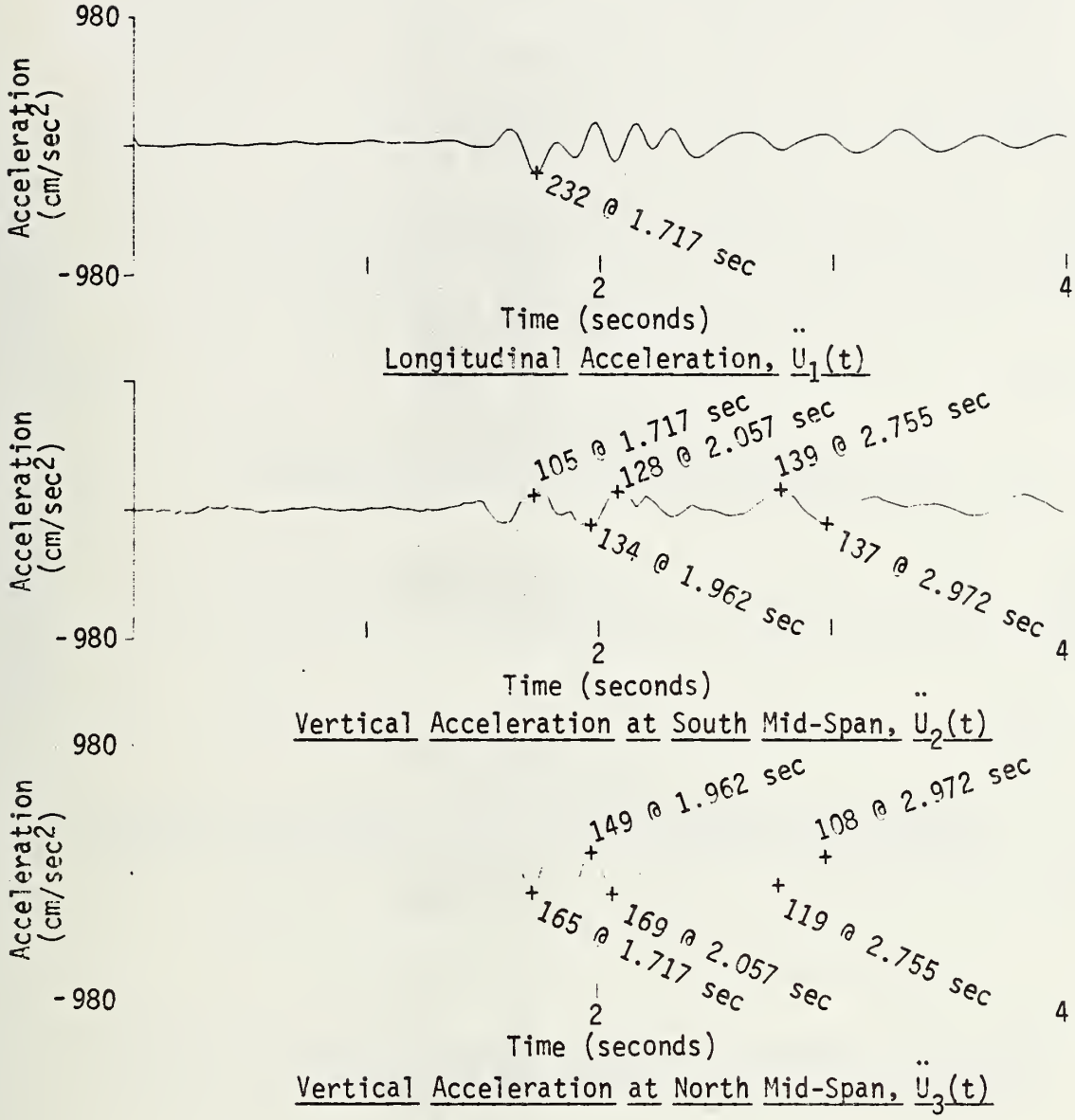

Figure 28.- Continuous two-span bridge, structure accelerations.

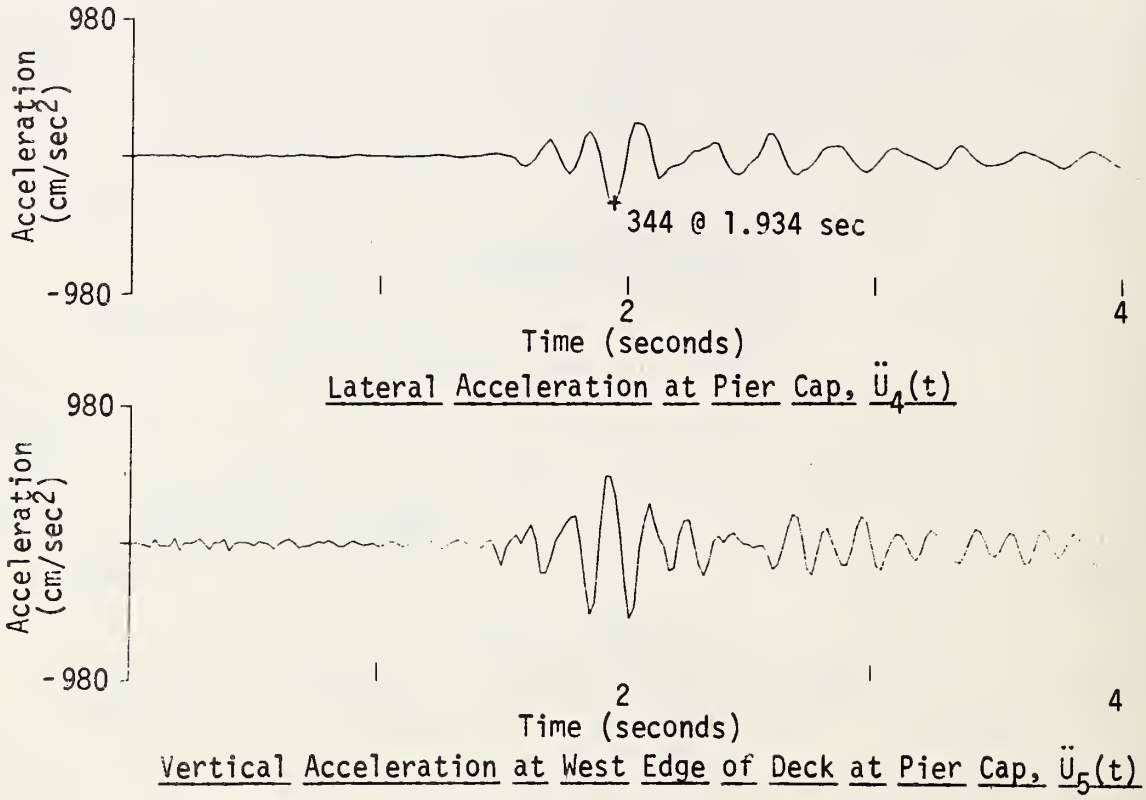

Figure 29.- Continuous two-span bridge, structure accelerations.

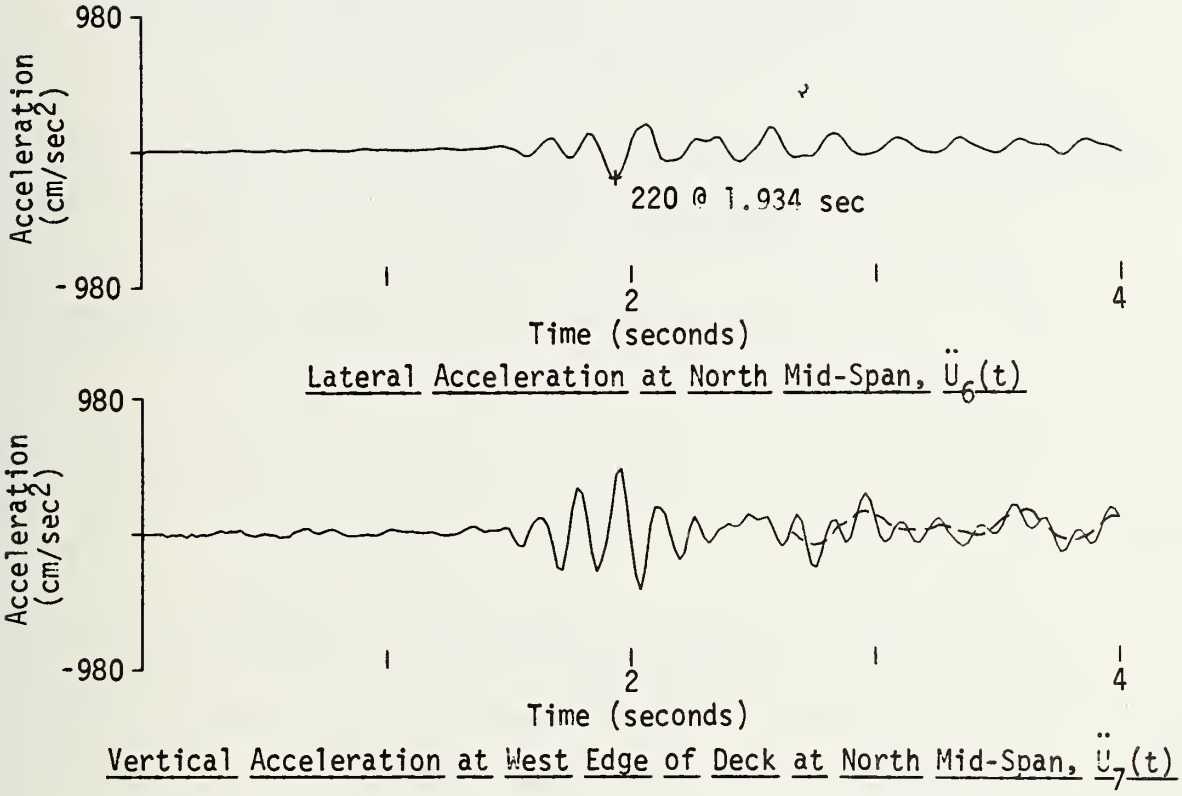

Figure 30.- Continuous two-span bridge, structure accelerations.

(a) Longitudinal Reactions

Rigid body motion in the x-direction and distortions in the first generalized coordinate direction only contribute to longitudinal reactions. The extreme absolute acceleration in the $\ddot{U}_1$ direction is given by

$$\ddot{U}_1|_{extreme} = -232.34 \text{ cm/sec}^2 \text{ @ } t = 1.72 \text{ seconds}$$

At t = 1.72 seconds, the longitudinal ground acceleration is given by

$$\ddot{U}_{xg} = 483 \text{ cm/sec}^2$$

By definition the corresponding generalized acceleration is obtained from

$$\ddot{U}_1 = \ddot{U}_{xg} + \psi_1(150)\ddot{\alpha}_1 \qquad \text{(see equation 27)}$$

where $\psi_1(150) = 1$ is the amplitude of the first assumed distortion at the instrument 1 location. Therefore

$$\ddot{\alpha}_1 = \ddot{U}_1 - \ddot{U}_{xg} \tag{83}$$

and at t = 1.72 seconds

$$\ddot{\alpha}_1 = -715.34 \text{ cm/sec}^2$$

From figures 25 and 26 and equation 83 the total longitudinal reaction is found as the linear combination of reactions from $\ddot{\alpha}_1(1.72)$ and $\ddot{U}_{xg}(1.72)$. This maximum reaction of 753.5 kips is shown graphically in figure 31. Although, in this case, this reaction could have been found directly from $\ddot{U}_1|_{extreme} = -232.34 \text{ cm/sec}^2$, it is of value to decompose this force into components associated with structural distortions and rigid body motions.

(b) Lateral (transverse) Reactions

Rigid body motion in the y-direction and distortions in the fourth and fifth generalized coordinate directions contribute to lateral bridge reactions (R_2, R_3, and R_4). Maximum lateral forces are likely to occur when $\ddot{U}_4$ and $\ddot{U}_6$ are at or near their extreme values. Both have their extreme values at

$\ddot{\alpha}_1(1.72) = -23.469\ \text{fps}^2\ (-715.34\ \text{cm/sec}^2)$

$R_{11}\ddot{\alpha}_{11}(1.72) = (-98.85\ \text{kips/fps}^2)\cdot(-23.469\ \text{fps}^2)$

$\ddot{U}_{xg}(1.72) = 15.846\ \text{fps}^2\ (483\ \text{cm/sec}^2)$

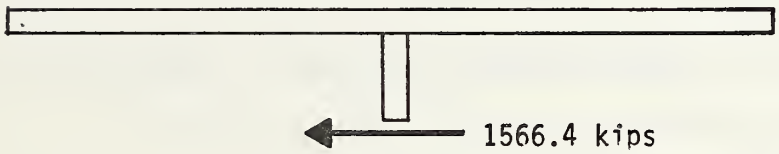

$R_{1x}\ddot{U}_{xg}(1.72) = (-98.85\ \text{kips/fps}^2)\cdot(15.846\ \text{fps}^2)$

Total Longitudinal Force

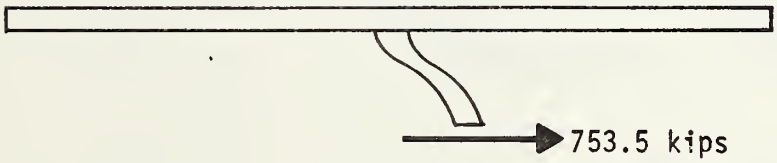

$R_1(1.72) = R_{11}\ddot{\alpha}_{11}(1.72)+R_{1x}\ddot{U}_{xg}(1.72)$

Figure 31.- Continuous two-span bridge, maximum longitudinal reactions.

t = 1.93 seconds (see figures 29 and 30)

$$\ddot{U}_4|_{extreme} = -344.33 \text{ cm/sec}^2$$

$$\ddot{U}_6|_{extreme} = -220.59 \text{ cm/sec}^2$$

At t = 1.93 seconds

$$\ddot{U}_{yg} = 217 \text{ cm/sec}^2$$

By definition the absolute accelerations at the instrument locations 4 and 6 can be expanded in terms of the generalized coordinates by

$$\ddot{U}_4 = \ddot{U}_{yg}+\psi_4(150)\ddot{\alpha}_4+\psi_5(150)\ddot{\alpha}_5 \tag{84}$$

$$\ddot{U}_6 = \ddot{U}_{yg}+\psi_4(225)\ddot{\alpha}_4+\psi_5(225)\ddot{\alpha}_5 \tag{85}$$

Using the measured values of $\ddot{U}_4$, $\ddot{U}_6$ and $\ddot{U}_{yg}$ at t = 1.93 seconds, and the known distortions, equations 84 and 85 are equivalent to

$$1.000\ddot{\alpha}_4(1.93)-1.000\ddot{\alpha}_5(1.93) = -561.33$$

$$.707\ddot{\alpha}_4(1.93)+ .707\ddot{\alpha}_5(1.93) = -437.59$$

from which

$$\ddot{\alpha}_4(1.93) = -590.14 \text{ cm/sec}^2$$

$$\ddot{\alpha}_5(1.93) = -28.81 \text{ cm/sec}^2$$

and

$$\ddot{U}_{yg}(1.93) = 217.00 \text{ cm/sec}^2$$

Since lateral reactions are presently known for $\ddot{\alpha}_4=\ddot{\alpha}_5=\ddot{U}_{yg}=1$ (foot/sec^2), lateral reactions to the above accelerations at t = 1.93 seconds can be scaled and combined as shown in figure 32.

(c) Vertical Reactions

Rigid body motion in the z-direction and distortions in the second and third generalized coordinate directions contribute to vertical force reactions. Extreme vertical reactions are likely to occur when $\ddot{U}_2$ and/or $\ddot{U}_3$ are extreme. Note that extreme seismic-induced reactions only are being

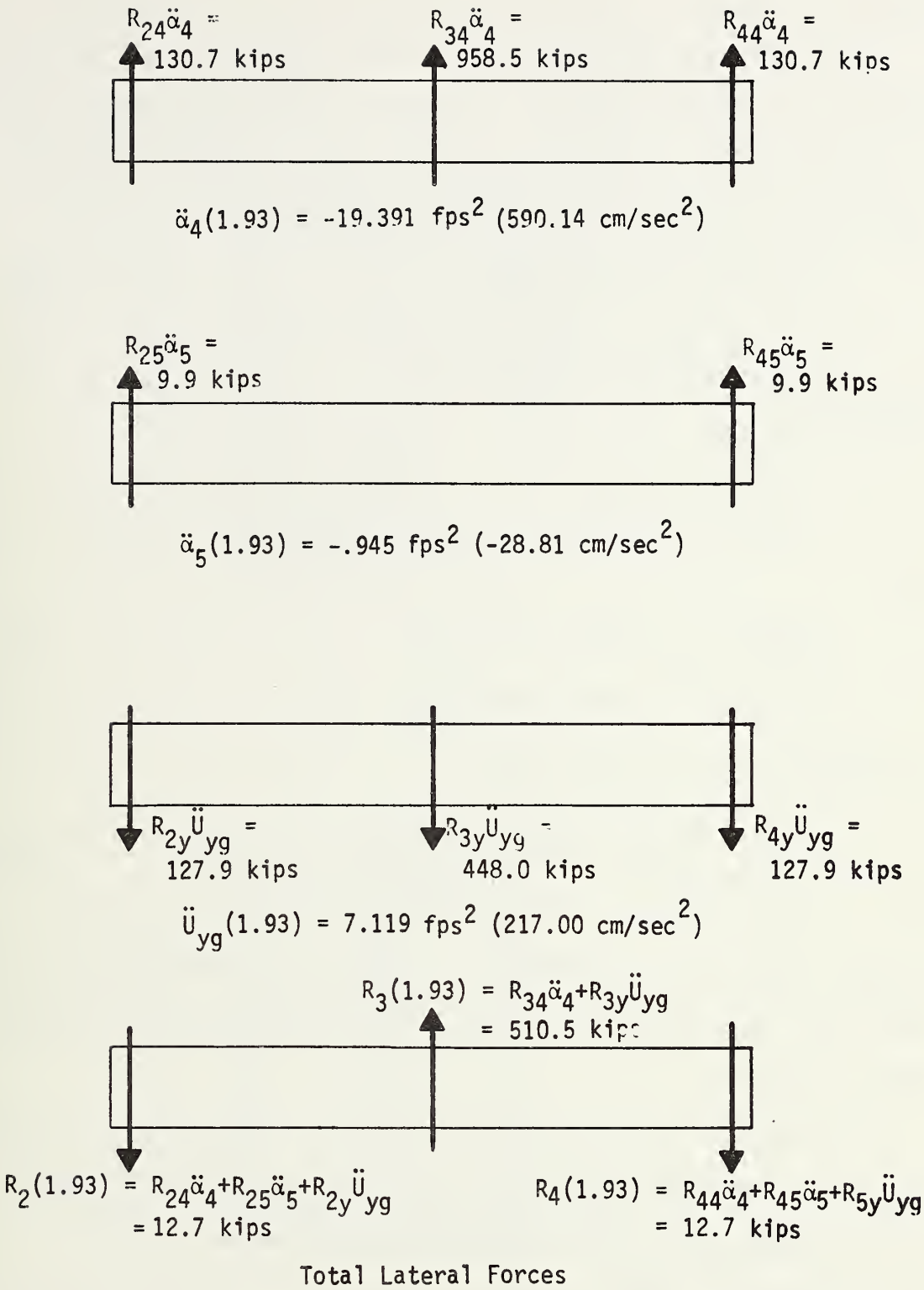

Figure 32.- Continuous two-span bridge, maximum lateral reactions.

found and no attempt is made to include dead loads in this analysis.

The times and accelerations scaled from figures 27 and 28 (and shown in table 4) are possible candidates for producing maximum vertical reactions. By definition, the structure accelerations can be expanded in terms of ground accelerations and generalized accelerations by

$$\ddot{U}_2 = \ddot{U}_{zg}+\psi_2(75)\ddot{\alpha}_2+\psi_3(75)\ddot{\alpha}_3 \tag{86}$$

$$\ddot{U}_3 = \ddot{U}_{zg}+\psi_2(225)\ddot{\alpha}_2+\psi_3(225)\ddot{\alpha}_3 \tag{87}$$

From figure 23

$$\psi_2(75) = 1.000 \qquad \psi_3(75) = 1.414$$

$$\psi_2(225) = -1.000 \qquad \psi_3(225) = 1.414$$

so

$$\begin{Bmatrix} \ddot{U}_2-\ddot{U}_{zg} \\ \ddot{U}_3-\ddot{U}_{zg} \end{Bmatrix} = \begin{bmatrix} 1.000 & 1.414 \\ -1.000 & 1.414 \end{bmatrix} \begin{Bmatrix} \ddot{\alpha}_2 \\ \ddot{\alpha}_2 \end{Bmatrix} \tag{88}$$

or inverted (Gere and Weaver, 1965)

$$\begin{Bmatrix} \ddot{\alpha}_2 \\ \ddot{\alpha}_3 \end{Bmatrix} = \begin{bmatrix} 0.500 & -0.500 \\ 0.354 & -.354 \end{bmatrix} \begin{Bmatrix} \ddot{U}_2-\ddot{U}_{zg} \\ \ddot{U}_3-\ddot{U}_{zg} \end{Bmatrix} \tag{89}$$

The peak generalized accelerations are then computed from equation 78, and the scaled values are shown in table 4. Peak generalized accelerations are shown in table 5.

The reactions R_5, R_6, R_7 sought are shown in figure 33. At any time, the vertical reactions are found as the linear combination of reactions due to unit generalized accelerations $\ddot{\alpha}_2$ and $\ddot{\alpha}_3$, and a unit vertical acceleration $\ddot{U}_{zg}$. Shown in table 6 are the vertical reactions for the five candidate times for producing extreme vertical reactions. As can be seen from table 6, the extreme seismically induced value of R_5 (-96.58 kips)

Accelerations (cm/sec^2)			
Time	$\ddot{U}_2$	$\ddot{U}_3$	$\ddot{U}_{zg}$
1.72	105.00	-164.90	165.79
1.96	-133.93	149.03	-85.00
2.06	128.33	-168.72	148.47
2.76	139.13	-119.00	-22.67
2.97	-136.73	107.67	17.00

Table 4.- Continuous Two-Span Bridge, Peak Vertical Accelerations

Acceleration (fps^2)			
Time	$\ddot{\alpha}_2$	$\ddot{\alpha}_3$	$\ddot{U}_{zg}$
1.72	4.427	-4.547	5.439
1.96	-4.462	2.150	-2.789
2.06	4.873	-3.918	4.871
2.76	4.235	.760	-.744
2.97	-4.009	-.732	.558

Table 5.- Continuous Two-Span Bridge, Peak Generalized accelerations

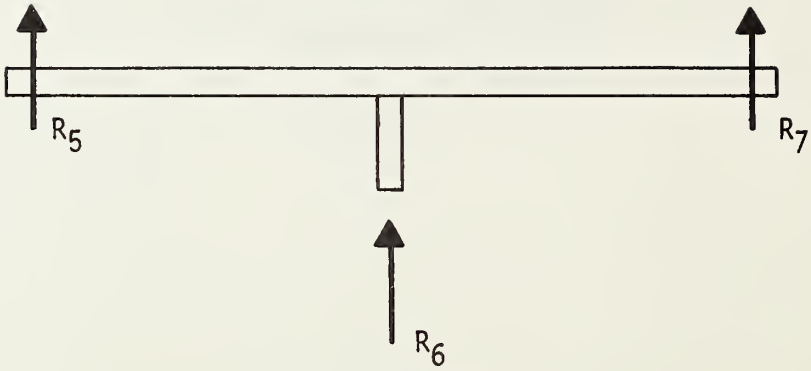

Figure 33.- Continuous two-span bridge, desired vertical reactions.

Time	Source	Reactions (kips) R_5	R_6	R_7
1.72	$R_{i2}\ddot{\alpha}_2$	-69.64	0	69.64
	$R_{i3}\ddot{\alpha}_3$	78.39	224.76	78.39
	$R_{iz}\ddot{U}_{zg}$	-97.68	-342.28	-97.68
	Total	-88.93	-117.52	-50.35
1.96	$R_{i2}\ddot{\alpha}_2$	70.19	0	-70.19
	$R_{i3}\ddot{\alpha}_3$	-37.07	-106.27	-37.07
	$R_{iz}\ddot{U}_{zg}$	50.09	175.51	50.09
	Total	83.21	69.24	-57.17
2.06	$R_{i2}\ddot{\alpha}_2$	-76.65	0	76.65
	$R_{i3}\ddot{\alpha}_3$	67.55	193.67	67.55
	$R_{iz}\ddot{U}_{zg}$	-87.48	-306.53	-87.48
	Total	-96.58	-112.86	56.72
2.76	$R_{i2}\ddot{\alpha}_2$	-66.62	0	66.62
	$R_{i3}\ddot{\alpha}_3$	-13.10	-37.57	-13.10
	$R_{iz}\ddot{U}_{zg}$	13.36	46.82	13.36
	Total	-66.36	9.25	66.88
2.97	$R_{i2}\ddot{\alpha}_2$	63.06	0	-63.06
	$R_{i3}\ddot{\alpha}_3$	12.62	36.18	12.62
	$R_{iz}\ddot{U}_{zg}$	-10.02	-35.11	-10.02
	Total	65.66	1.07	-60.46

Table 6.- Continuous Two-Span Bridge, Peak Vertical Reactions

occurs at t = 2.06 sec, of R_6 (-117.52 kips) occurs at t = 1.72 sec, and of R_7 (66.88 kips) occurs at t = 2.76 sec. Total extreme loads must include the dead load of the structure.

(2) Structural Model Parameters

Structural model parameters can best be obtained by hand analysis in normal coordinates only. In normal coordinates, the model is completely described by natural frequencies, damping ratios, mode shapes, and participation factors. Because of the many modes of vibration which respond, even for this very simple two-span continuous bridge, it is difficult to estimate damping from the free-vibration portions of the structure motions. As a consequence, only natural frequencies and natural mode shapes are expected to be found from this hand analysis. Participation factors are readily computed from known mass distribution and mode shapes using equations 60, 61, and 62.

Natural modes of vibration are generally sought in regions of the record where there is relatively little input motion. A natural mode will vibrate at the forcing frequency when forced to vibrate, but after excited it will vibrate at a unique natural frequency. For that natural mode of vibration, all parts of the structure will vibrate in phase at its natural frequency. For a single mode of vibration the <u>relative</u> amplitudes of motion for any two points will remain constant for all time. These properties of a mode will be used to identify their presence. It should be noted that, precisely speaking, normal modes of vibration are mathematical entities only. It is fortunate, however, that the distortions of structures in general can be expanded in terms of natural modes quite accurately for some structures and reasonably accurately for most structures.

It is unrealistic to assume that natural modes of vibration will be found in all analyses. It is particularly unrealistic to assume that they will be found for large amplitude, highly nonlinear, damaging motions. Unfortunately, it is often the case that these motions are the most interesting of all, and yet are the most difficult to analyze and are rarely recorded.

The characteristics of normal modes described above will be used to identify the existence of normal modes in the analysis to follow. Five modes of vibration are identified from the hypothetical response time histories shown in figures 19, 20, and 21. The expanded time histories shown in figures 28, 29, and 30 are also used to find structure model parameters for $t < 4$ sec. The identified modes of vibration are as follows:

Mode 1 - Observed in $\ddot{U}_2$ and $\ddot{U}_3$ for $t > 8$ seconds. It is an asymmetric vertical flexural mode of vibration.

Mode 2 - Observed in $\ddot{U}_1$, $\ddot{U}_2$, and $\ddot{U}_3$ for $2\ 1/2 < t < 6$ seconds. It is an asymmetric vertical and longitudinal flexural mode of vibration.

Mode 3 - Observed in $\ddot{U}_4$ and $\ddot{U}_6$ for $t > 2$ seconds. It is an assumed symmetric, lateral, flexural mode of vibration that probably has a torsional component which is not observed.

Mode 4 - Observed in $\ddot{U}_2$ and $\ddot{U}_3$ for $t < 2$ seconds. It is a symmetric vertical mode of vibration.

Mode 5 - Observed in $\ddot{U}_5$ and $\ddot{U}_7$ for $t > 2$ seconds. It is an assumed symmetric torsional mode of vibration that probably has a lateral component which is not observed.

(a) Mode Number 1

Information needed to determine properites of this mode of vibration

are obtained from $\ddot{U}_2$ and $\ddot{U}_3$. Because the observed motions in this mode are 180% out of phase (asymmetric vertical flexure) it is likely that there should exist some longitudinal component to the mode, but none is observed in $\ddot{U}_1$.

Natural frequency information is obtained from both $\ddot{U}_2$ and $\ddot{U}_3$ from t = 7.3 seconds to 11.8 seconds. For this time increment both $\ddot{U}_{xg}$ and $\ddot{U}_{zg}$ are assumed to be negligible, and so the response is essentially a free vibration. Frequency information is tabulated in table 7; the natural frequency ω_1 is computed from the equation $\omega_1 = 2\pi/T_1$ where T_1 = (time for n cycles)/n.

Mode shape information is obtained by comparing the relative amplitudes of $\ddot{U}_2$ and $\ddot{U}_3$for free vibrations at this frequency. From the average of sixteen peak values in the above time period, for $\ddot{U}_3$ arbitrarily given the value -1.000, then $\ddot{U}_2$ = 1.025. Mode 1 characteristics are summarized in figure 34.

(b) Mode Number 2

Natural frequency and mode shape information for this mode is obtained from $\ddot{U}_1$, $\ddot{U}_2$, and $\ddot{U}_3$. This mode is excited primarily in the early part of the earthquake response, and so information is most accurately obtained from the expanded acceleration records shown in figure 28.

Frequency information is obtained from $\ddot{U}_1$ from t = 2.5 to 5 seconds. Seven cycles of motion are observed in 2.386 seconds yielding ω_2 = 18.434 radians/sec.

Mode shape information is obtained from the average of four peaks from 3 to 4 seconds into the record. It is assumed that the motion is essentially free vibration. For $\ddot{U}_1$ scaled to 1.000, the relative amplitudes of $\ddot{U}_2$ and $\ddot{U}_3$ in this mode of vibration are -2.005 and 2.130 respectively.

Mode 2 characteristics are summarized in figure 35.

(c) Mode Number 3

Mode 3 information is obtained from the lateral accelerations $\ddot{U}_4$ and $\ddot{U}_6$. Because the bridge is supported by a single column, it is highly likely that there should exist significant torsional motion, but none is observed at this lateral mode frequency. Mode shape data is taken from t = 2.5 to 4.0 seconds even though significant lateral ground motion exists in this interval. The ground motion during this time has a predominant frequency significantly different from this natural frequency. Therefore, mode shape information will be obtained from averaging many response peaks, assuming free vibration behavior.

This mode of vibration is the fundamental, symmetric, lateral flexural mode of vibration. This behavior is anticipated, as there exists only one side-span instrumented with a lateral motion accelerometer. The symmetric nature of this mode is assumed.

From five cycles of motion from t = 2.5 to 4.0 seconds, from both $\ddot{U}_4$ and $\ddot{U}_6$, the natural frequency was measured to be ω_3 = 23.957 rps. At this natural frequency both $\ddot{U}_4$ and $\ddot{U}_6$ were in phase, and an average of eleven peaks of motion yielded the relative amplitudes ($\ddot{U}_4$ arbitrarily scaled to unity) of $\ddot{U}_4$ = 1.000 and $\ddot{U}_6$ = 0.862. Mode 3 characteristics are summarized in figure 36.

(d) Mode Number 4

Mode 4 was anticipated and is a symmetric, vertical flexural mode of the deck. Motion in the mode is observed in $\ddot{U}_2$ and $\ddot{U}_3$ only for $t < 2$ seconds. Evidently, a small vertical earthquake motion preceded the significant ground motion and excited, to a small extent, this symmetric

vertical mode of vibration. Undoubtedly motion in this mode exists throughout $\ddot{U}_2$ and $\ddot{U}_3$ but is overshadowed by the large vertical components of Modes 1 and 2.

Frequency and mode shape information is obtained from three cycles of motion before t = 2 sec. The natural frequency was found to be ω_4 = 17.527 rps. Both $\ddot{U}_2$ and $\ddot{U}_3$ are in phase in this mode and are approximately equal in amplitude. No more accurate quantitative measurements are justified from the data. Mode 4 characteristics are summarized in figure 37.

(e) Mode Number 5

Mode 5 is a torsional mode of vibration observed in the eccentrically located vertical accelerations $\ddot{U}_5$ and $\ddot{U}_7$. Such motions have very high accelerations, but because of the high natural frequency of this mode, torsional displacements may not be large. Frequency and mode shape information is obtained for t = 2.7 to 4.0 seconds. The torsional component is obtained as $(\ddot{U}_5-\ddot{U}_{zg})/c$ and $(\ddot{U}_7-\ddot{U}_3)/c$ where c is half of the deck width. For t > 2.5 seconds the motion is essentially free, so $\ddot{U}_{zg}$ can be ignored relative to $\ddot{U}_5$, but $\ddot{U}_3$ must still be removed from $\ddot{U}_7$.

Frequency data are obtained from nine cycles of motion between t = 2.7 and 4.0 seconds from $\ddot{U}_5$ and $\ddot{U}_7$, and are summarized in table 8. Mode shape data were taken from the average of eighteen peak values after the vertical motion $\ddot{U}_3$ had been subtracted from $\ddot{U}_7$ (see dashed line on $\ddot{U}_7$ trace on figure 30). Torsional motion at mid-side-span is in phase with torsional motion at the center of the bridge. Although motion on one side only was recorded, it is assumed that this mode is symmetric. Furthermore, although it is not measurable, it is assumed that there must exist some lateral component to this mode (it is also assumed that there must exist

Instru.	No. of Cycles	Time (sec)	ω_1(rad/sec)
2	8	4.381	11.474
3	8	4.427	11.354
		Average	= 11.414

Table 7.- Continuous Two-Span Bridge, Mode 1 Frequency Summary

Instru.	No. of Cycles	Time	ω_5(rad/sec)
5	9	1.283	44.075
7	9	1.292	43.768
		Average	= 43.922

Table 8.- Continuous Two-Span Bridge, Mode 5 Frequency Summary

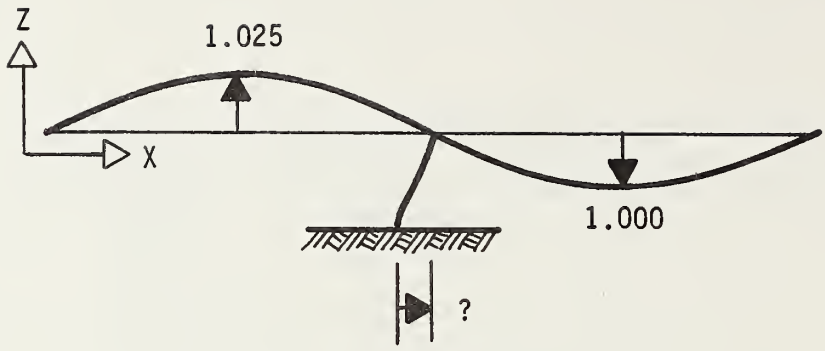

ω_1 = 11.414 rps

Figure 34.- Continuous two-span bridge, mode 1 characteristics.

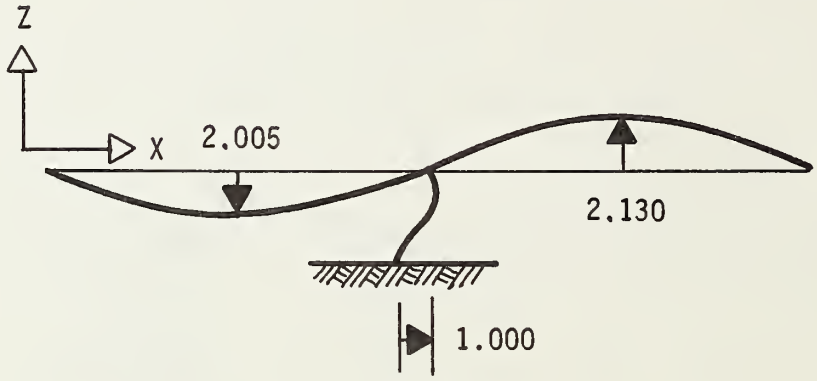

ω_2 = 18.434 rps

Figure 35.- Continuous two-span bridge, mode 2 characteristics.

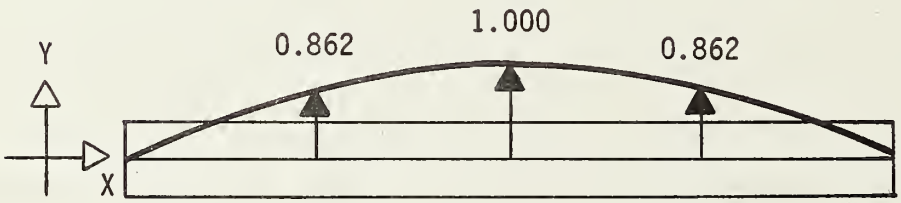

ω_3 = 23.957 rps

Figure 36.- Continuous two-span bridge, mode 3 characteristics.

some torsional component to the lateral mode). For a rotation at the center of the bridge of 1.000, the rotation at mid-side-span is measured to be 0.794. Mode 5 characteristics are summarized in figure 38.

(f) Discussion

It is of value to compare the structure model parameters which have been found from this hand analysis to those known parameters which were used to generate these hypothetical records. A summary of the actual structure model parameters are shown in figure 39. As can be seen the natural frequencies were found quite accurately. On the other hand, mode shapes were found only in a qualitative sense, with numerical accuracy for a few components. In order that mode shapes be found with any quantitative accuracy, even for this simple example, the records must be analyzed on a digital computer.

Note that damping estimates were not even attempted for this example. In certain cases numerical accuracy may be achieved. In other cases, damping estimates may be highly erroneous. Because of the great inconsistency which may exist in damping estimates obtained from hand analyses (except for the simplest of examples like the triple simple span bridge) it is not recommended to find damping ratios from hand analyses.

These two examples, as well as one additional example, will be reanalyzed with the aid of a high-speed digital computer in the next section.

One last comment is in order. Note that at most, mode shapes may be found with numerical accuracy at a few points where instruments exist. Deformations between instruments can only be assumed. Unless bridges are very heavily instrumented, mode shapes are not likely to be found with great accuracy. The results from these analyses are best used to verify

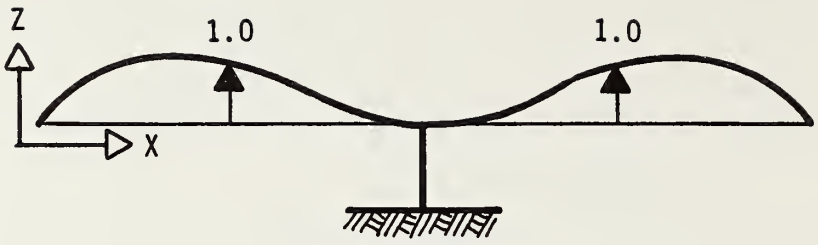

ω_4 = 17.527 rps

Figure 37.- Continuous two-span bridge, mode 4 characteristics.

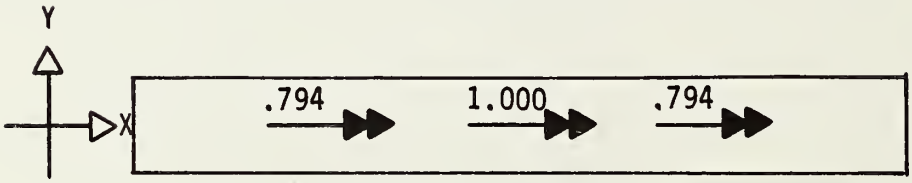

ω_5 = 43.914 rps

Figure 38.- Continuous two-span bridge, mode 5 characteristics.

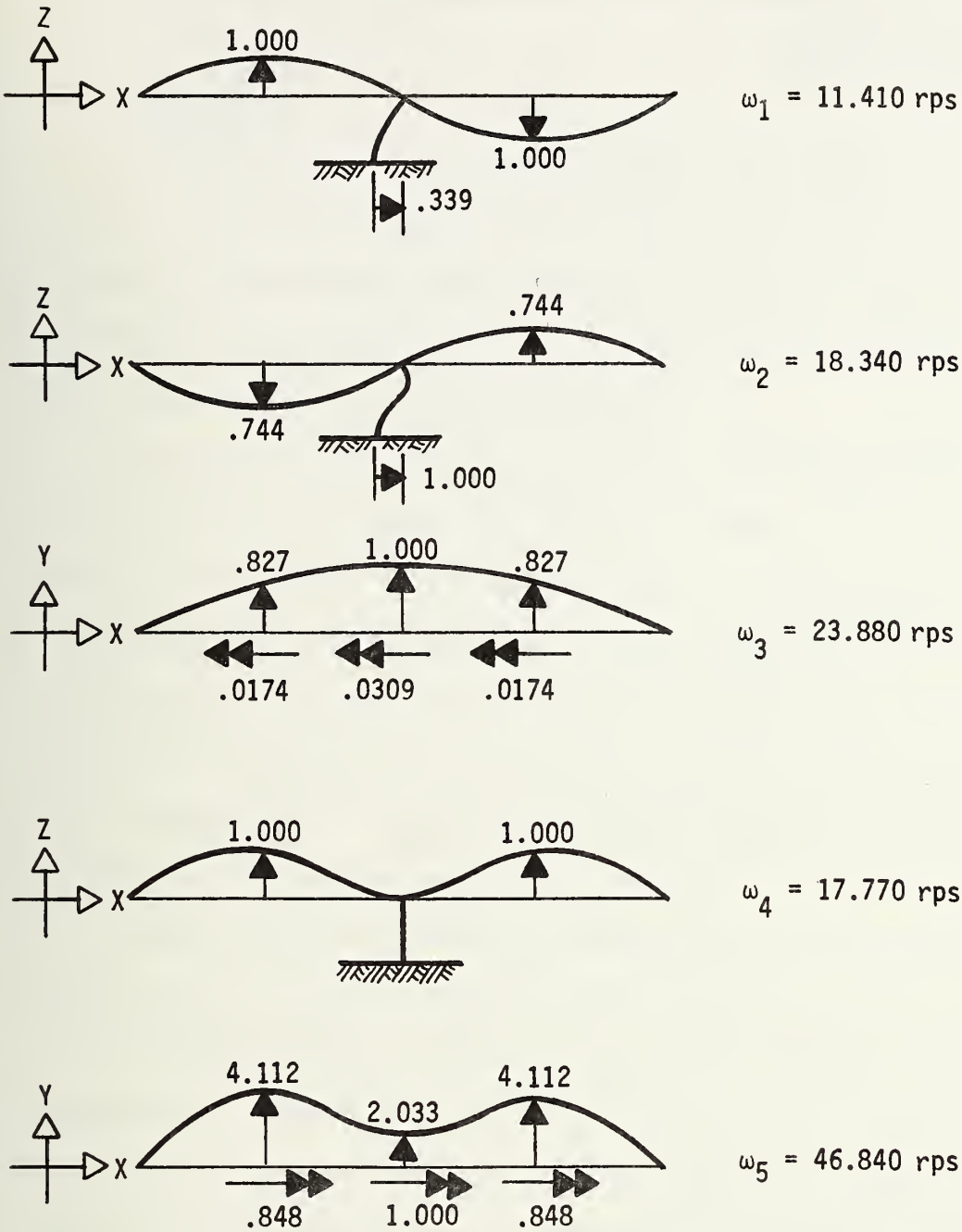

Figure 39.- Continuous two-span bridge, actual modal characteristics.

theoretical behavior of a few points. Experimentally obtained structure models will rarely have sufficient detail to be used by themselves for complete earthquake analyses.

IV. ANALYSIS OF DIGITIZED STRONG-MOTION RECORDS WITH THE ASSISTANCE OF A HIGH-SPEED COMPUTER

A. Introduction

The objectives of this section are the same as those for the previous section: to compute force levels throughout the bridge for a given earthquake, and to deduce what mathematical model would have best duplicated the measured response to the measured ground motion. Again, this second objective is the more important.

Once deflected shapes and corresponding coordinate amplitudes have been obtained by any means, force levels throughout the bridge may be computed as outlined in the previous section. Again those force levels may be computed from assumed shapes $\tilde{\psi}_i(s)$ and corresponding coordinate accelerations $\alpha_i(t)$, or computed normal mode shapes $\tilde{\phi}_i(s)$ and corresponding modal accelerations $\eta_i(t)$. The remainder of this section will be devoted to the second objective; to identify mathematical model properties of the bridge from the measured strong-motion records.

Identification of a best-fit mathematical model from strong-motion records (called system or parameter identification) is still very much in the developmental stage, particularly for bridges because their natural frequencies of vibration are so often closely spaced. Traditionally, mathematical models of the dynamic bridge behavior are formulated, theoretical bridge responses are compared to the measured responses, and finally the theoretical model is evaluated by comparing theoretical and measured responses. If the fit is good, nothing more need be done, but if the fit is poor, many or all of the model parameters must be changed in hopes of improving the fit. Unfortunately, even for the simplest bridge, a

mathematical model may include hundreds if not thousands of parameters that may be varied. Since the possible combinations of changed parameters is enormous, system identification by this unsystematic trial and error procedure is extremely tedious if not entirely impractical. Since it is not within the scope of this report to discuss mathematical modeling (Biggs, 1964; Clough and Penzien, 1975, Hurty and Rubinstein, 1964), system identification by modifying an a priori model will not be considered. In any event, this approach has not yet been demonstrated to be the best; therefore in this report no a priori model will be formulated.

There are two fundamental methods of identifying the mathematic model from strong-motion records when no a priori model is formulated: frequency domain methods and time domain methods. Traditionally in the fields of electrical and mechanical engineering, the frequency domain method has been used. Specifically, Fourier transforms (Clough and Penzien, 1975; Hurty and Rubinstein, 1964) of the ground motion and the bridge motion are computed. The bridge motion transform is then divided by the ground-motion transform to yield a complex transfer function, $H(\omega)$, or frequency response function. The amplitude of a typical transfer function is shown in figure 40. The transfer function amplitude between a point on the bridge and the ground is the ratio of peak bridge response to peak ground motion for a steady harmonic ground motion with constant frequency, ω. For input motion frequencies near a natural frequency of the bridge, resonance will occur causing large modal motions. For input motion frequencies away from natural frequencies the bridge may act as a vibration isolator and filter out those input motions entirely.

From a transfer function, natural frequencies can be found as the locations of the dominant peaks; damping ratios can be found from the peak

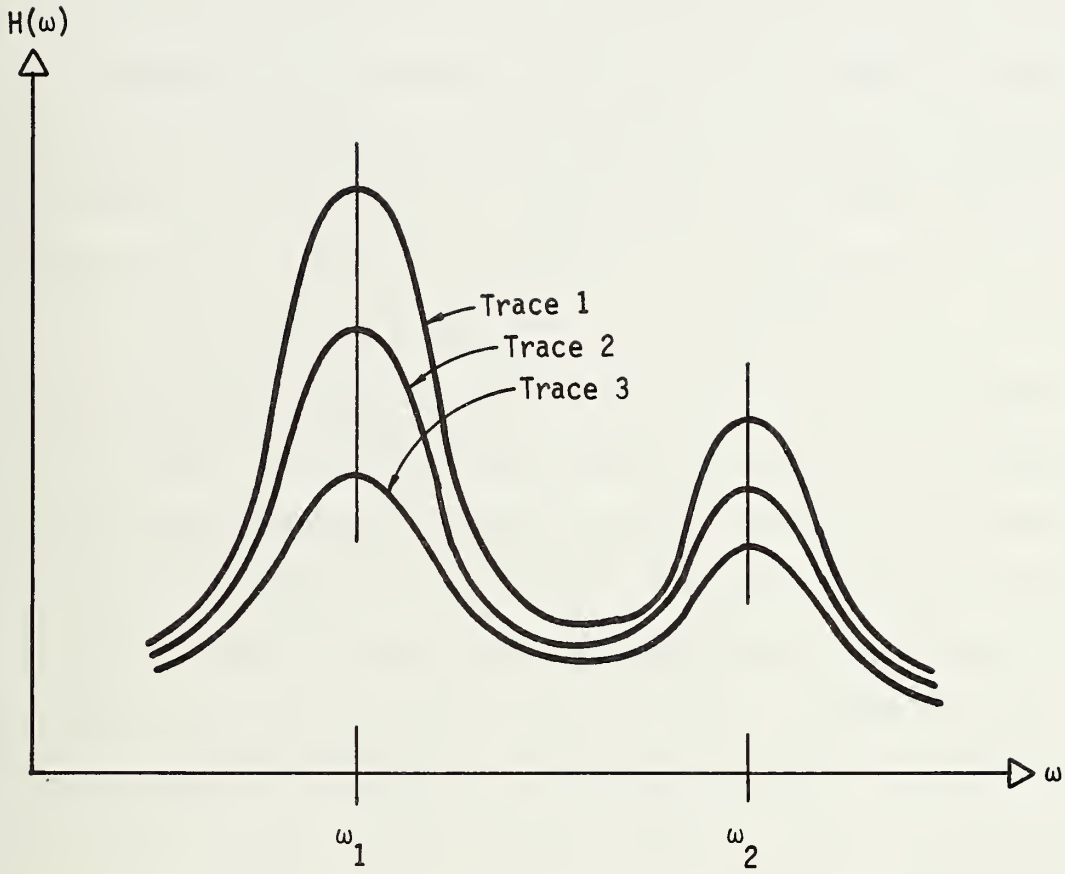

Figure 40.- Transfer function amplitude.

widths; and mode shapes can be found from the relative record amplitudes at a specific natural frequency (Clough and Penzien, 1975; Hurty and Rubinstein, 1964). Once mode shapes have been found, participation factors can be computed from equations 60, 61, and 62 from the bridge geometry and mass distribution, M(s).

Although this procedure sounds very simple once computer subroutines are available to compute Fourier transforms, it is not particularly accurate when used to analyze earthquake induced bridge motions. Inherent in any frequency domain method using Fourier transforms is the assumption that the input and output motions are periodic indefinitely; namely motion begins at $t=-\infty$ and continues to $t=\infty$. Obviously earthquakes are not periodic, and most cannot even be approximated well as being periodic. The assumption of periodicity in the response implies that some sort of steady-state response exists. In actuality, by the time that significant ground motions have ceased, bridge motions may have just begun to grow towards a steady-state response. Consequently, when a transfer function between input and output motions is found, peaks at natural frequencies are deceptively small. As a result modal peaks may not even be identifiable against background "noise", and when identifiable may yield erroneous values of damping.

Because of the many uncertainties in the results obtained from frequency domain procedures, they are not recommended for general use in analyzing strong-motion records for highway bridges. In certain circumstances, natural frequencies may be identified from Fourier transforms of absolute bridge motions, but not reliably. Other publications (Biggs, 1964; Clough and Penzien, 1975; Hurty and Rubinstein, 1964; Newmark and Rosenblueth, 1971; Wiegel, 1970) have further information

regarding frequency domain analysis procedures.

Most reliable strong-motion record analysis procedures seem to be time domain procedures. Recent summaries of system identification procedures are given in Hart and Yao (1976) and Ibanez (1977). The methods described were developed to analyze building structures, and may be used with only some success for highway bridges. Consequently, a time domain analysis procedure has been developed to analyze highway bridge motions from a general least-squares fitting procedure described by Kozin and Kozin (1968.)

B. Time Domain Analysis Procedure

A time domain analysis procedure which has been developed primarily for the analysis of highway bridges will be described here. Although highway bridges are simple in outward appearance, their dynamic behavior is in general very complex because natural frequencies of vibration may be closely spaced, and modes of vibration may be excited by all components of the ground motion. The procedure described here is unaffected by these complexities.

The objective of this system identification analysis is to describe completely, from the recorded motions, the mathematical model that duplicates the actual motion best. The mathematical model to be identified can be either in physical coordinates associated with lumped masses

$$[M]\{\ddot{U}\}+[C]\{\dot{U}\}+[K]\{U\} = -\{M_x\}\ddot{U}_{xg}-\{M_y\}\ddot{U}_{yg}-\{M_z\}\ddot{U}_{zg} \qquad (90)$$

or in generalized coordinates associated with a set of assumed distorted shapes

$$[m]\{\ddot{\alpha}\}+[c]\{\dot{\alpha}\}+[k]\{\alpha\} = -\{m_x\}\ddot{U}_{xg}-\{m_y\}\ddot{U}_{yg}\{m_z\}\ddot{U}_{zg} \tag{91}$$

In either case, the ground accelerations $\ddot{U}_{xg}$, $\ddot{U}_{yg}$, and $\ddot{U}_{zg}$ are recorded as such and need no further processing before analysis.

The following paragraphs describe the preprocessing required to identify the mathematical model in physical coordinates described by equation 90.

Relative motions, or distortions, $\{\ddot{u}\}$, $\{\dot{u}\}$, $\{u\}$ must first be computed from the set of recorded absolute bridge accelerations $\{\ddot{U}\}$. A bridge acceleration relative to the ground, $\ddot{u}_i(t)$, is found simply as the recorded bridge acceleration, less the component of the recorded ground acceleration in the direction of that transducer. Relative bridge velocities, $\dot{u}_i(t)$, and displacements, $u_i(t)$, must then be computed from the relative acceleration. These time histories may be computed by any technique, but typically the accelerations are first digitized and assumed to be linear between points. These piecewise linear functions are then integrated numerically to yield the corresponding velocities and displacements (Conte, 1965). Often, after one and particularly after two integrations, low-frequency noise becomes obvious. For ground motions with frequencies that are low with respect to the lowest natural frequency of the bridge, the bridge will respond essentially as a rigid body with negligible distortions. Consequently, large-amplitude and low-frequency components in the relative velocities and displacements must be errors and can therefore justifiably be filtered from the time histories. A reasonable lower limit to the frequencies passed by the filter is $\omega_1/4$, where ω_1 is the estimated lowest natural frequency for the bridge. The time histories $u_i(t)$, $\dot{u}_i(t)$, and $\ddot{u}_i(t)$ are now in suitable form for

analysis.

It is assumed that the bridge geometry and mass distribution can be obtained accurately from material weights and the bridge drawings. The rule for lumping masses differs for each bridge, and is demonstrated graphically in the example analyses which follow. The participation factor M_{xi} simply equals the corresponding mass M_i if the ith transducer is directed parallel to $\ddot{U}_{xg}$ or equals zero if it is perpendicular to $\ddot{U}_{xg}$. The participation factors M_{yi} and M_{zi} are similarly defined. If the ith mass is a rotational inertia, then all corresponding participation factors M_{xi}, M_{yi}, and M_{zi} equal zero.

Equation 90 can now be written in a more convenient form for analysis:

$$[C]\{\dot{u}\}+[K]\{u\} = \{B\} \tag{92}$$

where the vector {B} is a vector of known time histories defined by

$$\{B\} = -[M]\{\ddot{U}\}-\{M_x\}\ddot{U}_{xg}-\{M_y\}\ddot{U}_{yg}-\{M_z\}\ddot{U}_{zg} \tag{93}$$

and the damping coefficients, C_{ij}, and the stiffness coefficients, K_{ij}, are the unknowns to be determined from this identification procedure.

This completes the preprocessing required to identify the mathematical model in physical coordinates (equation 90). The following paragraphs describe the required preprocessing to identify the mathematical model in generalized coordinates (equation 91).

In order to compute the appropriate masses and time histories in generalized coordinates, assumed distorted shapes, $\tilde{\psi}_i(s)$, must be selected. One distorted shape is allowed for each independent bridge motion recorded. Although the success of this analysis procedure does not depend upon it, the accuracy of the analysis is improved if the first n assumed shapes $\tilde{\psi}_i(s)$, i=1, ..., n. most closely approximate the first n most significant normal mode shapes $\tilde{\phi}_i(s)$ i=1, ..., n. Time histories associated with the

assumed distorted shapes are computed as follows.

Let ψ_{ij} be the amplitude of the jth assumed shape at the ith transducer location in the ith transducer direction. There will exist a coordinate transformation between the vector of relative bridge accelerations, $\{\ddot{u}(t)\}$, defined earlier, and the vector of generalized accelerations, $\{\ddot{\alpha}(t)\}$, given by

$$\{\ddot{u}(t)\} = [\psi]\{\ddot{\alpha}(t)\} \tag{94}$$

As the assumed distorted shapes must be linearly independent, the inverse transformation exists:

$$\{\ddot{\alpha}(t)\} = [\psi]^{-1}\{\ddot{u}(t)\} \tag{95}$$

yielding the generalized accelerations immediately. The generalized velocities, $\{\dot{\alpha}(t)\}$, and generalized displacements, $\{\alpha(t)\}$, may be computed from the generalized accelerations, $\{\ddot{\alpha}(t)\}$, by the numerical integration procedure outlined earlier.

Given the mass distribution, M(s), and the assumed shapes, $\tilde{\psi}_i(s)$, the masses and participation factors needed for analysis are computed again by

$$m_{ij} = \int M(s)\tilde{\psi}_i(s)\cdot\tilde{\psi}_j(s)ds \tag{96}$$

$$m_{xi} = \int M(s)\tilde{\psi}_i(s)\cdot\tilde{i}ds \tag{97}$$

$$m_{yi} = \int M(s)\tilde{\psi}_i(s)\cdot\tilde{j}ds \tag{98}$$

$$m_{zi} = \int M(s)\tilde{\psi}_i(s)\cdot\tilde{k}ds \tag{99}$$

Equation 91 can now be written in the more convenient form for analysis (similar to equation 92):

$$[c]\{\dot{\alpha}\}+[k]\{\alpha\} = \{b\} \tag{100}$$

where {b} is another vector of known time histories

$$\{b\} = -[m]\{\ddot{\alpha}\}-\{m_x\}\ddot{U}_{xg}-\{m_y\}\ddot{U}_{yg}-\{m_z\}\ddot{U}_{zg} \tag{101}$$

and the damping coefficients, c_{ij}, and the stiffness coefficients, k_{ij},

are the unknowns in generalized coordinates to be identified from this identification procedure.

This completes the preprocessing required to identify the mathematical model in generalized coordinates (equation 91). The procedure to identify the coefficients in equation 92 is obviously identical to the procedure required to identify the unknown coefficients in equation 100. The latter equation, in generalized coordinates, will be used in the description of this procedure.

The unknown coefficients are found by a linear least-squares fitting procedure in the time domain. Specifically, the left-hand side of equation (100) is fitted in a least-squares sense to the right-hand side as a function of the unknown coefficients c_{ij} and k_{ij}.

Equation (100) is a system of n equations linear with respect to the unknown coefficients. The total squared error, E, is defined to be the sum of the squared errors between left-hand and right-hand sides of all equations:

$$E = \sum_{i=1}^{n} \int_{t_1}^{t_2} (c_{i1}\dot{\alpha}_1+\cdots+c_{in}\dot{\alpha}_n+k_{i1}\alpha_1+\cdots+k_{in}\alpha_n-b_i)^2 dt \qquad (102)$$

where the integral is over a time interval of any size, located anywhere in the total record, i.e., the initial conditions for the time interval analyzed are not restricted to be zero.

The squared error is minimum or maximum for c_{ij} and k_{ij} that satisfy

$$\partial E/\partial c_{ij} = 0 \qquad (103)$$

$$\partial E/\partial k_{ij} = 0 \qquad (104)$$

for all independent c_{ij} and k_{ij}.

Equations (103) and (104) when expanded yield a system of linear equations with respect to the unknowns c_{ij} and k_{ij}. The exact form of the equations depends upon the choice of independent unknowns. In general, it is assumed that $c_{ij} = c_{ji}$ and $k_{ij} = k_{ji}$. These off-diagonal terms may be evaluated independently, however, or other dependence amongst the unknowns may be assumed, if justified. The resulting system of linear equations may then be readily solved for the unknown coefficients c_{ij} and k_{ij} using any accepted procedure (Conte, 1965; Gere and Weaver, 1965).

The actual fitting procedure is performed on a high-speed digital computer. Therefore, recorded motions are analyzed as time series. Integrals, which result when equations 103 and 104 are expanded, are replaced by summations. Listings and descriptions of all computer programs necessary to perform the various phases of this analysis are included in Appendix C. Use of these programs is demonstrated in the example analyses.

C. Transformation to Normal Coordinates

Once the records are analyzed, the best-fit linear mathematical model of the dynamic bridge behavior, either equation 90 in physical coordinates or equation 91 in generalized coordinates, is completely defined. However, as discussed in Section II, this mathematical model is not in its most useful form. The model is often most informative when expressed in normal coordinates. By making this transformation no new information is obtained, but what has been obtained is simply changed into a more useful form. The transformation from generalized to normal coordinates will be used to demonstrate the procedures; the transformation from physical to normal coordinates is identical.

Related to equation 91 is the eigenvalue problem (Biggs, 1964; Clough

and Penzien 1975; Hurty and Rubinstein, 1964)

$$[[k]-\omega^2[m]]\{\theta\} = \{0\} \tag{105}$$

where ω^2 (the natural frequencies squared) are the eigenvalues and $\{\theta\}$ are the corresponding eigenvectors (natural mode shapes of the bridge in terms of generalized coordinates). Equation 105 will have a solution (non-unique) if and only if the determinant

$$|[k]-\omega^2[m]| = 0 \tag{106}$$

Equation 106 when expanded is an nth order polynomial which can be solved for the unknown natural frequencies, ω. For each natural frequency ω_i found, equation 105 can then be solved for a corresponding mode shape $\{\theta_i\}$. Since the solution to equation 105 is non-unique on satisfying equation 106, the mode shapes can be found only in terms of some arbitrary constant. Often the maximum term in $\{\theta_i\}$ is arbitrarily set to unity, but any normalization scheme is acceptable.

The mode shapes found in this manner have the desirable property of diagonalizing both the mass and stiffness matrices. Specifically, for the mode shapes arranged as columns in the transformation matrix, $[\theta]$,

$$[\theta]^T[m][\theta] = [M] \tag{107}$$

$$[\theta]^T[k][\theta] = [K] \tag{108}$$

where both $[M]$ and $[K]$ are diagonal matrices.

The matrix $[\theta]$ is in fact the desired transformation matrix defining the transformation from generalized to normal coordinates. For the transformation defined by

$$\{\alpha(t)\} = [\theta]\{\eta(t)\} \tag{109}$$

equation 91 is transformed to

$$[M]\{\ddot{\eta}\}+[C]\{\dot{\eta}\}+[K]\{\eta\} = -\{M_x\}\ddot{U}_{xg}-\{M_y\}\ddot{U}_{yg}-\{M_z\}\ddot{U}_{zg} \tag{110}$$

where $[M]$ and $[K]$ are defined by equations 107 and 108 and

$$[C] = [\theta]^T[c][\theta] \tag{111}$$

$$\{M_x\} = [\theta]^T\{m_x\} \tag{112}$$

$$\{M_y\} = [\theta]^T\{m_y\} \tag{113}$$

$$\{M_z\} = [\theta]^T\{m_z\} \tag{114}$$

The mass and stiffnesses are diagonal by definition of this transformation. The damping matrix [C] may or may not be diagonalized. Often this determination of the character of [C] is in itself an objective of the analysis, whether or not a specific modal damping ratio does exist. Again if it is assumed that [C] is diagonalized, or if the off-diagonal terms are small and can be ignored, then equation 110 premultiplied by $[M]^{-1}$ yields n uncoupled modal equations of motion

$$\ddot{\eta}_i+2\xi_i\omega_i\dot{\eta}_i+\omega_i^2\eta_i = -\gamma_{xi}\ddot{U}_{xg}-\gamma_{yi}\ddot{U}_{yg}-\gamma_{zi}\ddot{U}_{zg} \tag{115}$$

where ξ_i, ω_i, γ_{xi}, γ_{yi}, and γ_{zi} are defined from equation 17.

It is to be noted that the mode shapes, $\{\theta\}_i$, are found in terms of generalized coordinates. It is more useful to know the mode shapes, $\tilde{\phi}_i(s)$, in physical coordinates. Specifically these are given by

$$\tilde{\phi}_i(s) = \theta_{1i}\tilde{\psi}_1(s)+\theta_{2i}\tilde{\psi}_2(s)+\cdots+\theta_{ni}\tilde{\psi}_n(s) \tag{116}$$

Had the transformation been from physical to normal coordinates directly, the mode shapes $\{\theta_i\}$ would have been in physical coordinates already, and no further expansion with equation 116 would have been necessary.

This concludes the description of how strong-motion records may be analyzed with the aid of a high-speed digital computer. Many extensions to this analysis method are possible, including the assumption of nonlinear behavior, but a description of these extensions is beyond the scope of this manual.

D. Example Analyses

In all of the example analyses which follow, the motions of the highway bridges to an actual earthquake are simulated mathematically on a high-speed, digital computer. For all examples, the earthquake ground motions used were the three ground accelerations recorded at D. Johnson Ranch, Oroville, Calif., for the aftershock recorded 6 August 1975 (Sherburne and Hauge, 1975). Plots of the three recorded ground accelerations are shown in figure 13.

As a first step in the development of the simulated responses, lumped-mass models of all examples were made and their natural frequencies, natural mode shapes, and participation factors were obtained using the structural analysis program SAP IV (Bathe, Wilson, and Peterson, 1973). Modal damping ratios were assumed, and simulated bridge accelerations were computed at hypothetical instrument locations using the modal superposition technique (Biggs, 1964; Clough and Penzien, 1975; Hurty and Rubinstein, 1964). These absolute bridge accelerations were then used in the analyses which follow as though they had been recorded by strong-motion instruments.

Of the three examples which follow, the continuous two-span bridge and the triple simple span bridge are the same bridges subjected to the same ground motions as the two examples in Section III. The three-span continuous bridge example is introduced in this section.

Two-Span Continuous Bridge - The subject bridge is a simple continuous two-span highway grade separation bridge with geometry and section properties as shown in figure 17. It is a typical reinforced concrete box girder bridge supported by a single central column. Both ends of the bridge deck are restrained laterally and free to move longitudinally. The column

is fixed at its base and rigidly cast into a stiff transverse beam in the bridge deck.

The instrumentation required to identify the significant distortions of the bridge is shown in figure 41. This instrumentation is minimal and is expected to be in keeping with what has been used or what should at least be used on such a simple bridge. Again it should be noted that the abutment and column base motions have been assumed to be identical. Furthermore, no instrumentation is provided to measure relative bridge-abutment motions at either of the two ends. The instrumentation shown is designed principally for the identification of the best-fit mathematical model. The mathematical model of the bridge motion to be identified cannot be expected to be more than approximate without additional instrumentation. The expected distortions recorded by this instrumentation are the following: (1) longitudinal deck motion; (2) antisymmetric vertical flexure; (3) symmetric vertical flexure; (4) lateral flexural motion; and (5) longitudinal torsional motion. There is one, and only one, instrument to record each of these distortions. Since the spanwise distributions of these five distortions are not measured, they must be assumed. For this reason the results expected from this analysis will be approximate, unless of course the assumed spanwise distributions of the distortions happen to be exact.

Before analyzing these bridge motions, the data must be processed as described in the previous section. Let $\ddot{U}_i (i=1,2,3,4,5)$ be the five absolute accelerations recorded on the bridge.

The absolute accelerations must first be transformed into accelerations relative to the ground. If all bridge instruments are aligned with at least one ground instrument, this transformation is achieved simply through subtraction. The relative bridge accelerations, $\ddot{u}_i$ $(i=1,2,3,4,5)$, are then

$$\ddot{u}_1 = \ddot{U}_1 - \ddot{U}_{xg} \tag{117}$$

$$\ddot{u}_2 = \ddot{U}_2 - \ddot{U}_{zg} \tag{118}$$

$$\ddot{u}_3 = \ddot{U}_3 - \ddot{U}_{zg} \tag{119}$$

$$\ddot{u}_4 = \ddot{U}_4 - \ddot{U}_{yg} \tag{120}$$

$$\ddot{u}_5 = \ddot{U}_5 - \ddot{U}_{zg} \tag{121}$$

Because masses are difficult to estimate for coordinates corresponding to these instrument motions, it is advantageous, as described in earlier sections, to transform these relative accelerations to generalized accelerations in coordinates corresponding to the five principal distortions. If $\tilde{i}$, $\tilde{j}$, $\tilde{k}$, are unit vectors corresponding to the $\ddot{U}_{xg}$, $\ddot{U}_{yg}$, and $\ddot{U}_{zg}$ accelerations respectively, the five deck distortions are assumed to be

Longitudinal motion	$\tilde{\psi}_1(x) = \tilde{i}$
Antisymmetric Vertical Flexure	$\tilde{\psi}_2(x) = [\sin(\pi x/150)]\tilde{k}$
Symmetric Vertical Flexure	$\tilde{\psi}_3(x) = [\sin(\pi x/(300)+\sin(\pi x/100)]\tilde{k}$
Lateral Flexure	$\tilde{\psi}_4(x) = [\sin(\pi x/300)]\tilde{j}$
Longitudinal Torsion	$\tilde{\psi}_5(x) = [\mathrm{Sin}(\pi x/300)]\tilde{i}$

The first four of these distorted shapes are shown in figure 23 and the fifth has the identical distribution with the fourth. For $\ddot{\alpha}_i(t)$ equal to the generalized accelerations corresponding to these assumed distortions, the transformation from relative accelerations to generalized accelerations is given by equation 122. The term ψ_{55} equals $c \cdot \sin(150\pi/300)$, where c equals 18 feet, half the deck width.

$$\begin{Bmatrix} \ddot{u}_1 \\ \ddot{u}_2 \\ \ddot{u}_3 \\ \ddot{u}_4 \\ \ddot{u}_5 \end{Bmatrix} = \begin{bmatrix} 1.000 & 0 & 0 & 0 & 0 \\ 0 & 1.000 & 1.414 & 0 & 0 \\ 0 & -1.000 & 1.414 & 0 & 0 \\ 0 & 0 & 0 & 1.000 & 0 \\ 0 & 0 & 0 & 0 & 18.000 \end{bmatrix} \begin{Bmatrix} \ddot{\alpha}_1(t) \\ \ddot{\alpha}_2(t) \\ \ddot{\alpha}_3(t) \\ \ddot{\alpha}_4(t) \\ \ddot{\alpha}_5(t) \end{Bmatrix} \tag{122}$$

Equation 122 is equation 94 expanded for this example. The generalized accelerations are readily obtained from the relative accelerations by inverting the transformation above. Therefore,

$$\begin{Bmatrix} \ddot{\alpha}_1(t) \\ \ddot{\alpha}_2(t) \\ \ddot{\alpha}_3(t) \\ \ddot{\alpha}_4(t) \\ \ddot{\alpha}_5(t) \end{Bmatrix} = \begin{bmatrix} 1.000 & 0 & 0 & 0 & 0 \\ 0 & .500 & -.500 & 0 & 0 \\ 0 & .354 & .354 & 0 & 0 \\ 0 & 0 & 0 & 1.000 & 0 \\ 0 & 0 & 0 & 0 & .056 \end{bmatrix} \begin{Bmatrix} \ddot{u}_1(t) \\ \ddot{u}_2(t) \\ \ddot{u}_3(t) \\ \ddot{u}_4(t) \\ \ddot{u}_5(t) \end{Bmatrix} \tag{123}$$

The generalized accelerations must be integrated once to yield generalized velocities $\dot{\alpha}_i(t)$ and again to yield generalized displacements $\alpha_i(t)$. As shown in figure 42, linear acceleration approximation is made (acceleration is assumed to be linear between points) in the integration computations. Integrating the expression in figure 42 two times yields

$$\dot{\alpha}(t) = \dot{\alpha}_n + \ddot{\alpha}_n t + (\ddot{\alpha}_{n+1} - \ddot{\alpha}_n) t^2 / 2\Delta t \tag{124}$$

$$\alpha(t) = \alpha_n + \dot{\alpha}_n t + \ddot{\alpha}_n t^2/2 + (\ddot{\alpha}_{n+1} - \ddot{\alpha}_n) t^3 / 6\Delta t \tag{125}$$

Evaluating these expressions at $t=\Delta t$ yields the next increments in velocity and displacement

$$\dot{\alpha}_{n+1} = \dot{\alpha}_n + (\ddot{\alpha}_{n+1} + \ddot{\alpha}_n)\Delta t/2 \tag{126}$$

$$\alpha_{n+1} = \alpha_n + \dot{\alpha}_n \Delta t + (\ddot{\alpha}_n/3 + \ddot{\alpha}_{n+1}/6)\Delta t^2 \tag{127}$$

At the start of each record $\dot{\alpha}_1=0$ and $\alpha_1=0$, by assumption.

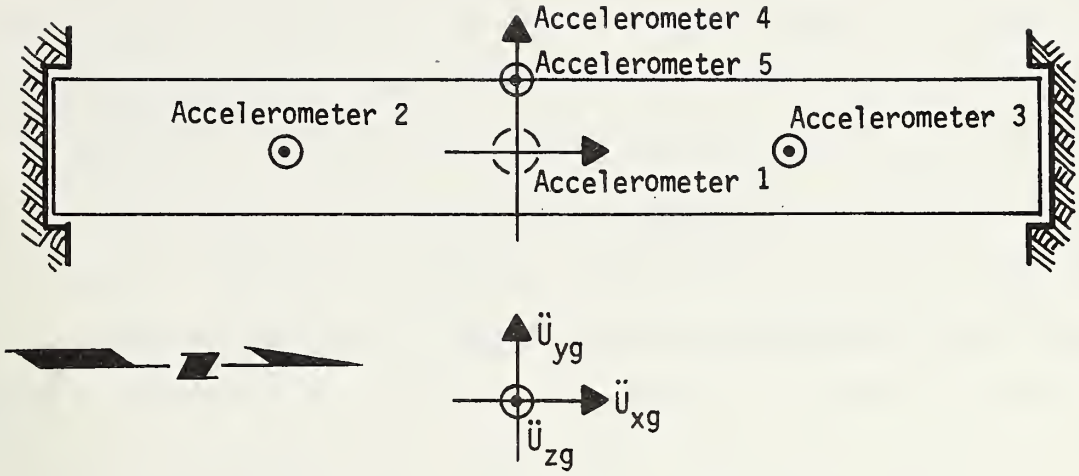

Figure 41.- Continuous two-span bridge, instrumentation plan.

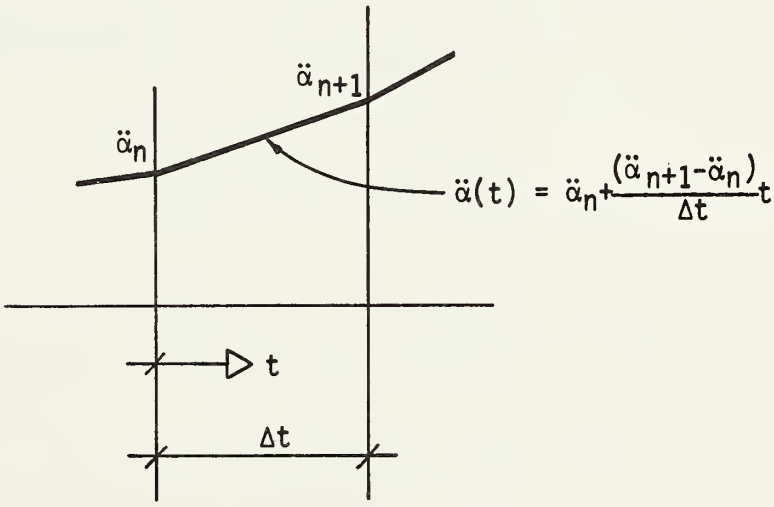

Figure 42.- Linear acceleration approximation.

Numerically integrating real records two times often amplifies tremendously the low-frequency errors in the recorded accelerations. Since all signals in the generalized velocities and displacements having frequencies low with respect to the lowest natural frequency ($<\frac{\omega_1}{4}$ or so) must be errors, they may justifiably be filtered from the records. From the relative accelerations, the lowest natural frequency of this bridge is estimated to be 2.0 cps (12.566 rps). Therefore all signals in the velocities and displacements having frequencies less than 0.5 cps (3.142 rps) are removed. A phaseless, Fast Fourier Transform filter could be used to remove these errors (Taoka, 1976). Since the time histories analyzed here are artificially generated, there are no low frequency errors after the numerical integrations, and therefore the velocities and displacements have not been filtered.

Masses for this bridge are calculated from the drawings and the unit weight of concrete, taken as 150 pcf. Therefore, they will not be considered as unknowns, but as knowns. As outlined earlier, the generalized masses corresponding to the generalized coordinate system are given by

$$m_{ij} = \int_0^{300} M(x)\tilde{\psi}_i(x)\cdot\tilde{\psi}_j(x)dx \tag{128}$$

and the participation factors by

$$m_{xi} = \int_0^{300} M(x)\tilde{\psi}_i(x)\cdot\tilde{i}dx \tag{129}$$

$$m_{yi} = \int_0^{300} M(x)\tilde{\psi}_i(x)\cdot\tilde{j}dx \tag{130}$$

$$m_{zi} = \int_0^{300} M(x)\tilde{\psi}_i(x)\cdot\tilde{k}dx \tag{131}$$

for assumed deck distortions 1 through 4. The mass of the column has been ignored in the calculations relative to the mass of the deck. Finally,

$$m_{55} = \int_0^{300} I(x)\tilde{\psi}_5(x)\cdot\tilde{\psi}_5(x)dx \tag{132}$$

Since $\tilde{\psi}_5(x)$ is a rotation, the appropriate inertia to use in the above integral is a rotational inertia per unit length of bridge, I(x). Since the ground <u>rotations</u> are assumed to equal zero, all participation factors for this mode, m_{x5} m_{y5}, m_{z5}, will be zero. All off-diagonal mass terms with respect to the torsional mode, and all three participation factors for this mode are zero. These generalized masses and participation factors expanded for this example bridge are, for M(x)=0.3295 kip-sec^2/ft^2 and I(x) = 50.939 kip-sec^2,

$$[m] = \begin{bmatrix} 98.85 & 0 & 0 & 0 & 0 \\ 0 & 49.42 & 0 & 0 & 0 \\ 0 & 0 & 98.85 & 0 & 0 \\ 0 & 0 & 0 & 49.42 & 0 \\ 0 & 0 & 0 & 0 & 7641. \end{bmatrix}$$

$$\{m_x\} = \begin{Bmatrix} 98.85 \\ 0 \\ 0 \\ 0 \\ 0 \end{Bmatrix} \quad \{m_y\} = \begin{Bmatrix} 0 \\ 0 \\ 0 \\ 62.93 \\ 0 \end{Bmatrix} \quad \{m_z\} = \begin{Bmatrix} 0 \\ 0 \\ 83.90 \\ 0 \\ 0 \end{Bmatrix}$$

The final preprocessing required before analysis is to combine all inertial time histories into a single vector

$$\{b(t)\} = -[m]\{\ddot{\alpha}(t)\}-\{m_x\}\ddot{U}_{xg}(t)-\{m_y\}\ddot{U}_{yg}(t)-\{m_z\}\ddot{U}_{zg}(t) \tag{133}$$

Specifically,

$$b_1(t) = -98.85\ddot{\alpha}_1(t)-98.85\ddot{U}_{xg}(t)$$

$$b_2(t) = -49.42\ddot{\alpha}_2(t)$$

$$b_3(t) = -98.85\ddot{\alpha}_3(t)-83.90\ddot{U}_{zg}(t)$$

$$b_4(t) = -49.42\ddot{\alpha}_4(t)-62.93\ddot{U}_{yg}(t)$$

$$b_5(t) = -7641.\ddot{\alpha}_5(t)$$

All input quantities are in suitable form for analysis, namely

$$\begin{array}{l} c_{11}\dot{\alpha}_1+ \cdots +c_{15}\dot{\alpha}_5+k_{11}\alpha_1+ \cdots +k_{15}\alpha_5 = b_1 \\ c_{12}\dot{\alpha}_1+ \cdots +c_{25}\dot{\alpha}_5+k_{12}\alpha_1+ \cdots +k_{25}\alpha_5 = b_2 \\ \quad\vdots \qquad\qquad \vdots \qquad \vdots \qquad\qquad \vdots \qquad \vdots \\ c_{15}\dot{\alpha}_1+ \cdots +c_{55}\dot{\alpha}_5+k_{15}\alpha_1+ \cdots +k_{55}\alpha_5 = b_5 \end{array} \tag{134}$$

where the c_{ij} and k_{ij} (both assumed symmetric) are the unknown damping and stiffness coefficients to be found.

Although the analysis may be performed at this stage, numerical errors may be reduced if motions known to be decoupled are in fact decoupled before analysis. This is true because even though the motions are decoupled (motions in one direction entirely independent from motions in another direction) the actual time histories representing those motions may be correlated. Any correlations existing between uncoupled motions will lead to numerical errors in the analysis.

This example problem may justifiably be separated into three uncoupled problems, due to the symmetry in the structure. The three uncoupled problems become the following: (1) longitudinal motion and antisymmetric vertical flexure; (2) symmetric vertical flexure; and (3) lateral motion and longitudinal torsion. Mathematically this division corresponds to dividing the above system of equations, equation 134, into the following

sets:

$$c_{11}\dot{\alpha}_1+c_{12}\dot{\alpha}_2+k_{11}\alpha_1+k_{12}\alpha_2 = b_1$$
$$c_{12}\dot{\alpha}_1+c_{22}\dot{\alpha}_2+k_{12}\alpha_1+k_{22}\alpha_2 = b_2 \tag{135}$$

for longitudinal motion and antisymmetric vertical flexure;

$$c_{33}\dot{\alpha}_3+k_{33}\alpha_3 = b_3 \tag{136}$$

for symmetric vertical flexure; and

$$c_{44}\dot{\alpha}_4+c_{45}\dot{\alpha}_5+k_{44}\alpha_4+k_{45}\alpha_5 = b_4$$
$$c_{45}\dot{\alpha}_4+c_{55}\dot{\alpha}_5+k_{45}\alpha_4+k_{55}\alpha_5 = b_5 \tag{137}$$

for lateral motion and longitudinal torsion. All other coefficients c_{ij} and k_{ij} must equal zero due to symmetry in the bridge.

Subroutine FIT was used to identify the best-fit values of the unknown damping coefficients, c_{ij} and stiffness coefficients, k_{ij}. Results of the analyses, corresponding to equations 135, 136, and 137 are as follows:

$$69.6\dot{\alpha}_1-5.48\dot{\alpha}_2+27{,}900\alpha_1-5530\alpha_2 = -98.85\ddot{\alpha}_1-98.85\ddot{U}_{xg}$$
$$-5.48\dot{\alpha}_1+23.4\dot{\alpha}_2-5530\alpha_1+8400\alpha_2 = -49.42\ddot{\alpha}_2 \tag{138}$$

and

$$69.8\dot{\alpha}_3+31{,}300\alpha_3 = -98.85\ddot{\alpha}_3-83.90\ddot{U}_{zg} \tag{139}$$

and

$$49.4\dot{\alpha}_4+338\dot{\alpha}_5+39{,}400\alpha_4+369{,}000\alpha_5 = -49.42\ddot{\alpha}_4-62.93\ddot{U}_{yg}$$
$$338\dot{\alpha}_4+16{,}800\dot{\alpha}_5+369{,}000\alpha_4+16{,}600{,}000\alpha_5 = -7641\ddot{\alpha}_5 \tag{140}$$

Once again these equations of motion may be recombined in the more usual form

$$[m]\{\ddot{\alpha}\}+[c]\{\dot{\alpha}\}+[k]\{\alpha\} = -\{m_x\}\ddot{U}_{xg}-\{m_y\}\ddot{U}_{yg}-\{m_z\}\ddot{U}_{zg} \tag{141}$$

where

$$[m] = \begin{bmatrix} 98.85 & 0 & 0 & 0 & 0 \\ 0 & 49.42 & 0 & 0 & 0 \\ 0 & 0 & 98.85 & 0 & 0 \\ 0 & 0 & 0 & 49.42 & 0 \\ 0 & 0 & 0 & 0 & 7641 \end{bmatrix}$$

$$[c] = \begin{bmatrix} 69.6 & -5.48 & 0 & 0 & 0 \\ -5.48 & 23.4 & 0 & 0 & 0 \\ 0 & 0 & 69.8 & 0 & 0 \\ 0 & 0 & 0 & 49.4 & 338. \\ 0 & 0 & 0 & 338. & 16,800 \end{bmatrix}$$

$$[k] = \begin{bmatrix} 27,900 & -5530 & 0 & 0 & 0 \\ -5530 & 8400 & 0 & 0 & 0 \\ 0 & 0 & 31,300 & 0 & 0 \\ 0 & 0 & 0 & 39,400 & 369,000 \\ 0 & 0 & 0 & 369,000 & 16,600,000 \end{bmatrix}$$

and

$$\{m_x\} = \begin{Bmatrix} 98.85 \\ 0 \\ 0 \\ 0 \\ 0 \end{Bmatrix} \{m_y\} = \begin{Bmatrix} 0 \\ 0 \\ 0 \\ 62.93 \\ 0 \end{Bmatrix} \{m_z\} = \begin{Bmatrix} 0 \\ 0 \\ 83.90 \\ 0 \\ 0 \end{Bmatrix}$$

At this point the mathematical model of the bridge has been entirely defined from the analysis of the strong-motion records. The model, however, is not in its most useful form. It is much more useful for comparative

purposes to transform these equations of motion into uncoupled equations of motion in terms of normal coordinates. At this time we do not know if such a transformation will exist, but we can find a coordinate transformation which will diagonalize the mass and stiffness matrices (Biggs, 1964; Clough and Penzien, 1975; Hurty and Rubinstein, 1964); there is no guarantee, however, that the transformation will also diagonalize the damping matrix.

A transformation matrix is found which transforms the above equations of motion from generalized coordinates $\{\alpha\}$ to normal coordinates $\{\eta\}$

$$\{\alpha\} = [\theta]\{\eta\} \tag{142}$$

by solving the related eigenvalue problem (Biggs, 1964; Clough and Penzien, 1975; Hurty and Rubinstein, 1964):

$$[[k]-\omega^2[m]]\{\theta\} = \{0\} \tag{143}$$

The transformation matrix (matrix of eigenvectors arranged as columns) found is

$$[\theta] = \begin{bmatrix} 1.00 & 1.00 & 0 & 0 & 0 \\ 2.74 & -.730 & 0 & 0 & 0 \\ 0 & 0 & .707 & 0 & 0 \\ 0 & 0 & 0 & 1.00 & 1.00 \\ 0 & 0 & 0 & -.0302 & .214 \end{bmatrix}$$

The equations of motion, equation 141, may then be transformed into normal equations of motion in the following manner:

$$[m]\{\ddot{\alpha}\}+[c]\{\dot{\alpha}\}+[k]\{\alpha\} = -\{m_x\}\ddot{U}_{xg}-\{m_y\}\ddot{U}_{yg}-\{m_z\}\ddot{U}_{zg} \tag{144}$$

$$[m][\theta]\{\ddot{\eta}\}+[c][\theta]\{\dot{\eta}\}+[k][\theta]\{\eta\} = -\{m_x\}\ddot{U}_{xg}-\{m_y\}\ddot{U}_{yg}-\{m_z\}\ddot{U}_{zg} \tag{145}$$

$$[\theta]^T[m][\theta]\{\ddot{\eta}\}+[\theta]^T[c][\theta]\{\dot{\eta}\}+[\theta]^T[k][\theta]\{\eta\} = -[\theta]^T\{m_x\}\ddot{U}_{xg}-[\theta]^T m_y \ddot{U}_{yg}-[\theta]^T\{m_z\}\ddot{U}_{zg} \tag{146}$$

For the obvious definitions this last equation can be rewritten as

$$[M]\{\ddot{\eta}\}+[C]\{\dot{\eta}\}+[K]\{\eta\} = -\{M_x\}\ddot{U}_{xg}-\{M_y\}\ddot{U}_{yg}-\{M_z\}\ddot{U}_{zg} \tag{147}$$

where

$$[M] = \begin{bmatrix} 469.9 & 0 & 0 & 0 & 0 \\ 0 & 125.2 & 0 & 0 & 0 \\ 0 & 0 & 49.42 & 0 & 0 \\ 0 & 0 & 0 & 56.39 & 0 \\ 0 & 0 & 0 & 0 & 399.3 \end{bmatrix}$$

$$[C] = \begin{bmatrix} 215.3 & 11.78 & 0 & 0 & 0 \\ 11.78 & 90.07 & 0 & 0 & 0 \\ 0 & 0 & 34.89 & 0 & 0 \\ 0 & 0 & 0 & 44.31 & 2.930 \\ 0 & 0 & 0 & 2.930 & 963.4 \end{bmatrix}$$

$$[K] = \begin{bmatrix} 60{,}660 & 0 & 0 & 0 & 0 \\ 0 & 40{,}450 & 0 & 0 & 0 \\ 0 & 0 & 15{,}650 & 0 & 0 \\ 0 & 0 & 0 & 32{,}250 & 0 \\ 0 & 0 & 0 & 0 & 957{,}500 \end{bmatrix}$$

$$\{M_x\} = \begin{Bmatrix} 98.85 \\ 98.85 \\ 0 \\ 0 \\ 0 \end{Bmatrix} \quad \{M_y\} = \begin{Bmatrix} 0 \\ 0 \\ 0 \\ 62.93 \\ 62.93 \end{Bmatrix} \quad \{M_z\} = \begin{Bmatrix} 0 \\ 0 \\ 59.32 \\ 0 \\ 0 \end{Bmatrix}$$

As can be seen, the off-diagonal damping terms are small but are not

negligible. The off-diagonal damping forces, when compared to inertial and restoring forces, are negligible, and so the off-diagonal damping terms in the end will be ignored.

The system of equations of motion in normal coordinates can be rewritten as five uncoupled single-degree-of-freedom equations of motion (each equation has been divided by its mass):

$$\ddot{\eta}_1+0.458\dot{\eta}_1+129.1\eta_1 = -0.210\ddot{U}_{xg} \tag{148}$$

$$\ddot{\eta}_2+0.719\dot{\eta}_2+323.1\eta_2 = -0.790\ddot{U}_{xg} \tag{149}$$

$$\ddot{\eta}_3+0.706\dot{\eta}_3+316.7\eta_3 = -1.200\ddot{U}_{zg} \tag{150}$$

$$\ddot{\eta}_4+0.786\dot{\eta}_4+571.9\eta_4 = -1.116\ddot{U}_{yg} \tag{151}$$

$$\ddot{\eta}_5+2.413\dot{\eta}_5+2398.\eta_5 = -0.158\ddot{U}_{yg} \tag{152}$$

Each equation is compared to the standard form (equation 17)

$$\ddot{\eta}+2\xi\omega\dot{\eta}+\omega^2\eta = -\gamma_x\ddot{U}_{xg}-\gamma_y\ddot{U}_{yg}-\gamma_z\ddot{U}_{zg} \tag{153}$$

where again

ω = natural circular frequency of vibration (radians/second),

ξ = damping ratio, and

γ = participation factor

For the natural period, $T=2\pi/\omega$, the final results are found and are given in table 9. The natural modes of vibration are obtained from the eigenvectors (columns in the transformation matrix $[\theta]$), and the assumed shapes of distortion, $\tilde{\psi}_i(x)$. Specifically, the ith mode shape in physical coordinates is given by

$$\tilde{\phi}_i(x) = \theta_{1i}\tilde{\psi}_1(x)+\theta_{2i}\tilde{\psi}_2(x)+ \cdots +\theta_{5i}\tilde{\psi}_5(x) \tag{154}$$

The natural modes of vibration found from this identification procedure are shown in figure 43.

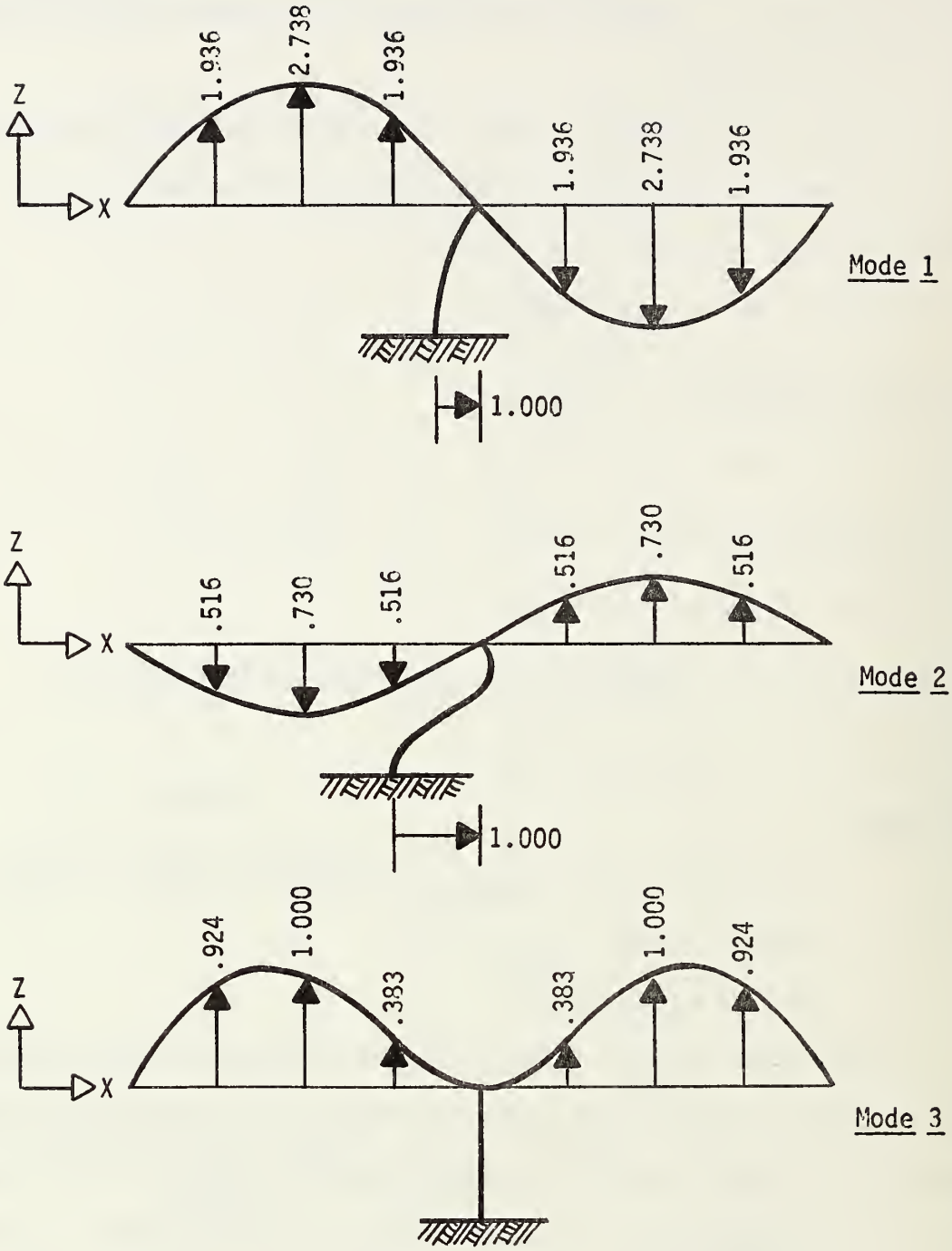

Figure 43.- Continuous two-span bridge, mode shapes found from analysis.

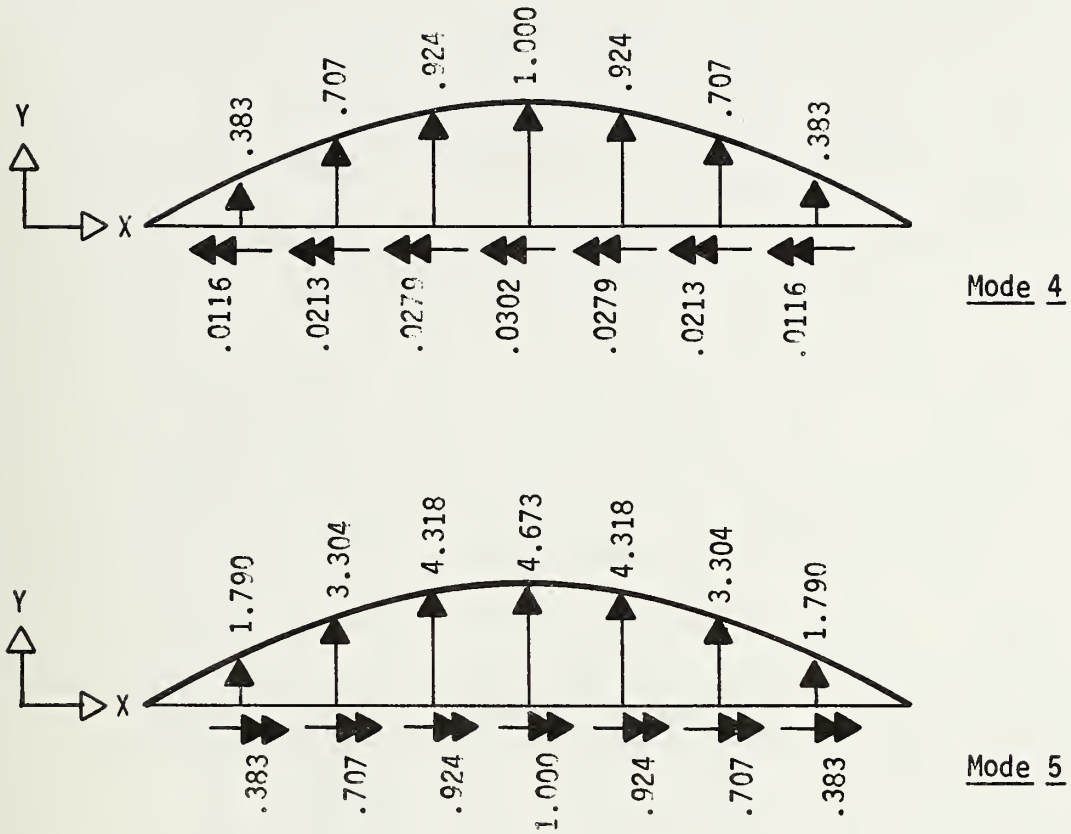

Figure 43 (continued).- Continuous two-span bridge, mode shapes found from analysis.

This completes the analysis for the best-fit mathematical model for this bridge from the strong-motion records alone. Now that the modal properties have been identified, forces in various elements of the bridge may be found in exactly the same manner as was described in Section III. For comparison, the exact modal properties are given in table 10, and the exact mode shapes are shown in figure 44. These properties were used to generate the hypothetical responses used to demonstrate this analysis.

In comparing the tabulated values identified from the time histories to the actual values used to create the theoretical time histories, one can see that the values identified are quite acceptable for the first three modes. On the other hand, the values identified for modes 4 and 5 are somewhat in error. These discrepancies are due to the large errors in the shapes of the assumed lateral and torsional distortions. Better results may have resulted had the assumed distortions more closely resembled the actual modes of vibration. These differences, however, would never have been detected without further instrumentation. An additional transverse and vertical accelerometer at midspan would most likely improve the accuracy of the fourth and fifth modal properties found.

Although the fifth mode shape identified looks particularly erroneous, in fact it is quite reasonable. Mode 5 is primarily a torsional mode. Although the numerical amplitudes of rotation are comparable (actually slightly smaller) than the numerical values of lateral translation for the actual mode shape, the vertical translations at the bridge deck edges due to the torsional displacements are in fact very large. Specifically for a rotation of unity, the vertical displacement at the deck edges is ±18.000. A comparison of the identified and actual mode 5 deck rotations is fairly reasonable. It can therefore be concluded that the <u>significant</u> deck

Mode	ω(rps)	T(sec)	ξ(%)	γ_x	γ_y	γ_z
1	11.362	.553	2.0	.210	0	0
2	17.975	.350	2.0	.790	0	0
3	17.796	.353	2.0	0	0	1.200
4	23.914	.263	1.6	0	1.116	0
5	48.969	.128	2.5	0	.034	0

Table 9.- Continuous Two-Span Bridge Model, Parameters Identified

Mode	ω(rps)	T(sec)	ξ(%)	γ_x	γ_y	γ_z
1	11.410	.551	2.0	.189	0	0
2	18.340	.343	2.0	.780	0	0
3	17.770	.354	2.0	0	0	1.208
4	23.880	.263	2.0	0	1.062	0
5	46.840	.134	2.0	0	.027	0

Table 10.- Continuous Two-Span Bridge , Exact Model Parameters

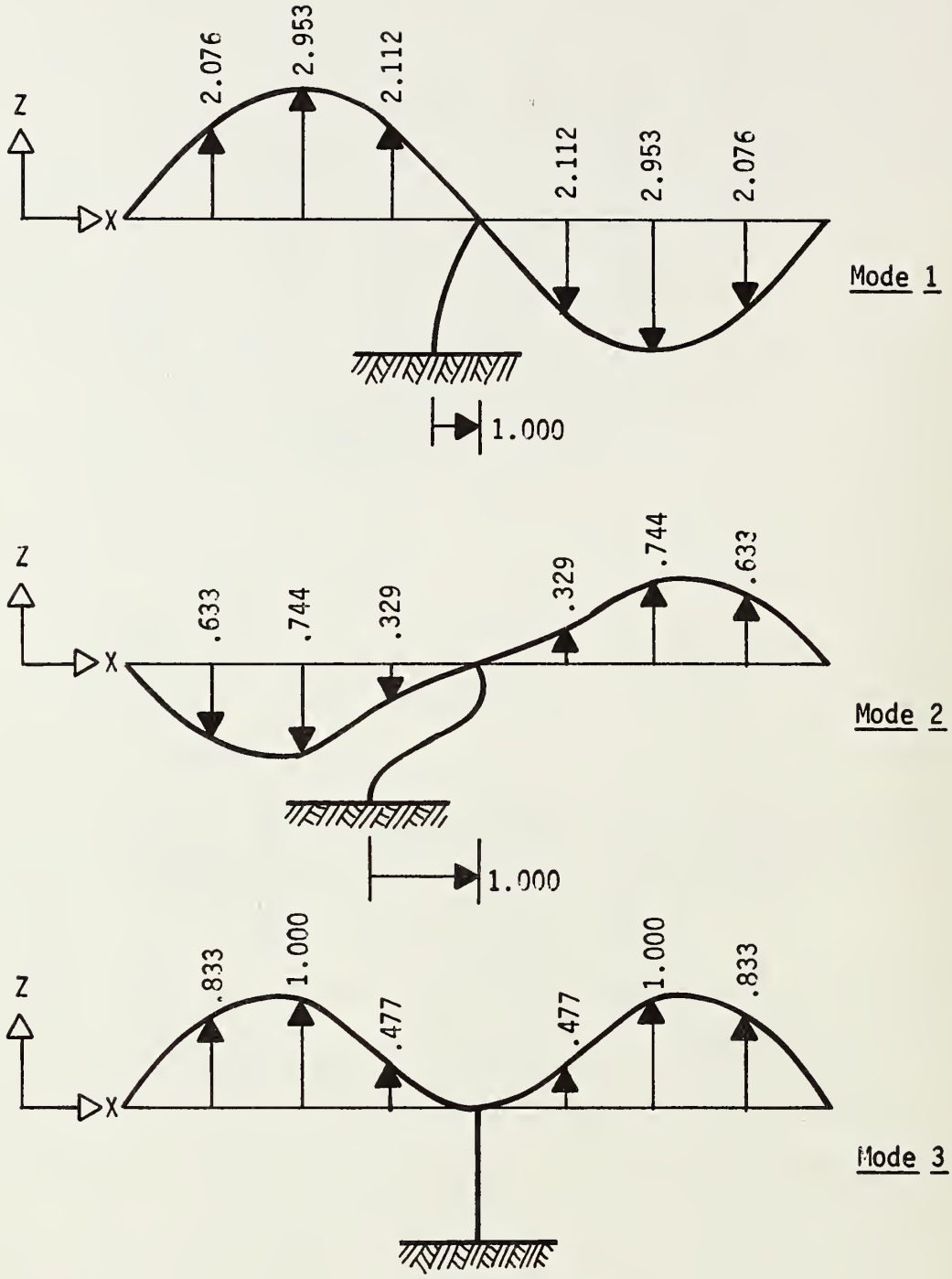

Figure 44.- Continuous two-span bridge, actual mode shapes.

Figure 44 (continued).- Continuous two-span bridge, actual mode shapes.

displacements, even for mode 5, have been found reasonably accurately.

Three-Span Simply Supported Bridge

The subject bridge for this example is a straight highway grade separation bridge with three simple spans. The geometry and properties of the bridge as well as the accelerometer locations are shown in figure 12. The instruments are on the pier caps and are assumed to sense the motion of the pinned ends of the simple spans. All spans are assumed to be restrained laterally.

Bridge accelerations $\ddot{u}_i(t)$ relative to the ground are first computed from the recorded bridge accelerations $\ddot{U}_i(t)$ and the ground accelerations. Specifically,

$$\ddot{u}_1(t) = \ddot{U}_1(t)-\ddot{U}_{xg}(t) \tag{155}$$

$$\ddot{u}_2(t) = \ddot{U}_2(t)-\ddot{U}_{xg}(t) \tag{156}$$

$$\ddot{u}_3(t) = \ddot{U}_3(t)-\ddot{U}_{yg}(t) \tag{157}$$

$$\ddot{u}_4(t) = \ddot{U}_4(t)-\ddot{U}_{yg}(t) \tag{158}$$

Since masses corresponding to each recorded motion may easily be estimated from the bridge plans, there is no need to transform the relative accelerations to a generalized coordinate system. Therefore parameters of a lumped mass model in physical coordinates are to be identified.

As described before, the relative accelerations $\ddot{u}_i(t)$ are now numerically integrated to yield the relative bridge velocities $\dot{u}_i(t)$ and relative displacements $u_i(t)$. Again, if these had been computed from actually recorded bridge accelerations, low-frequency errors would undoubtably exist in the velocities and displacements. These errors must be filtered from the bridge velocities and displacements as suggested in the first example. Since no low-frequency errors exist in these

artificially generated time histories, they have not been filtered; the time histories are already in suitable form for analysis.

In addition to these time histories, bridge masses and participation factors are needed. It is assumed that it is sufficiently accurate to lump bridge deck masses at the pier caps corresponding to the accelerometer coordinates. Note that lateral flexural motion of the individual spans have been ignored relative to the rigid body translations. In any event, such flexural distortions cannot be detected with this instrumentation. The masses corresponding to coordinates at the instrument locations have been found for this example and are shown graphically in figure 15 (M_4 is equal to M_3).

$$[M] = \begin{bmatrix} 64.463 & 0 & 0 & 0 \\ 0 & 26.588 & 0 & 0 \\ 0 & 0 & 34.163 & 0 \\ 0 & 0 & 0 & 34.163 \end{bmatrix}$$

Since the masses are assumed to be lumped at the degrees of freedom, the participation factors equal the corresponding masses and are given by

$$\{M_x\} = \begin{Bmatrix} 64.463 \\ 26.588 \\ 0 \\ 0 \end{Bmatrix} \qquad \{M_y\} = \begin{Bmatrix} 0 \\ 0 \\ 34.163 \\ 34.163 \end{Bmatrix}$$

There are no vertical degrees of freedom, and the horizontal degrees of freedom corresponding to each accelerometer direction are not excited by vertical ground motion; therefore all M_{zi} equal zero.

For the time histories defined by

$$B_1(t) = -64.463[\ddot{u}_1(t)+\ddot{U}_{xg}(t)]$$

$$B_2(t) = -26.588[\ddot{u}_2(t)+\ddot{U}_{xg}(t)]$$

$$B_3(t) = -34.163[\ddot{u}_3(t)+\ddot{U}_{yg}(t)]$$

$$B_4(t) = -34.163[\ddot{u}_4(t)+\ddot{U}_{yg}(t)]$$

the system of equations to be analyzed by this method is

$$\begin{array}{ccccccccc} C_{11}\dot{u}_1 & + \cdots & +C_{14}\dot{u}_4 & +K_{11}u_1 & + \cdots & +K_{14}u_4 & = B_1 \\ \vdots & \vdots & \vdots & & \vdots & & \vdots \\ C_{14}\dot{u}_1 & + \cdots & +C_{44}\dot{u}_4 & +K_{14}u_1 & + \cdots & +K_{44}u_4 & = B_4 \end{array} \tag{159}$$

Again, this system of equations can be simplified by anticipating structural behavior. By assumption there is no inertial coupling (no off-diagonal mass terms), and by inspection, there will be no stiffness coupling (a force applied in any individual accelerometer direction will produce a distortion only in that individual direction). Furthermore, because the example bridge really consists of three independent simple spans there is not likely to be any significant damping coupling. Therefore, all off-diagonal damping and stiffness coefficients can reasonably be assumed to equal zero, and the system of equations to be identified reduces to the following four uncoupled single-degree-of-freedom equations of motion:

$$C_{11}\dot{u}_1+K_{11}u_1 = B_1 \tag{160}$$

$$C_{22}\dot{u}_2+K_{22}u_2 = B_2 \tag{161}$$

$$C_{33}\dot{u}_3+K_{33}u_3 = B_3 \tag{162}$$

$$C_{44}\dot{u}_4+K_{44}u_4 = B_4 \tag{163}$$

Subroutine FIT was used to identify the unknown coefficients, and yielded, after a slight rearrangement of terms in the $B_i(t)$,

$$64.463\ddot{u}_1+63.1\dot{u}_1+9650u_1 = -64.463\ddot{U}_{xg} \tag{164}$$

$$26.588\ddot{u}_2+40.5\dot{u}_2+9650u_2 = -26.588\ddot{U}_{xg} \tag{165}$$

$$34.163\ddot{u}_3+45.9\dot{u}_3+38{,}600u_3 = -34.163\ddot{U}_{yg} \tag{166}$$

$$34.163\ddot{u}_4+45.9\dot{u}_4+38{,}600u_4 = -34.163\ddot{U}_{yg} \tag{167}$$

By comparing these single-degree-of-freedom equations of motion, equations 164 to 167, to the standard form, equation 153, the model parameters are identified and shown in table 11. For comparison, the exact values which were used to generate the artificial bridge motions are given in table 12. In essence, the results are identical.

Three-Span Continuous Bridge

The subject bridge for this example is a continuous box girder bridge of three spans. The geometry of this reinforced concrete bridge is shown in figure 45.

Because the column heights vary, the response of this bridge is not expected to be symmetrical. Also, because the ends of the bridge are torsionally restrained, as well as at the column pairs, no significant longitudinal torsional deck motion is expected. Therefore, adequate instrumentation to describe all significant structure distortions is given in figure 46. All structure instruments are located at mid-span positions.

If $U_i(t)(i=1,\cdots,7)$ are the recorded absolute accelerations, relative structure accelerations are computed as

$$\ddot{u}_1(t) = \ddot{U}_1(t)-\ddot{U}_{yg}(t) \tag{168}$$

$$\ddot{u}_2(t) = \ddot{U}_2(t)-\ddot{U}_{yg}(t) \tag{169}$$

$$\ddot{u}_3(t) = \ddot{U}_3(t)-\ddot{U}_{yg}(t) \tag{170}$$

$$\ddot{u}_4(t) = \ddot{U}_4(t)-\ddot{U}_{xg}(t) \tag{171}$$

$$\ddot{u}_5(t) = \ddot{U}_5(t)-\ddot{U}_{zg}(t) \tag{172}$$

Mode	ω(rps)	T(sec)	ξ(%)	γ_x	γ_y
1	12.235	.514	4.0	1.000	0
2	19.051	.330	4.0	1.000	0
3	33.614	.187	2.0	0	1.000
4	33.614	.187	2.0	0	1.000

Table 11.- Three-Span Simply Supported Bridge, Model Parameters Identified

Mode	ω(rps)	T(sec)	ξ(%)	γ_x	γ_y
1	12.236	.513	4.0	1.000	0
2	19.052	.330	4.0	1.000	0
3	33.615	.187	2.0	0	1.000
4	33.615	.187	2.0	0	1.000

Table 12.- Three-Span Simply Supported Bridge, Exact Model Parameters

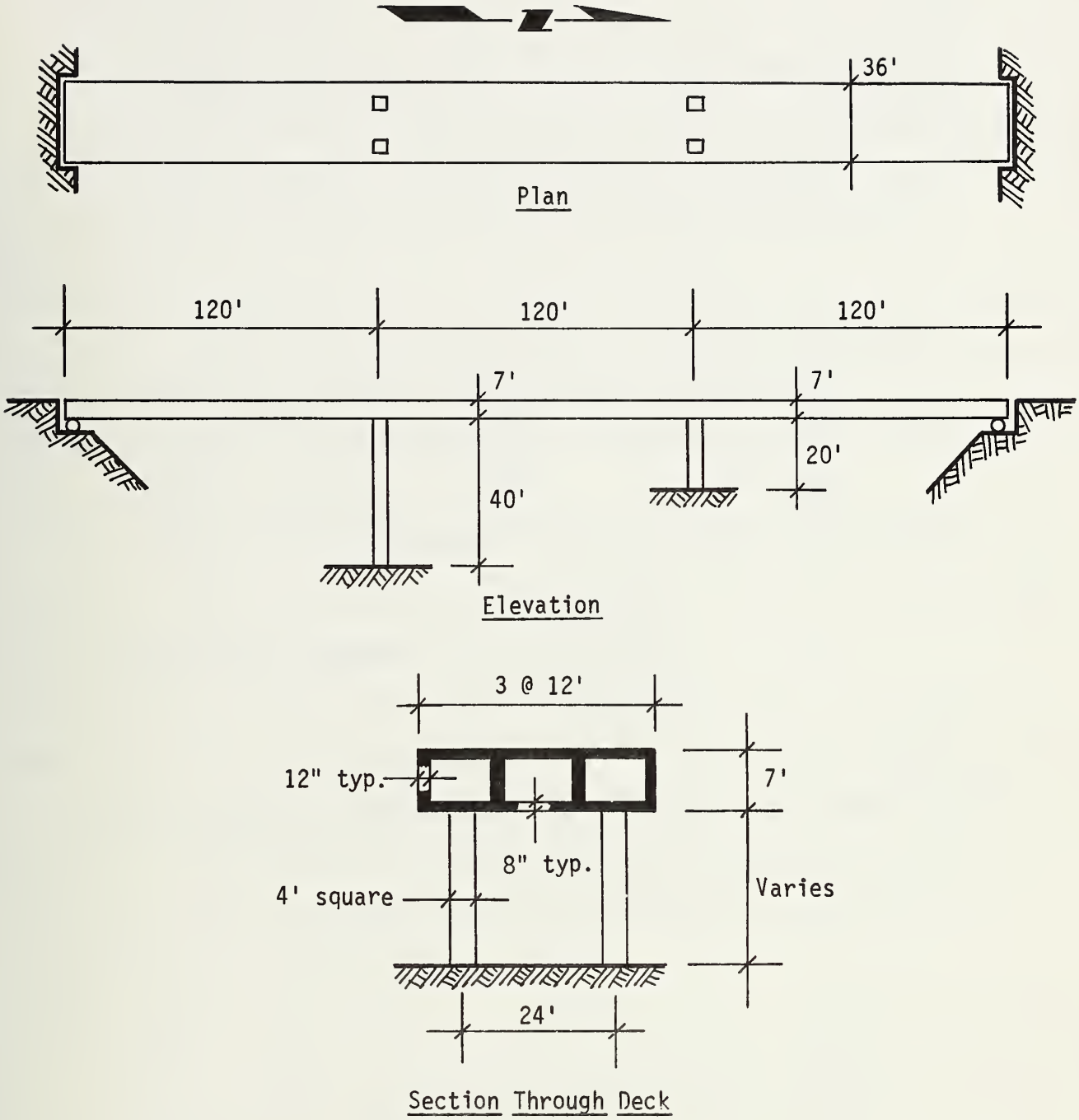

Figure 45.- Continuous three-span bridge.

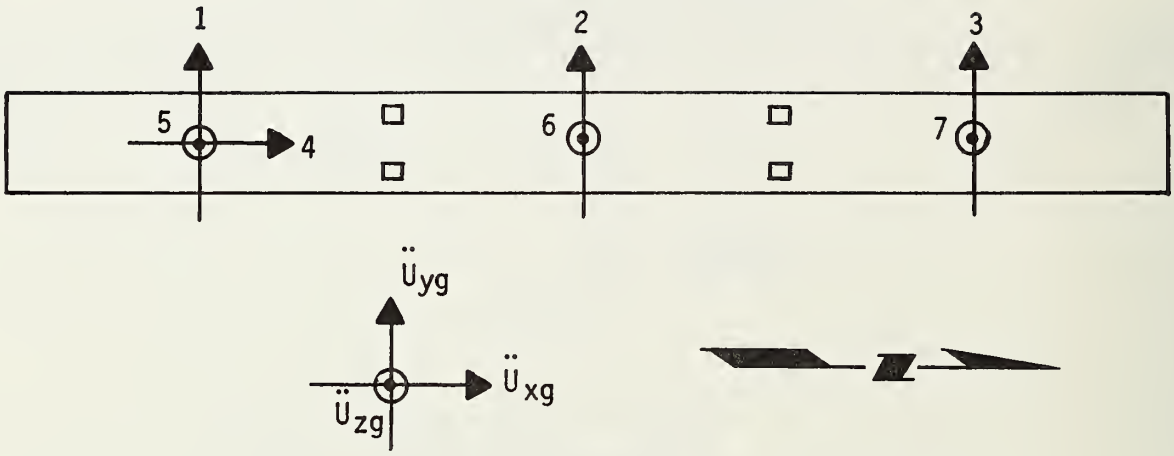

Figure 46.- Continuous three-span bridge, instrumentation plan.

$$\ddot{u}_6(t) = \ddot{U}_6(t) - \ddot{U}_{zg}(t) \tag{173}$$

$$\ddot{u}_7(t) = \ddot{U}_7(t) - \ddot{U}_{zg}(t) \tag{174}$$

As described previously, relative velocities $\dot{u}_i$ and relative displacements u_i are numerically calculated from the relative accelerations computed above. Again, if the data were real, some filtering would undoubtedly be required to remove amplified low-frequency errors in the computed velocities and displacements.

For this example, a lumped mass approach is taken and coordinates describing structure distortions (relative motions) corresponding to accelerometer directions and locations are assumed. All axial distortions of the columns and bridge deck are ignored.

Again the mass matrix is computed from bridge geometry and material properties. Masses associated with the three lateral degrees of freedom are assumed to equal one-third of the total bridge mass; the mass associated with the longitudinal degree of freedom is assumed to equal the total bridge mass; and masses associated with the three vertical degrees of freedom are assumed to equal half of each span mass. Masses are chosen so that the kinetic energy in the lumped-mass system approximately equals the kinetic energy in the actual bridge, when vibrating. The mass matrix and vectors of participation factors become

$$[M] = \begin{bmatrix} 39.54 & 0 & 0 & 0 & 0 & 0 & 0 \\ 0 & 39.54 & 0 & 0 & 0 & 0 & 0 \\ 0 & 0 & 39.54 & 0 & 0 & 0 & 0 \\ 0 & 0 & 0 & 118.62 & 0 & 0 & 0 \\ 0 & 0 & 0 & 0 & 19.77 & 0 & 0 \\ 0 & 0 & 0 & 0 & 0 & 19.77 & 0 \\ 0 & 0 & 0 & 0 & 0 & 0 & 19.77 \end{bmatrix}$$

$$\{M_x\} = \begin{Bmatrix} 0 \\ 0 \\ 0 \\ 118.62 \\ 0 \\ 0 \\ 0 \end{Bmatrix} \qquad \{M_y\} = \begin{Bmatrix} 39.54 \\ 39.54 \\ 39.54 \\ 0 \\ 0 \\ 0 \\ 0 \end{Bmatrix} \qquad \{M_z\} = \begin{Bmatrix} 0 \\ 0 \\ 0 \\ 0 \\ 19.77 \\ 19.77 \\ 19.77 \end{Bmatrix}$$

Lumped-mass models are always inertially uncoupled, and so all off-diagonal mass terms by definition equal zero.

For the time histories defined by

$$B_1(t) = -39.54\ [\ddot{u}_1(t)+\ddot{U}_{yg}(t)]$$

$$B_2(t) = -39.54\ [\ddot{u}_2(t)+\ddot{U}_{yg}(t)]$$

$$B_3(t) = -39.54\ [\ddot{u}_3(t)+\ddot{U}_{yg}(t)]$$

$$B_4(t) = -118.62[\ddot{u}_4(t)+\ddot{U}_{xg}(t)]$$

$$B_5(t) = -19.77[\ddot{u}_5(t)+\ddot{U}_{zg}(t)]$$

$$B_6(t) = -19.77[\ddot{u}_6(t)+\ddot{U}_{zg}(t)]$$

$$B_7(t) = -19.77[\ddot{u}_7(t)+\ddot{U}_{zg}(t)]$$

the system of equations describing the bridge motions becomes

$$\begin{matrix} C_{11}\dot{u}_1+ \cdots +C_{17}\dot{u}_7+K_{11}u_1+ \cdots +K_{17}u_7 = B_1 \\ \vdots \qquad\qquad \vdots \qquad \vdots \qquad\qquad \vdots \qquad \vdots \\ C_{17}\dot{u}_1+ \cdots +C_{77}\dot{u}_7+K_{17}u_1+ \cdots +K_{77}u_7 = B_7 \end{matrix} \tag{175}$$

Numerical errors in the solution for the unknown parameters C_{ij} and K_{ij} again are greatly reduced if the motions known to be uncoupled are analyzed as such. It is assumed, from the geometry of the bridge and anticipated structural behavior, that the lateral or transverse response will be

independent of the longitudinal and vertical motion. Therefore, the equations of motion describing the bridge motions can be separated into the following two systems:

$$
\begin{aligned}
C_{11}\dot{u}_1+C_{12}\dot{u}_2+C_{13}\dot{u}_3+K_{11}u_1+K_{12}u_2+K_{13}u_3 &= B_1 \\
C_{12}\dot{u}_1+C_{22}\dot{u}_2+C_{23}\dot{u}_3+K_{12}u_1+K_{22}u_2+K_{23}u_3 &= B_2 \\
C_{13}\dot{u}_1+C_{23}\dot{u}_2+C_{33}\dot{u}_3+K_{13}u_1+K_{23}u_2+K_{33}u_3 &= B_3
\end{aligned}
\tag{176}
$$

and

$$
\begin{aligned}
C_{44}\dot{u}_4+C_{45}\dot{u}_5+C_{46}\dot{u}_6+C_{47}\dot{u}_7+K_{44}u_4+K_{45}u_5+K_{46}u_6+K_{47}u_7 &= B_4 \\
C_{45}\dot{u}_4+C_{55}\dot{u}_5+C_{56}\dot{u}_6+C_{57}\dot{u}_7+K_{45}u_4+K_{55}u_5+K_{56}u_6+K_{57}u_7 &= B_5 \\
C_{46}\dot{u}_4+C_{56}\dot{u}_5+C_{66}\dot{u}_6+C_{67}\dot{u}_7+K_{46}u_4+K_{56}u_5+K_{66}u_6+K_{67}u_7 &= B_6 \\
C_{47}\dot{u}_4+C_{57}\dot{u}_5+C_{67}\dot{u}_6+C_{77}\dot{u}_7+K_{47}u_4+K_{57}u_5+K_{67}u_6+K_{77}u_7 &= B_7
\end{aligned}
\tag{177}
$$

Notice that the damping matrix and stiffness matrix are assumed to be symmetric; and, by the assumption that these two systems are decoupled, all other C_{ij} and K_{ij} not shown are equal to zero.

Subroutine FIT was used to find the best-fit values of C_{ij} and K_{ij} for the two systems above. Regrouped back into a single system of equations

$$[M]\{\ddot{u}\}+[C]\{\dot{u}\}+[K]\{u\} = -\{M_x\}\ddot{U}_{xg}-\{M_y\}\ddot{U}_{yg}-\{M_z\}\ddot{U}_{zg} \tag{178}$$

where $[M]$, $\{M_x\}$, $\{M_y\}$, and $\{M_u\}$ are given previously, the best fit damping and stiffness matrices found are

$$
[C] = \begin{bmatrix}
64.1 & -24.5 & 6.82 & 0 & 0 & 0 & 0 \\
-24.5 & 61.4 & -4.74 & 0 & 0 & 0 & 0 \\
6.82 & -4.74 & 53.7 & 0 & 0 & 0 & 0 \\
0 & 0 & 0 & 54.1 & .288 & 6.16 & -7.35 \\
0 & 0 & 0 & .288 & 14.3 & -6.18 & -5.41 \\
0 & 0 & 0 & 6.16 & -6.18 & .193 & -.800 \\
0 & 0 & 0 & -7.35 & -5.41 & -.800 & 1.82
\end{bmatrix}
$$

$$[K] = \begin{bmatrix} 75{,}200 & -54{,}600 & 32{,}200 & 0 & 0 & 0 & 0 \\ -54{,}600 & 64{,}300 & -44{,}000 & 0 & 0 & 0 & 0 \\ 32{,}200 & -44{,}000 & 86{,}900 & 0 & 0 & 0 & 0 \\ 0 & 0 & 0 & 24{,}800 & -1330 & -2770 & 2500 \\ 0 & 0 & 0 & -1330 & 10{,}800 & 4510 & 291 \\ 0 & 0 & 0 & -2770 & 4510 & 17{,}300 & 4140 \\ 0 & 0 & 0 & 2500 & 291 & 4140 & 11{,}100 \end{bmatrix}$$

At this point the mathematical model describing the significant bridge distortions is completely defined. Again it is not in its most useful form. Mathematical models are most usefully described in terms of normal coordinates characterized by natural frequencies, natural mode shapes, damping ratios, and modal participation factors.

By solving the related eigenvalue problem

$$[[K]-\omega^2[M]]\{\phi\} = \{0\} \tag{179}$$

the following natural frequencies are found

$\omega_1 = 17.7144$ rps

$\omega_2 = 36.0280$ rps

$\omega_3 = 64.1405$ rps

$\omega_4 = 13.7408$ rps

$\omega_5 = 19.5835$ rps

$\omega_6 = 23.4614$ rps

$\omega_7 = 32.6969$ rps

The first three are lateral modes of vibration and the following four are coupled longitudinal and vertical modes of vibration.

Corresponding to each natural frequency is a natural mode of vibration. These natural mode shapes, in physical coordinates, are arranged as columns

in the transformation matrix $[\phi]$ as follows:

$$[\phi] = \begin{bmatrix} .7280 & -.7429 & -.9934 & 0 & 0 & 0 & 0 \\ 1.000 & .2648 & 1.000 & 0 & 0 & 0 & 0 \\ .2760 & 1.0000 & -1.0029 & 0 & 0 & 0 & 0 \\ 0 & 0 & 0 & 1.0000 & 1.0000 & .0912 & -.0227 \\ 0 & 0 & 0 & -.0344 & 8.6506 & -.7880 & .4511 \\ 0 & 0 & 0 & .3845 & -6.2609 & -.0520 & 1.0000 \\ 0 & 0 & 0 & -.5535 & 5.9418 & 1.0000 & .4200 \end{bmatrix}$$

The mass matrix, damping matrix, and stiffness matrix are transformed into corresponding mass, damping and stiffness matrices in normal coordinates by

$$[M] = [\phi]^T[M][\phi]; \; [C] = [\phi]^T[C][\phi]; \; [K] = [\phi]^T[K][\phi]$$

By definition, all off-diagonal terms of the mass and stiffness matrices are zero, but they are not necessarily zero for the damping matrix. The transformed matrices become

$$[M] = \begin{bmatrix} 63.508 & 0 & 0 & 0 & 0 & 0 & 0 \\ 0 & 64.135 & 0 & 0 & 0 & 0 & 0 \\ 0 & 0 & 118.329 & 0 & 0 & 0 & 0 \\ 0 & 0 & 0 & 127.623 & 0 & 0 & 0 \\ 0 & 0 & 0 & 0 & 3071.007 & 0 & 0 \\ 0 & 0 & 0 & 0 & 0 & 33.086 & 0 \\ 0 & 0 & 0 & 0 & 0 & 0 & 27.342 \end{bmatrix}$$

$$[C] = \begin{bmatrix} 63.915 & 8.371 & 3.278 & 0 & 0 & 0 & 0 \\ 8.371 & 90.378 & 29.180 & 0 & 0 & 0 & 0 \\ 3.278 & 29.180 & 250.442 & 0 & 0 & 0 & 0 \\ 0 & 0 & 0 & 67.855 & -29.404 & -3.644 & 2.141 \\ 0 & 0 & 0 & -29.404 & 1209.331 & 140.761 & -9.892 \\ 0 & 0 & 0 & -3.644 & -140.761 & 17.812 & -.387 \\ 0 & 0 & 0 & 2.141 & -9.892 & -.387 & -4.991 \end{bmatrix}$$

$$[K] = \begin{bmatrix} 19{,}928. & 0 & 0 & 0 & 0 & 0 & 0 \\ 0 & 83{,}248. & 0 & 0 & 0 & 0 & 0 \\ 0 & 0 & 486{,}810. & 0 & 0 & 0 & 0 \\ 0 & 0 & 0 & 24{,}094. & 0 & 0 & 0 \\ 0 & 0 & 0 & 0 & 1{,}177{,}767. & 0 & 0 \\ 0 & 0 & 0 & 0 & 0 & 18{,}213. & 0 \\ 0 & 0 & 0 & 0 & 0 & 0 & 29{,}231. \end{bmatrix}$$

The vectors of participation factors become

$$\{M_x\} = \begin{Bmatrix} 0 \\ 0 \\ 0 \\ 118.62 \\ 118.62 \\ 10.818 \\ -2.693 \end{Bmatrix} \qquad \{M_y\} = \begin{Bmatrix} 79.238 \\ 20.636 \\ -39.394 \\ 0 \\ 0 \\ 0 \\ 0 \end{Bmatrix} \qquad \{M_z\} = \begin{Bmatrix} 0 \\ 0 \\ 0 \\ -4.021 \\ 164.714 \\ 3.163 \\ 36.992 \end{Bmatrix}$$

Off-diagonal damping terms are in general not negligible but are small in most cases. However, those off-diagonal damping terms are ignored, and it

is assumed that the equations of motion in normal coordinates can be separated without significant error. Errors will be evaluated after the analysis.

Ignoring the off-diagonal damping terms the modal equations of motion become

$$\ddot{\eta}_1+1.006\dot{\eta}_1+313.8\eta_1 = -1.248\ddot{U}_{yg} \tag{180}$$

$$\ddot{\eta}_2+1.409\dot{\eta}_2+1298.\eta_2 = -.322\ddot{U}_{yg} \tag{181}$$

$$\ddot{\eta}_3+2.117\dot{\eta}_3+4114.\eta_3 = .333\ddot{U}_{yg} \tag{182}$$

$$\ddot{\eta}_4+.532\dot{\eta}_4+188.8\eta_4 = -.929\ddot{U}_{xg}+.032\ddot{U}_{zg} \tag{183}$$

$$\ddot{\eta}_5+.394\dot{\eta}_5+383.5\eta_5 = -.039\ddot{U}_{xg}-.054\ddot{U}_{zg} \tag{184}$$

$$\ddot{\eta}_6+.538\dot{\eta}_6+550.5\eta_6 = -.327\ddot{U}_{xg}-.096\ddot{U}_{zg} \tag{185}$$

$$\ddot{\eta}_7-.183\dot{\eta}_7+1069.\eta_7 = .099\ddot{U}_{xg}-1.353\ddot{U}_{zg} \tag{186}$$

Comparing these equations to

$$\ddot{\eta}+2\xi\omega\dot{\eta}+\omega^2\eta = -\gamma_x\ddot{U}_{xg}-\gamma_y\ddot{U}_{yg}-\gamma_z\ddot{U}_{zg} \tag{187}$$

yields the modal parameters found by this analysis shown in table 13. The mode shapes identified are shown in figure 47. For comparison, the actual modal parameters used to generate the artificial time histories are shown in table 14, and the exact mode shapes are shown in figure 48.

From this example analysis it is apparent that frequencies, participation factors, and mode shapes can be found with acceptable accuracy using this technique. Errors in the damping ratios are significant for those modes of vibration not significantly excited (note in particular the negative damping ratio found for the seventh mode of vibration). These errors in damping ratios are not likely, however, to

Mode	ω(rps)	ξ(%)	γ_x	γ_y	γ_z
1	17.714	2.84	0	1.248	0
2	36.028	1.96	0	.322	0
3	64.141	1.65	0	-.333	0
4	13.741	1.94	.929	0	-.032
5	19.584	1.01	.039	0	.054
6	23.461	1.15	.327	0	.096
7	32.697	-.28	-.099	0	1.353

Table 13 - Three-Span Continuous Bridge Model Parameters Identified

Mode	ω(rps)	ξ(%)	γ_x	γ_y	γ_z
1	17.780	2.00	0	1.1888	0
2	36.040	2.00	0	.3291	0
3	64.310	2.00	0	-.4002	0
4	13.730	2.00	.9380	0	-.0446
5	19.660	2.00	.0413	0	.0639
6	23.360	2.00	.3240	0	.0546
7	31.740	2.00	-.6340	0	1.6910

Table 14.- Three-Span Continuous Bridge Exact Model Parameters

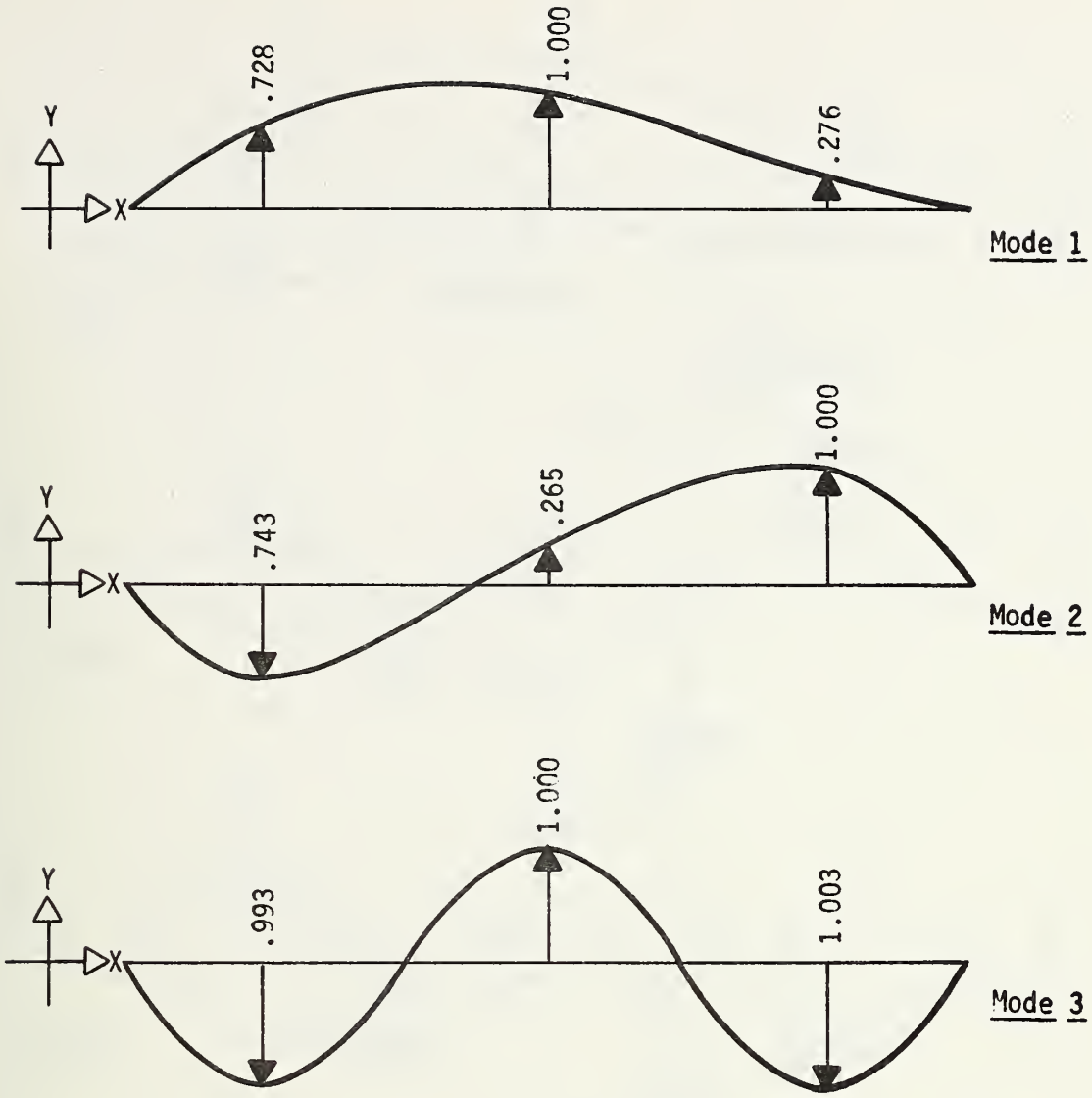

Figure 47.- Continuous three-span bridge, mode shapes found from analysis.

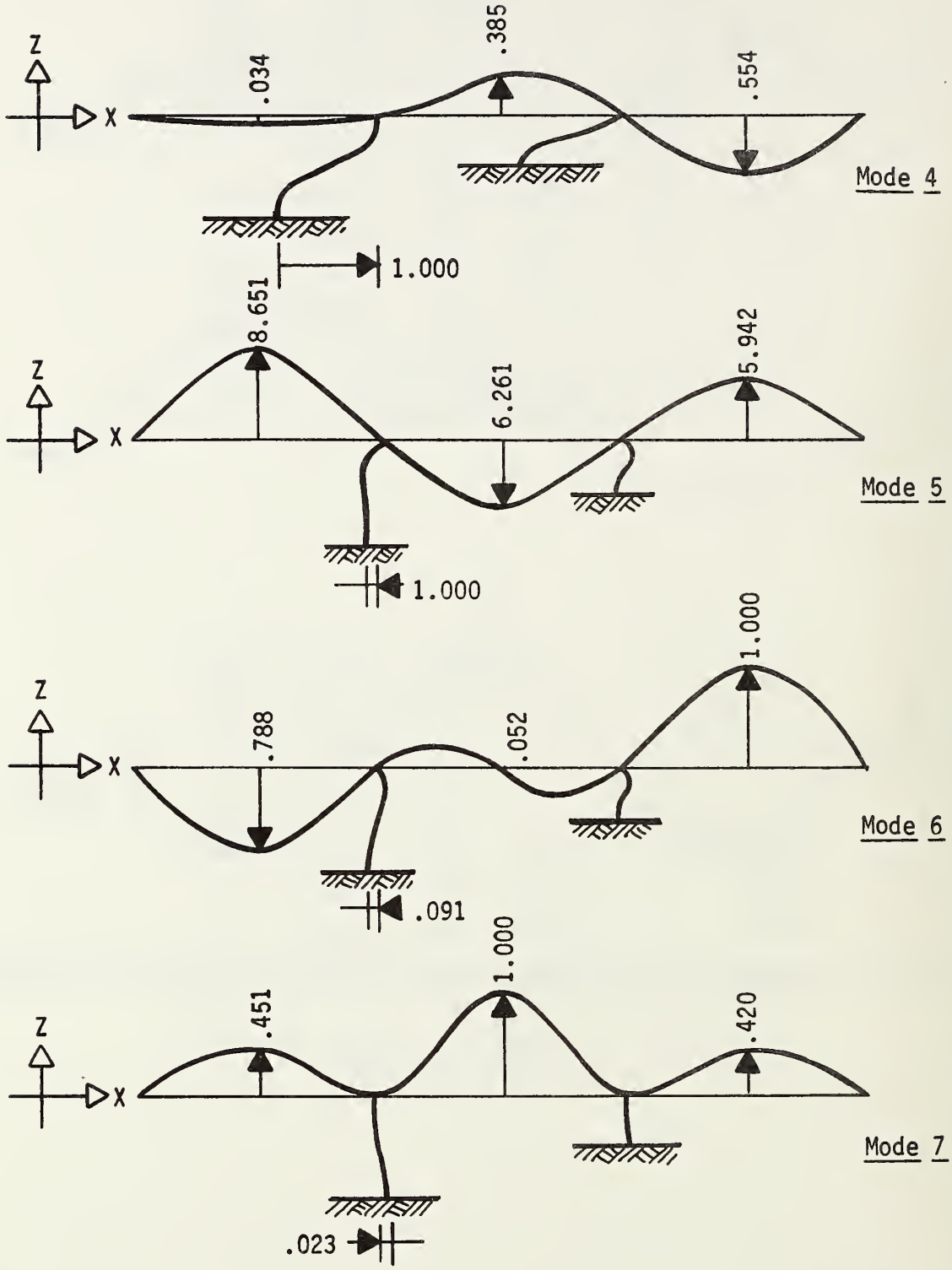

Figure 47 (continued).- Continuous three-span bridge, mode shapes found from analysis.

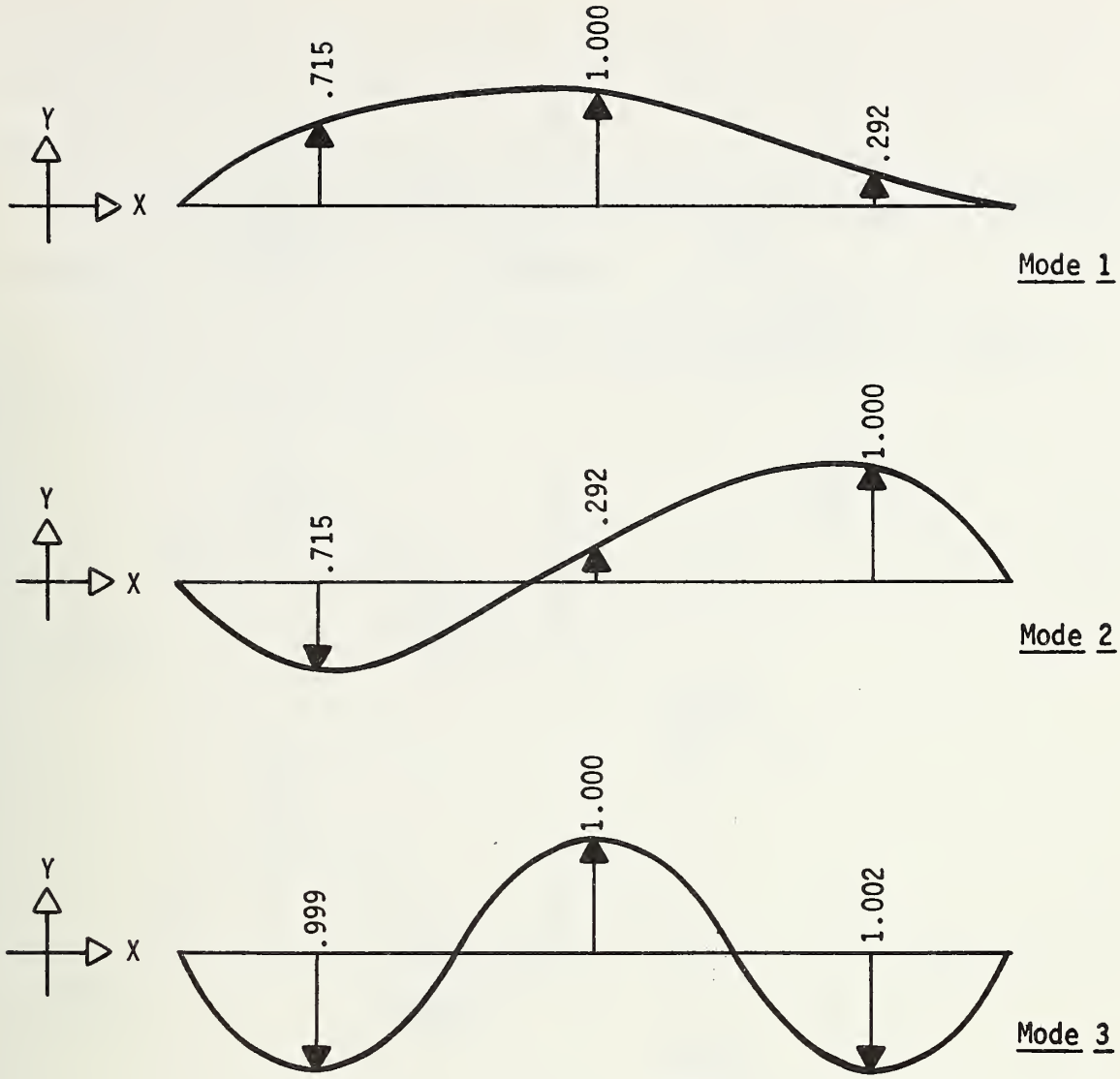

Figure 48.- Continuous three-span bridge, actual mode shapes.

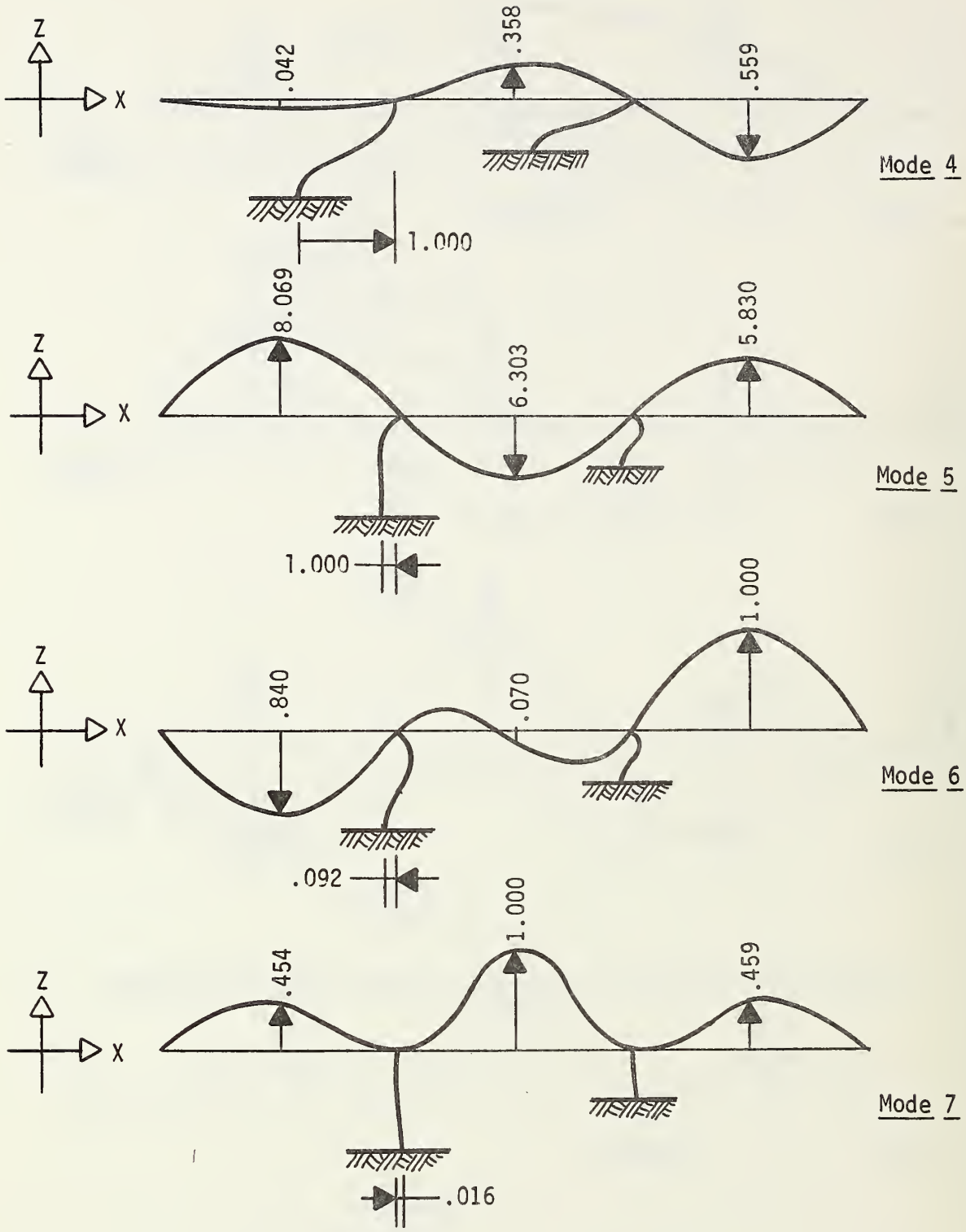

Figure 48 (continued).- Continuous three-span bridge, actual mode shapes.

produce significant errors in response. Although response amplitudes of resonating systems are highly dependent upon damping ratios, response amplitudes of seismically induced motions generally are not highly sensitive to variations in damping within the range of values to be found in practice. One general rule of thumb in time history analyses is that if the response is particularly sensitive to a parameter, that parameter will be found with accuracy.

V. CONCLUDING REMARKS

This report has discussed methods of analyzing strong-motion records obtained from highway bridges. There have been two objectives of the analyses: (1) obtain maximum force levels throughout the bridge, and (2) identify a mathematical model which best describes the observed dynamic behavior. There are few uncertainties regarding the calculation of maximum force levels, and few assumptions needed to be made. On the other hand, many uncertainties are associated with the identification of the best-fit mathematical model. Some of those uncertainties and additional limitations are discussed here.

This report has one procedure to identify one mathematical model of observed dynamic behavior. Two fundamental assumptions have been made about that model: (1) the model is linear, and (2) all support motions are identical and in phase. These assumptions may seem overly restrictive since it is well known that bridge response can be highly non-linear, and support motions can vary significantly, particularly if the foundation material differs from one support to another. Unfortunately, the ability to identify non-linear models with variable support motions lags far behind the ability to formulate such models and generate acceptable response. In fact, it is almost beyond the state of the art to identify linear mathematical models with identical support motions when the natural frequencies of the bridge are closely spaced. Unfortunately, this is often the case for highway bridges. The procedure described in this report will yield adequate results for structures that do or do not have closely spaced frequencies. In fact, it was developed with that purpose in mind.

Any non-linear model can be interpreted as a linear model with time-

dependent parameters. Since the identification procedure described in this report can identify a best-fit linear model over a small time slice, variations in the best-fit linear models identified can be analyzed as non-linearities in the bridge behavior. Bridge motions with variable support motions can also be analyzed with this identification procedure. In many cases, embankment motions could be interpreted not as input motions to the bridge but as response motions to bedrock motion. If it is appropriate to assume that column base motions are identical to bedrock motions under an embankment, then embankment motions can be included with other bridge motions as response motions, and can be analyzed using the procedure described in this manual. Bridge motions produced from ground motions propogating from one support to another, however, cannot be analyzed using this procedure.

REFERENCES

Bathe, K. J., Wilson, E. L. and Peterson, F. E., 1973, SAP IV, A structural analysis program for static and dynamic response of linear systems: Univ. of Calif., Berkeley, Earthquake Engineering Research Center Report No. EERC 73-11, 59 p.

Biggs, J. M., 1964, Introduction to structural dynamics: New York, McGraw-Hill, 341 p.

Brady, A. G., and Perez, V., 1976, Strong-motion earthquake accelerograms, digitization and analysis, 1971 records: U.S. Geological Survey Open-file Report 76-609, 117 p.

Clough, R. W., and Penzien, J., 1975, Dynamics of structures: New York, McGraw-Hill, 634 p.

Conte, S. D., 1965, Elementary numerical analysis: New York, McGraw-Hill, 278 p.

Douglas, B. M., 1976, Quick release pullback testing and analytical seismic analysis of a six span composite girder bridge: Department of Transportation Federal Highway Administration Report No. FHWA-RD-76-173, 73 p.

Gere, J. M., and Weaver, W., 1965, Matrix algebra for engineers: Princeton, N.J., Van Nostrand, 168 p.

Hart, G. C., and Yao, J.T.P., 1976, System identification in structural dynamics: Univ. of Calif., Los Angeles, Proceedings of the ASCE/EMD Specialty Conference, Dynamic Response of Structures: Instrumentation, Testing Methods and System Identification, p. 61-85.

Hurty, W. C., and Rubinstein, M. F., 1964, Dynamics of structures: Englewood Cliffs, N.J., Prentice-Hall, 455 p.

Ibanez, P., et al., 1977, Review of analytical and experimental techniques for improving structural dynamic models: Santa Monica, Calif., Applied

Nucleonics Co., Inc. Report No. 1149-1, 193 p.

Kozin, F., and Kozin, C. H., 1968, Identification of linear systems, final report of simulation studies: NASA Report No. CR-98738.

Miklofsky, H. A., and Mancini, W. B., 1977, Digitization and integration of strong-motion accelerograms: Department of Transportation Federal Highway Administration Report No. FHWA-RD-77-92, 279 p.

Newmark, N. M., and Rosenblueth, E., 1971, Fundamentals of earthquake engineering: Englewood Cliffs, N.J., Prentice-Hall, 640 p.

Sherburne, R.W., and Hauge, C.J., editors, 1975, Oroville, California, earthquake, 1 August 1975; Sacramento, Calif.: California Division of Mines and Geology Special Report 124, p. 103, 105, 106.

Taoka, G.T., 1976, Digital filtering of ambient response data: Univ. of Calif., Los Angeles, Proceedings of the ASCE/EMD Specialty Conference, Dynamic Response of Structures: Instrumentation, Testing Methods and System Identification, p. 253-262.

Trifunac, M.D., and Lee, V., 1973, Routine computer processing of strong-motion accelerograms: Pasadena, Calif., California Institute of Technology, Earthquake Engineering Research Laboratory Report No. EERL 73-03, 360 p.

Wiegel, R.L., editor, 1970, Earthquake engineering: Englewood Cliffs, N.J. Prentice-Hall, 518 p.

APPENDIX A

GLOSSARY OF TERMS

$\{B(t)\}$	vector of known inertial time histories in physical coordinates
$\{b(t)\}$	vector of known inertial time histories in generalized coordinates
C	constant
$[C]$	damping matrix in physical coordinates
$[C]$	damping matrix in normal coordinates
$[c]$	damping matrix in generalized coordinates
c	half of deck width
E	squared error
$\tilde{F}_i(t)$	force on i^{th} lumped mass
$\tilde{F}_j(s,t)$	Force per unit length for the jth generalized (normal) shape
F_{ci}	damping force in physical coordinates
F_{ki}	elastic force in physical coordinates
F_{mi}	inertial force in physical coordinates
f_{ci}	damping force in generalized coordinates
f_{ki}	elastic force in generalized coordinates
f_{mi}	inertial force in generalized coordinates
$I(x)$	rotational inertial per unit length
i,j	indeces
$\tilde{i},\tilde{j},\tilde{k}$	unit vectors in the Cartesian coordinate directions x,y,z respectively
$[K]$	stiffness matrix in physical coordinates

$[K]$	stiffness matrix in normal coordinates
$[k]$	stiffness matrix in generalized coordinates
L	length of bridge
$M(x)$	mass per unit length
M_x, M_y, M_z	internal bending moments in bridge deck
$[M]$	mass matrix in physical coordinates
$\{M_x\}, \{M_y\}, \{M_z\}$	vectors of participation factors in physical coordinates
$[M]$	mass matrix in normal coordinates
$\{M_x\}, \{M_y\}, \{M_z\}$	vectors of participation factors in normal coordinates
$[m]$	mass matrix in generalized coordinates
$\{m_x\}, \{m_y\}, \{m_z\}$	vectors of participation factors in generalized coordinates
N_x	internal axial force in bridge deck
n	number of lumped masses
Q_i	generalized force
$R_i(t)$	i^{th} reaction
R_{ij}	i^{th} reaction to a unit j^{th} generalized (normal) acceleration
R_{ix}, R_{iy}, R_{iz}	i^{th} reaction to unit rigid-body accelerations in the x-, y-, and z- directions respectively
R_{tx}, R_{ty}, R_{tz}	total reaction in the x-, y-, and z- directions due to unit rigid-body accelerations in the x-, y-, and z- directions respectively

$R_{tjx}, R_{tjy}, R_{tjz}$	total reaction in the x-, y-, and z- directions respectively due to a unit jth generalized (normal) acceleration
$\tilde{r}_i(s)$	vector of distortions due to a unit displacement corresponding to the ith reaction
$S_a(\omega)$	spectral acceleration
s	coordinate along the principal axis of the bridge
T	natural period ($=2\pi/\omega$)
t	temporal coordinate
$\{U(t)\}$	vector of absolute bridge displacements
$\ddot{U}_{xg}(t), \ddot{U}_{yg}(t), \ddot{U}_{zg}(t)$	ground accelerations in x-, y-, and z- directions respectively
$\{u(t)\}$	vector of bridge distortions relative to the ground
$\tilde{u}(s,t)$	vector distortion relative to the ground of point on bridge axis
V_x, V_y	internal shears on bridge deck
x,y,z	Cartesian coordinates
$\{\alpha(t)\}$	vector of bridge distortions in generalized coordinates
$\{\gamma_x\}, \{\gamma_y\}, \{\gamma_z\}$	vectors of participation factors in normal coordinates when masses are normalized to unity
δ	virtual displacement
$\{\eta(t)\}$	vector of bridge distortions in normal coordinates
$[\theta]$	transformation matrix from normal to generalized coordinates

$\{\xi\}$	vector of modal viscous damping ratios
$[\phi]$	transformation matrix from normal to physical coordinates
$\tilde{\phi}_i(s)$	ith normal mode shape
$[\psi]$	transformation matrix from generalized to physical coordinates
$\tilde{\psi}_i(s)$	ith generalized shape
$\{\omega\}$	vector of natural circular frequencies of vibration
$[\ ]$	brackets denoting a matrix quantity
$[\ ]^T$	transpose of a matrix
$\{\ \}$	braces denoting a vector quantity
Σ	summation
$(\dot{\ })=d/dt$	differentiation with respect to time
$(\tilde{\ })$	symbol of a vector quantity

APPENDIX B

INTRODUCTION TO STRUCTURAL DYNAMICS OF BRIDGES

Before any mathematical model of dynamic bridge behavior can be made, a coordinate system must be established which can describe the bridge motions accurately. The number and location of the coordinates to describe the bridge motion is purely arbitrary. To describe the bridge motion exactly requires an infinite number of coordinates. If the coordinates are chosen judiciously, however, only a few coordinates are necessary to describe the complete bridge motion with acceptable accuracy. In the case of a curved highway grade separation bridge, for example, there are many possible coordinate systems that may be chosen to describe the horizontal motion of the bridge. If vertical and twisting motion of the bridge deck are ignored (such motions may be very important but are not considered here in order to simplify the discussion), then the bridge deck motions and ground motions can be described by the coordinates shown in figure 49, for a total of twenty coordinates. The number of required coordinates can further be reduced if it is possible to make some additional assumptions. For most bridges, or isolated segments of bridges, it is reasonable to assume that bridges are inextensible in their longitudinal directions (the s direction for the bridge shown).

In many cases, it is also reasonable to assume that the ground motion exciting the bridge is identical under each support. This assumption is reasonable for short span bridges on firm foundation material. For long span bridges (such as the San Francisco Golden Gate Bridge), it is of course unreasonable to assume that the earthquake motion at one end is identical to the earthquake motion at the other end. It may also be erroneous to make

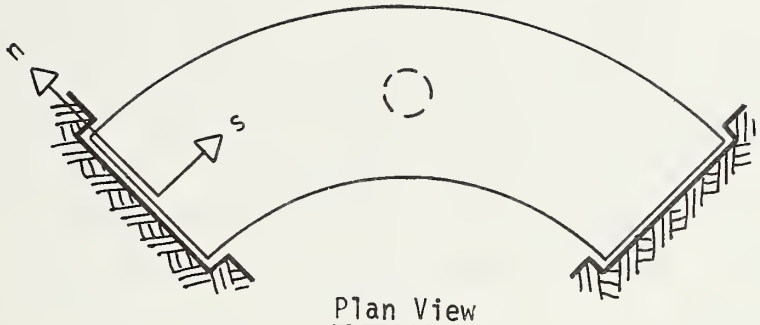

Plan View

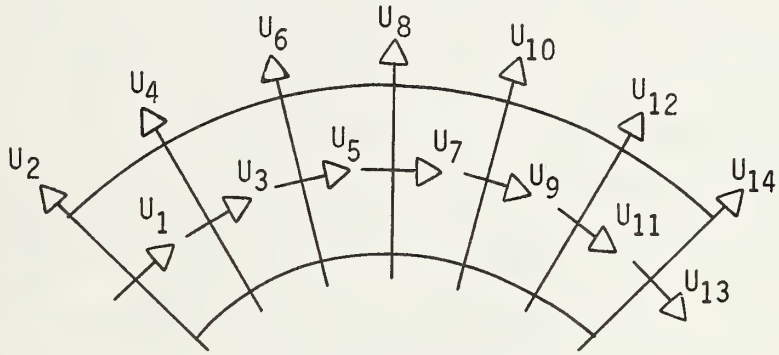

Deck Instrumentation

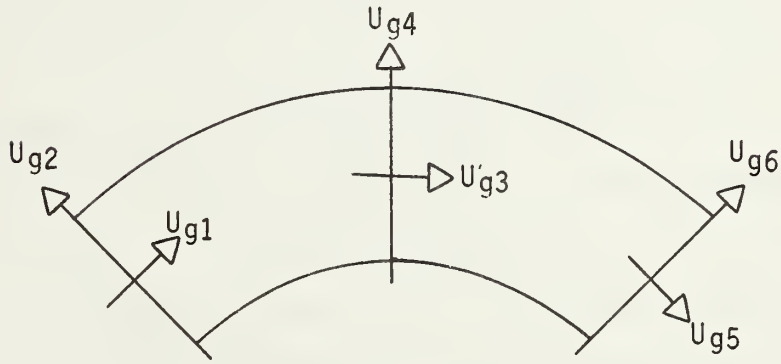

Ground Instrumentation

Figure 49.- Example curved bridge with complete instrumentation.

this assumption for a simple highway bridge if a central pier rests on firm rock, while the end abutments rest on fill. In any case the mathematical modeling assumptions are made primarily for mathematical convenience, and each should be evaluated from the analysis of the strong-motion records.

When the two assumptions described above are made, the bridge motion may be described accurately by the reduced coordinates shown in figure 50. In this case, the bridge and ground motions are described by a total of only eight coordinates. The five lateral motion coordinates at the bridge deck describe accurately the motions of those five points only. The lateral motions of the deck must be assumed for all locations between coordinate points. For typical highway bridges, significant motions involving more than a half wave length per span are not expected.

Instead of approximating the bridge displacements with the displacements of a few selected points, the bridge displacements can be approximated by a linear combination of assumed independent shape functions. For the assumed shapes shown in figure 51 and corresponding coordinates $\alpha_1(t)$, $\alpha_2(t)$, and $\alpha_3(t)$, the total lateral bridge deck displacement relative to the ground can be given by

$$\tilde{u}(s,t) = \tilde{\psi}_1(s)\alpha_1(t)+\tilde{\psi}_2(s)\alpha_2(t)+\tilde{\psi}_3(s)\alpha_3(t) \qquad \text{(B-1)}$$

The displacements in these coordinates $\alpha_i(t)$ are not in themselves measurable quantities but are related to measurable quantities $u_i(t)$ by the assumed deflected shapes $\tilde{\psi}_i(s)$. The bridge is not expected to vibrate freely, to any significant extent, in a mode like $\tilde{\psi}_3(s)$, but this assumed shape should be included nonetheless to improve the description of the actual lateral bridge deck motion, otherwise described entirely by the assumed shapes $\tilde{\psi}_1(s)$ and $\tilde{\psi}_2(s)$.

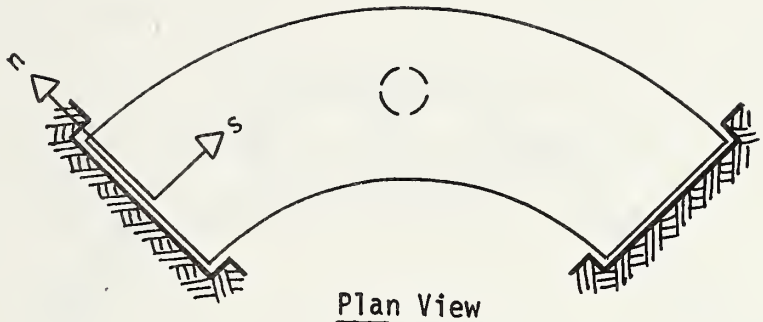

Plan View

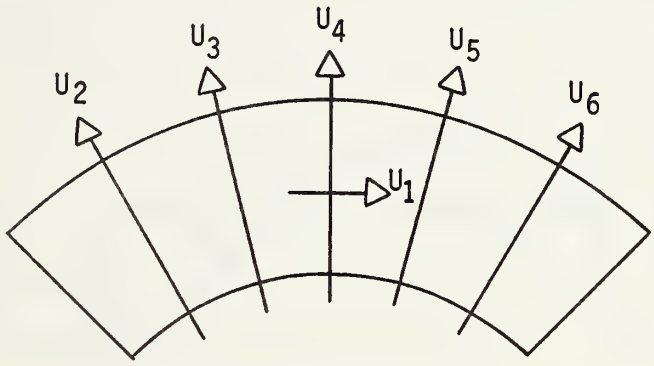

Deck Instrumentation

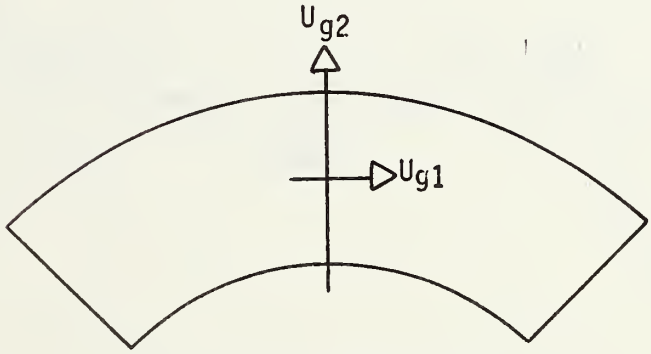

Ground Instrumentation

Figure 50.- Example curved bridge with reduced instrumentation.

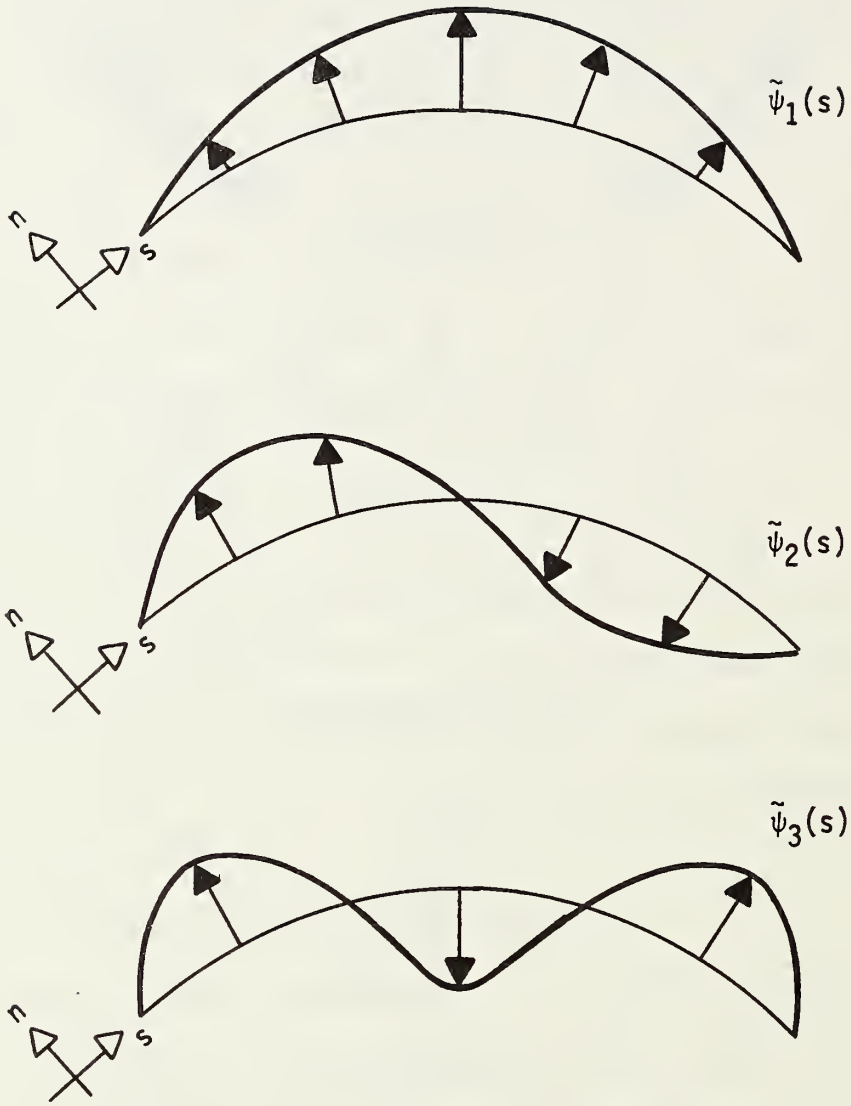

Figure 51.- Example curved bridge, assumed deflected shapes.

In addition to the three coordinates that describe the lateral bridge motion, a single longitudinal coordinate and two ground motion coordinates are also required. It is unlikely that fewer coordinates could describe the horizontal bridge motion with equal accuracy. It is also very important that significant bridge motions, yielding significant force levels are not lost when coordinates are hastily removed for the sake of simplicity and reduced cost. Once the information is lost, it can never be regained from the remaining coordinates.

The mathematical model used to describe the dynamic behavior of a bridge consists of a set of equations of motion. There will exist one equation for each unknown bridge displacement. For the coordinate system described above there will exist four equations of motion. Each equation of motion is nothing more than an equation of dynamic equilibrium including all forces acting on the bridge in that particular coordinate "direction". Forces acting in a coordinate direction that is not directly measurable will be defined later.

Specifically, there will exist inertial forces, damping forces (forces that damp the motion by dissipating energy), elastic forces, and externally applied forces. For the ith coordinate direction, the equation of dynamic equilibrium can be written

$$f_{mi} + f_{ci} + f_{ki} = f_{pi} \tag{B-2}$$

where

f_{mi} = inertial force,

f_{ci} = damping force,

f_{ki} = restoring force, and

f_{pi} = applied force.

A generally accurate assumption for non-damaging motion is that the above inertial, damping, and elastic forces are proportional to the coordinate accelerations, velocities, and displacements respectively. This assumption of linear behavior is one of the fundamental assumptions to be checked by the experimental data. The assumption of linear behavior is not made primarily because linear models are best but because linear models can be solved in closed form using general solution methods. The same cannot be said for non-linear equations. Whether or not a linear equation is the best to simulate bridge motion is to be evaluated by the experimental data.

Like $\tilde{u}(s,t)$ the displacements $\alpha i(t)$ are defined as displacements relative to the ground. Relative coordinates are important because force levels in bridges are proportional to relative displacements; damping forces are proportional to relative velocities. Inertial forces, on the other hand, are proportional to absolute accelerations.

In terms of constants of proportionality the inertial force in the ith coordinate direction can be expanded in the most general, linear manner to

$$f_{mi} = m_{i1}\ddot{\alpha}_1 + \ldots m_{in}\ddot{\alpha}_n + m_{xi}\ddot{U}_{xg} + m_{yi}\ddot{U}_{yg} + m_{zi}\ddot{U}_{zg} \qquad \text{(B-3)}$$

where $\ddot{U}_{xg}$, $\ddot{U}_{yq}$, and $\ddot{U}_{zg}$ are the three mutually perpendicular ground accelerations (the definitions and significance of m_{i1}, ..., m_{in}, m_{xi}, m_{yi}, and m_{zi} are discussed below). Similarly, by definition, the damping force in the ith direction is given by

$$f_{di} = c_{i1}\dot{\alpha}_1 + c_{i2}\dot{\alpha}_2 \ldots + c_{in}\dot{\alpha}_n \qquad \text{(B-4)}$$

and the elastic force

$$f_{ki} = k_{i1}\alpha_1 + k_{i2}\alpha_2 + \ldots + k_{in}\alpha_n \qquad \text{(B-5)}$$

where

$$\dot{\alpha}_j = d\alpha_j/dt \qquad \text{(B-6)}$$

$$\ddot{\alpha}_j = d^2\alpha_j/dt^2 \tag{B-7}$$

Earthquakes do not apply forces directly to bridges, so for all i, $f_{pi}=0$. All of the forces induced by earthquakes initially are inertial. Then, only after relative motion between the bridge and ground occurs, are damping and elastic forces developed.

The ith of n equations of motion can then be written as

$$m_{i1}\ddot{\alpha}_1 + \cdots + m_{in}\ddot{\alpha}_n + c_{i1}\dot{\alpha}_1 + \cdots + c_{in}\dot{\alpha}_n + k_{i1}\alpha_1 + \cdots + k_{in}\alpha_n =$$

$$-m_{xi}\ddot{U}_{xg} - m_{yi}\ddot{U}_{yg} - m_{zi}\ddot{U}_{zg} \tag{B-8}$$

For bookkeeping reasons, these n equations of motion can be regrouped in matrix form (Gere & Weaver, 1965).

$$\begin{bmatrix} m_{11} m_{12} & \cdots & m_{1n} \\ m_{21} m_{22} & \cdots & m_{2n} \\ \vdots \quad \vdots & & \vdots \\ m_{n1} m_{n2} & \cdots & m_{nn} \end{bmatrix} \begin{Bmatrix} \ddot{\alpha}_1 \\ \ddot{\alpha}_2 \\ \vdots \\ \ddot{\alpha}_n \end{Bmatrix} + \begin{bmatrix} c_{11} c_{12} & \cdots & c_{1n} \\ c_{21} c_{22} & \cdots & c_{2n} \\ \vdots \quad \vdots & & \vdots \\ c_{n1} c_{n2} & \cdots & c_{nn} \end{bmatrix} \begin{Bmatrix} \dot{\alpha}_1 \\ \dot{\alpha}_2 \\ \vdots \\ \dot{\alpha}_n \end{Bmatrix} +$$

$$\begin{bmatrix} k_{11} k_{12} & \cdots & k_{1n} \\ k_{21} k_{22} & \cdots & k_{2n} \\ \vdots \quad \vdots & & \vdots \\ k_{n1} k_{n2} & \cdots & k_{nn} \end{bmatrix} \begin{Bmatrix} \alpha_1 \\ \alpha_2 \\ \vdots \\ \alpha_n \end{Bmatrix} = - \begin{Bmatrix} m_{x1} \\ m_{x2} \\ \vdots \\ m_{xn} \end{Bmatrix} \ddot{U}_{xg}$$

$$- \begin{Bmatrix} m_{y2} \\ \vdots \\ \vdots \\ m_{yn} \end{Bmatrix} \ddot{U}_{yg} - \begin{Bmatrix} m_{z2} \\ \vdots \\ \vdots \\ m_{zn} \end{Bmatrix} \ddot{U}_{zg} \tag{B-9}$$

In simpler form this can be written as

$$[m]\{\ddot{\alpha}\}+[c]\{\dot{\alpha}\}+[k]\{\alpha\} = -\{m_x\}\ddot{U}_{xg} - \{m_y\}\ddot{U}_{yg} - \{m_z\}\ddot{U}_{zg} \tag{B-10}$$

The physical significance of the terms m_{ij}, c_{ij}, and k_{ij} can best be obtained from equations B-3, B-4, and B-5. Specifically the term m_{ij} is the force in the i coordinate direction due to a unit acceleration in the j direction only. The term c_{ij} is the force in the i coordinate direction due to a unit velocity in the j direction only. The term k_{ij} is the force in the i coordinate direction due to a unit displacement in the j direction only. Similarly the terms m_{xi}, m_{yi}, and m_{zi} are forces in the i coordinate direction due to unit ground accelerations $\ddot{U}_{xg}$, $\ddot{U}_{yg}$, and $\ddot{U}_{zg}$ respectively, with all relative bridge motions fixed.

The numerical evaluation of these terms is possible from the definitions above and with use of the theorem of virtual work (Clough and Penzien, 1975). Only the inertial terms will be evaluated using this theorem as they are the only terms that need to be evaluated from the weights and dimensions of the bridge for the analysis procedures that have been described in this report. The damping and elastic terms, in one form or another, are those modeling parameters that are to be identified from the bridge records. Formal procedures for their theoretical formulation are available in any of many texts on structural dynamics (Biggs, 1964, Clough and Penzien, 1975, Hurty and Rubinstein, 1964).

The theorem of virtual work is stated as follows (Clough and Penzien, 1975): "If a structure which is in static or dynamic equilibrium under the action of a set of forces is subjected to a virtual displacement, the total work done by those forces equals zero."

For the determination of m_{ij} consider the bridge subjected to a unit acceleration in the j coordinate direction only. All velocities and displacements are assumed to equal zero. Considering now the bridge to be composed of many line elements (including the deck as well as piers), the

acceleration at any point on the bridge is given by

$$d^2\tilde{u}(s,t)/dt^2 = \tilde{\psi}_j(s)\ddot{\alpha}_j(t) = \tilde{\psi}_j(s) \qquad \text{(B-11)}$$

where the last equality is due to the assumption that $\ddot{\alpha}_j(t) = 1$. The acceleration $\ddot{\tilde{u}}$ and assumed deflected shape $\tilde{\psi}$ are in general vector quantities having components in directions other than normal to the longitudinal axis s. For any element of the bridge, Δs, the inertial force due to that unit acceleration is given by

$$\Delta\tilde{F}(s) = M(s)\tilde{\psi}_j(s)\Delta s \qquad \text{(B-12)}$$

where M(s) is the mass per unit length of bridge element.

Let Q_k be a force corresponding to the k coordinate. For a set of virtual displacements $\delta\tilde{u}_k = \tilde{\psi}_k\delta\alpha_k (k=1, 2, \ldots, n)$ the total work produced by the $Q_k\delta\alpha_k$ plus the total work produced by the inertial forces undergoing the virtual displacements must add to zero by virtue of the theorem of virtual work:

$$Q_1\delta\alpha_1 + \ldots + Q_i\delta\alpha_i + \ldots + Q_n\delta\alpha_n + \int M(s)\tilde{\psi}_j(s)\cdot\delta\tilde{u}_1(s,t)\,ds$$
$$+\ldots+\int M(s)\tilde{\psi}_j(s)\cdot\delta\tilde{u}_j(s,t)ds+\ldots+\int M(s)\tilde{\psi}_j(s)\cdot\delta\tilde{u}_n(s,t)ds = 0 \qquad \text{(B-13)}$$

where the integrations are over the entire bridge. There are likely to exist many other forces, such as reactions, that result from the unit acceleration. However, since motions of the bridge are described completely by the coordinates, α_k, at least to within an acceptable error, none of those reactions or other forces will produce work.

If all but the ith virtual displacements equal zero, then

$$-Q_i\delta\alpha_i = \int M(s)\delta\tilde{u}_i(s,t)\cdot\tilde{\psi}_j(s)ds \qquad \text{(B-14)}$$

Since $\delta\tilde{u}_i(s,t) = \tilde{\psi}_i(s)\delta\alpha_i$ and since $\delta\alpha_i$ is non-zero, $\delta\alpha_i$ can be divided from both sides of equation B-14 to yield

$$-Q_i = \int M(s)\tilde{\psi}_i(s)\cdot\tilde{\psi}_j(s)ds \qquad \text{(B-15)}$$

Instead of considering the force in the i coordinate direction <u>resisting</u> the acceleration, consider the equivalent force in the i coordinate direction <u>produced</u> by the unit acceleration. By definition this force is m_{ij}, and therefore

$$m_{ij} = \int M(s)\tilde{\psi}_i(s)\cdot\tilde{\psi}_j(s)ds \tag{B-16}$$

In a similar manner the inertial terms m_{xi}, m_{yi}, and m_{zi} can be found. Assume that $\ddot{U}_{xg}=1$, while holding $\ddot{U}_{yg}$ and $\ddot{U}_{zg}$ and all relative bridge accelerations fixed. For $\tilde{i}$ equal to the unit vector in the $\ddot{U}_{xg}$ direction, an elemental inertial force due to this unit ground acceleration is

$$\Delta\tilde{F}(s) = M(s)\tilde{i}\Delta s \tag{B-17}$$

If the bridge is subjected to the single virtual displacement $\delta\tilde{u}_i(s,t)$, then from the theorem of virtual work,

$$Q_i\delta\alpha_i+\int M(s)\delta\tilde{u}_i(s,t)\cdot\tilde{i}ds = 0 \tag{B-18}$$

or again,

$$Q_i+\int M(s)\tilde{\psi}_i(s)\cdot\tilde{i}ds = 0 \tag{B-19}$$

By definition, m_{xi} is the force in the i coordinate direction produced by a unit acceleration $\ddot{U}_{xg}$; therefore

$$m_{xi} = \int M(s)\tilde{\psi}_i(s)\cdot\tilde{i}ds \tag{B-20}$$

In an analogous manner,

$$m_{yi} = \int M(s)\tilde{\psi}_i(s)\cdot\tilde{j}ds \tag{B-21}$$

and

$$m_{zi} = \int M(s)\tilde{\psi}_i(s)\cdot\tilde{k}ds \tag{B-22}$$

where $\tilde{j}$ and $\tilde{k}$ are unit vectors in the directions of $\ddot{U}_{yg}$ and $\ddot{U}_{zg}$, respectively.

Equation B-9 rewritten is again

$$[m]\{\ddot{\alpha}\}+[c]\{\dot{\alpha}\}+[k]\{\alpha\} = -\{m_x\}\ddot{U}_{xg}-\{m_y\}\ddot{U}_{yg}-\{m_z\}\ddot{U}_{zg} \tag{B-23}$$

where the inertial terms are defined by equations B-16, B-20, B-21, and B-22 in terms of the assumed deflected shapes $\tilde{\psi}_i(s)$. In practice the terms k_{ij} can also be found in a similar manner. The terms c_{ij} are rarely found in this form.

In general, all elements of the mass matrix [m], the damping matrix [c], and the stiffness matrix [k] are non-zero, making the solution difficult. There does exist a special set of deflected shapes, $\tilde{\phi}_i(s)$, called normal mode shapes, and corresponding coordinates $\eta_i(t)$ that greatly simplify the solution of equation B-10. Instead of expanding the displacement

$$\tilde{u}(s,t) = \tilde{\psi}_1(s)\alpha_1(t)+ \ldots +\tilde{\psi}_n(s)\alpha_n(t) \tag{B-24}$$

expand it in terms of normal modes:

$$\tilde{u}(s,t) = \tilde{\phi}_1(s)\eta_1(t)+ \ldots +\tilde{\phi}_n(s)\eta_n(t) \tag{B-25}$$

Then all off diagonal masses

$$m_{ij} = \int M(s)\tilde{\phi}_i(s).\tilde{\phi}(s)ds \tag{B-26}$$

equal zero for $i \neq j$, as well as all off-diagonal terms of [C] and [K]. It can be shown that for all real, symmetric, positive definite mass and stiffness matrices for stable structural systems a set of normal modes can in fact be found such that all $M_{ij} = 0$ and $K_{ij} = 0$ for $i \neq j$ (Biggs, 1964; Clough and Penzien, 1975; Hurty and Rubinstein, 1964). In general, the off-diagonal terms C_{ij} may not be zero but quite often are very small. In such cases it is usual to assume that they are zero so that all matrices [M], [C], and [K] are diagonalized by the coordinate selection.

Standard methods to find these normal coordinates are outlined in texts on structural dynamics (Biggs, 1964; Clough and Penzien, 1975; Hurty and

Rubinstein, 1964) and will not be considered further here. To analyze the vibration records it is enough to know that normal modes exist, and there is no special need to know how to find them analytically.

For the specific set of normal coordinates, equation B-10 is written

$$[M]\{\ddot{\eta}\}+[C]\{\dot{\eta}\}+[K]\{\eta\} = -\{M_x\}\ddot{U}_{xg}-\{M_y\}\ddot{U}_{yg}-\{M_z\}\ddot{U}_{zg} \tag{B-27}$$

where $[M]$, $[C]$, and $[K]$ are diagonal matrices (having all off-diagonal terms equal to zero). Because of the special diagonal form of all matrices, the n equations of motion can be written as n uncoupled single-degree-of-freedom simple-oscillator equations of motion, the ith of which is

$$M_i\ddot{\eta}_i+C_i\dot{\eta}_i+K_i\eta_i = -M_{xi}\ddot{U}_{xg}-M_{yi}\ddot{U}_{yg}-M_{zi}\ddot{U}_{zg} \tag{B-28}$$

where the inertial terms are defined by

$$M_i = \int M(s)\tilde{\phi}_i(s)\cdot\tilde{\phi}_i(s)ds \tag{B-29}$$

$$M_{xi} = \int M(s)\tilde{\phi}_i(s)\cdot\tilde{i}ds \tag{B-30}$$

$$M_{yi} = \int M(s)\tilde{\phi}_i(s)\cdot\tilde{j}ds \tag{B-31}$$

and

$$M_{zi} = \int M(s)\tilde{\phi}_i(s)\cdot\tilde{k}ds \tag{B-32}$$

Again, all integrals are over all elements of the bridge.

If equation B-28 is divided by M_i then this modal equation of motion can be written in the alternate form

$$\ddot{\eta}_i+2\xi_i\omega_i\dot{\eta}_i+\omega_i^2\eta_i = -\gamma_{xi}\ddot{U}_{xg}-\gamma_{yi}\ddot{U}_{yg}-\gamma_z\ddot{U}_{zg} \tag{B-33}$$

where the obvious definitions are made

$\xi_i = C_i/2\sqrt{K_iM_i}$ (damping ratio)

$\omega_i = \sqrt{K_i/M_i}$ (natural undamped circular frequency of vibration)

$\gamma_{xi} = M_{xi}/M_i$

$\gamma_{yi} = M_{yi}/M_i$ (participation factors)

$\gamma_{zi} = M_{zi}/M_i$

The ω_i have the physical significance that $\omega_i = 2\pi f_i$ where f_i is the approximate natural frequency of vibration (in Hz) of the ith mode. It is a property of the mode that if the mode could be perturbed alone, it would vibrate solely at that frequency. The damping ratio ξ_i also has the physical significance of equaling the ratio of damping in the bridge (capability of dissipating energy) to the value of critical damping. Critical damping is defined as the minimum damping for which a perturbed shape will return to its initial shape exponentially rather than in an oscillatory manner. In practice, most bridges are very lightly damped having $\xi < 0.1$.

Finally it can be said that a mathematical model of a bridge, if formulated under the assumptions presented here, can be characterized by the natural frequencies ω_i, the modal damping ratios ξ_i, and the participation factors γ_{xi}, γ_{yi}, and γ_{zi}. The participation factors are solely functions of the mass distribution M(s) and mode shapes $\tilde{\phi}_i(s)$, the usual third modal parameter. The normal mode formulation of the problem is powerful because typical bridge responses may be very accurately described in terms of a very few normal coordinates.

APPENDIX C

COMPUTER PROGRAM LISTINGS

Subroutine FIT

Subroutine FIT solves for the best-fit values of A(I,J) such that the left side of

$$[A]\{F(t)\} = \{B(t)\}$$

fits the right side in a least-squares sense. {F(t)} and {B(t)} are known time histories.

OUTPUT

A(NN,NM)	Matrix of unknown coefficients to be found [A] = [[C][K]]

INPUT

B(NN,NP)	Vector of known time histories
F(NM,NP)	Vector of known time histories
IJ(NN,NM)	Array of unknown coefficient indices: IJ(K,L) is the unknown coefficient index for the term A(K,L)
NE	Number of independent unknown coefficients in [A]
NM	Twice NN
NN	Number of system degrees of freedom
NP	Number of points in known time histories
NS	Starting index of known time histories
NF	Finishing index of known time histories
P(NE,NE)	Scratch array
Q(NE)	Do.
R(NE)	Do.

```
      subroutine fit(a,b,f,p,q,r,ij,ne,nm,nn,np,ns,nf,err)
      dimension a(nn,nm),b(nn,np),f(nm,np),ij(nn,nm)
      dimension p(ne,ne),q(ne),r(ne)
      do 10 i=1,ne
      q(i)=0.
      do 10 j=1,ne
   10 p(i,j)=0.
      do 50 l=1,ne
      do 50 i=1,nn
      do 40 j=1,nm
      if (ij(i,j).ne.l) go to 40
      do 20 k=1,nm
      m=ij(i,k)
      do 20 n=ns,nf
   20 p(l,m)=p(l,m)+f(k,n)*f(j,n)
      do 30 n=ns,nf
   30 q(l)=q(l)+b(i,n)*f(j,n)
   40 continue
   50 continue
      call solve(p,q,r,ne)
      do 60 i=1,nn
      do 60 j=1,nm
      k=ij(i,j)
   60 a(i,j)=r(k)
      err=0.
      cbb=0.
      do 80 i=1,nn
      do 80 n=ns,nf
      dum=b(i,n)
      cbb=cbb+dum*dum
      do 70 j=1,nm
   70 dum=dum-a(i,j)*f(j,n)
      err=err+dum*dum
   80 continue
      err=sqrt(err/cbb)
      return
      end
```

Subroutine SOLVE

Subroutine SOLVE solves the system of n linear equations [A]{X} = {B} for the vector of unknowns, {X}, using the Gaussian elimination procedure. The matrix [A] and vector {B} are destroyed in the process.

OUTPUT

X(N)	Vector of unknowns

INPUT

A(N,N)	Matrix of coefficients
B(N)	Vector of knowns
N	Number of equations to be solved

```
      subroutine solve(a,b,x,n)
      dimension a(n,n),b(n),x(n)
c subroutine solve solves the set of linear equations of order n
c [a][x]=[b]
      do 50 k=2,n
      m=k-1
      nn=0
    5 if(a(m,m)) 40,10,40
   10 nn=nn+1
      if(nn.gt.n) go to 200
      do 20 j=1,n
      ad=a(m,j)
      a(m,j)=a(m+nn,j)
   20 a(m+nn,j)=ad
      bd=b(m)
      b(m)=b(m+nn)
      b(m+nn)=bd
      go to 5
   40 do 50 i=k,n
      c=a(i,m)
      b(i)=b(i)-b(m)*c/a(m,m)
      do 50 j=m,n
      a(i,j)=a(i,j)-a(m,j)*c/a(m,m)
   50 continue
      x(n)=b(n)/a(n,n)
      l=n-1
      do 70 k=1,l
      m=n-k
      dum=0.
      do 60 j=m,l
   60 dum=dum+a(m,j+1)*x(j+1)
   70 x(m)=(b(m)-dum)/a(m,m)
      go to 300
  200 write(6,210)
  210 format(//," singular matrix")
  300 continue
      return
      end
```

APPENDIX D

CONVERSION FACTORS TO SI METRIC UNITS

		Conversion Factor
inches (in)	meters (m)	0.0254
inches (in)	centimeters (cm)	2.54
inches (in)	millimeters (mm)	25.4
feet (ft)	meters (m)	0.305
yards (yd)	meters (m)	0.914
miles (mi)	kilometers (km)	1.609
degrees (°)	radians (rad)	0.0174
acres (acre)	hectares (ha)	0.405
acre-feet (acre-ft)	cubic meters (m^3)	1233
gallons (gal)	cubic meters (m^3)	3.79×10^{-3}
gallons (gal)	liters (l)	3.79
pounds (lb)	kilograms (kg)	0.4536
tons (ton, 2000 lb)	kilograms (kg)	907.2
pound force (lbf)	newtons (N)	4.448
pounds per sq in (psi)	newtons per sq m (N/m^2)	6895
pounds per sq ft (psf)	newtons per sq m (N/m^2)	47.88
foot-pounds (ft-lb)	joules (J)	1.356
horsepowers (hp)	watts (W)	746
British thermal units (Btu)	joules (J)	1055
British thermal units (Btu)	kilowatt-hours (kWh)	2.93×10^{-4}

Definitions

newton - force that will give a 1-kg mass an acceleration of 1 m/s^2
joule - work done by a force of 1 N over a displacement of 1 m
1 newton per sq m (N/m^2) = 1 pascal
1 kilogram force (kgf) = 9.807 N
1 gravity acceleration (g) = 9.807 m/s^2
1 are (a) = 100 m^2
1 hectare (ha) = 10,000 m^2
1 kip (kip) = 1000 lb

☆U.S. GOVERNMENT PRINTING OFFICE: 1979 623-228/706 1-3

TE 662
.A3
no. FHWA-RD-
78-158
BORROWER

FEDERALLY COORDINATED PROGRAM OF HIGHWAY RESEARCH AND DEVELOPMENT (FCP)

The Offices of Research and Development of the Federal Highway Administration are responsible for a broad program of research with resources including its own staff, contract programs, and a Federal-Aid program which is conducted by or through the State highway departments and which also finances the National Cooperative Highway Research Program managed by the Transportation Research Board. The Federally Coordinated Program of Highway Research and Development (FCP) is a carefully selected group of projects aimed at urgent, national problems, which concentrates these resources on these problems to obtain timely solutions. Virtually all of the available funds and staff resources are a part of the FCP, together with as much of the Federal-aid research funds of the States and the NCHRP resources as the States agree to devote to these projects.*

FCP Category Descriptions

1. Improved Highway Design and Operation for Safety

Safety R&D addresses problems connected with the responsibilities of the Federal Highway Administration under the Highway Safety Act and includes investigation of appropriate design standards, roadside hardware, signing, and physical and scientific data for the formulation of improved safety regulations.

2. Reduction of Traffic Congestion and Improved Operational Efficiency

Traffic R&D is concerned with increasing the operational efficiency of existing highways by advancing technology, by improving designs for existing as well as new facilities, and by keeping the demand-capacity relationship in better balance through traffic management techniques such as bus and carpool preferential treatment, motorist information, and rerouting of traffic.

3. Environmental Considerations in Highway Design, Location, Construction, and Operation

Environmental R&D is directed toward identifying and evaluating highway elements which affect the quality of the human environment. The ultimate goals are reduction of adverse highway and traffic impacts, and protection and enhancement of the environment.

4. Improved Materials Utilization and Durability

Materials R&D is concerned with expanding the knowledge of materials properties and technology to fully utilize available naturally occurring materials, to develop extender or substitute materials for materials in short supply, and to devise procedures for converting industrial and other wastes into useful highway products. These activities are all directed toward the common goals of lowering the cost of highway construction and extending the period of maintenance-free operation.

5. Improved Design to Reduce Costs, Extend Life Expectancy, and Insure Structural Safety

Structural R&D is concerned with furthering the latest technological advances in structural designs, fabrication processes, and construction techniques, to provide safe, efficient highways at reasonable cost.

6. Prototype Development and Implementation of Research

This category is concerned with developing and transferring research and technology into practice, or, as it has been commonly identified, "technology transfer."

7. Improved Technology for Highway Maintenance

Maintenance R&D objectives include the development and application of new technology to improve management, to augment the utilization of resources, and to increase operational efficiency and safety in the maintenance of highway facilities.

---

* The complete 7-volume official statement of the FCP is available from the National Technical Information Service (NTIS), Springfield, Virginia 22161 (Order No. PB 242057, price $45 postpaid). Single copies of the introductory volume are obtainable without charge from Program Analysis (HRD-2), Offices of Research and Development, Federal Highway Administration, Washington, D.C. 20590.

DOT LIBRARY
00056144

FHWA

R&D